

# UC Santa Cruz

## UC Santa Cruz Previously Published Works

### Title

Magnetism in curved geometries

### Permalink

<https://escholarship.org/uc/item/2071m426>

### Journal

Journal of Applied Physics, 129(21)

### ISSN

0021-8979

### Authors

Streubel, Robert

Tsymbol, Evgeny Y

Fischer, Peter

### Publication Date

2021-06-01

### DOI

10.1063/5.0054025

Peer reviewed

# Magnetism in Curved Geometries

Robert Streubel,<sup>1,2,3,a)</sup> Evgeny Y. Tsybal,<sup>1,2</sup> and Peter Fischer<sup>3,4</sup>

<sup>1)</sup>*Department of Physics and Astronomy, University of Nebraska-Lincoln, Lincoln, NE 68588, USA*

<sup>2)</sup>*Nebraska Center for Materials and Nanoscience, University of Nebraska-Lincoln, Lincoln, NE 68588, USA*

<sup>3)</sup>*Materials Sciences Division, Lawrence Berkeley National Laboratory, Berkeley, CA 94720, USA*

<sup>4)</sup>*Physics Department, UC Santa Cruz, Santa Cruz, CA 95064, USA*

Curvature impacts physical properties across multiple length scales, ranging from macroscopic scales, where shape and size vary drastically with curvature, to the nanoscale at interfaces and inhomogeneities in materials with structural, chemical, electronic and magnetic short-range order. In quantum materials, where correlations, entanglement and topology dominate, curvature opens the path to novel characteristics and phenomena that have recently emerged and could have dramatic impact on future fundamental and applied studies of materials. Particularly, magnetic systems hosting non-collinear and topological states, and 3D magnetic nanostructures strongly benefit from treating curvature as a new design parameter to explore prospective applications in magnetic field and stress sensing, microrobotics, and information processing and storage. This perspective gives an overview of recent progress in synthesis, theory and characterization studies, and discusses future directions, challenges and application potential of harnessing curvature for 3D nanomagnetism.

## I. INTRODUCTION

Understanding the relationship between electronic and magnetic properties and structural and chemical quantities is one of the overarching themes in condensed matter and applied physics, and key to the discovery of novel quantum materials. Correlated electron systems and magnetic materials are particularly interesting because microscopic characteristics of entangled and topological states are heavily determined by local atomic and nanoscale features. To date, research efforts have largely been focusing on synthesizing planar single-crystals, epitaxial films and multilayer stacks with tailored functionalities originating from nearly perfect long-range order and symmetry. The existence or absence of symmetry is essential to many phenomena emergent in topological insulators, ferroelectric, multiferroic and magnetic materials whose physical properties are described by vector order parameters relying on, e.g., spin-orbit coupling<sup>1-3</sup>. In fact, current information processing and storage architectures as well as concepts for novel microelectronics, including the evolving field of spintronics<sup>4</sup>, rely on low-dimensional systems with well-defined symmetry and special types of spin-orbit coupling. However, structural and chemical inhomogeneities and disorder emerge even in the most perfect materials and at interfaces. A new way of describing those imperfections is to assign them a curvature in real, reciprocal or spin space (Fig. 1). A local curvature can be employed to design systems with spontaneous or inhomogeneous inversion symmetry breaking, and to stabilize 3D magnetization vector fields or to tailor topology and magneto-transport properties in amorphous correlated electron systems<sup>5-7</sup>. Sculpting

3D curved nanostructures provides means to tailor curvature on the nanoscale while simultaneously expanding 1D and 2D nanostructures into the third dimension<sup>8</sup>, and is heavily used in microrobotics<sup>9-11</sup>.

Topological vector fields, such as vortices<sup>12</sup>, skyrmions<sup>13</sup> and topological knots<sup>14-17</sup>, possess a curvature in the vector order parameter space, e.g., spin space. Compared with uniformly polarized or topologically trivial configurations, topological vector fields span the Bloch sphere  $N$  times with  $N$  referring to the topological charge. The representation in terms of a Bloch sphere is convenient to describe electromagnetism in solids<sup>18-20</sup> and to link topological properties to electronic transport phenomena<sup>21</sup>. The latter has stimulated a multitude of theoretical and experimental studies of magnetic<sup>22-27</sup> and polar<sup>28,29</sup> skyrmions in a large variety of materials systems in view of both basic sciences and novel information storage and processing units, such as the racetrack memory<sup>30-32</sup>. Alternative concepts propose to use topological states as 3D curved magnonic waveguides<sup>33</sup> for spin wave-based spintronics<sup>34</sup>, for neuromorphic<sup>35-38</sup> and probabilistic<sup>39</sup> computing, or for topological magnonics<sup>40,41</sup> taking advantage of their quasi-particle character. The vast majority of magnetic topological vector fields has been stabilized in systems with inversion symmetry breaking, provided either by virtue of their crystal structure<sup>42,43</sup> or through the presence of planar interfaces<sup>44-46</sup> causing an asymmetric vector spin exchange, known as the Dzyaloshinskii-Moriya interaction (DMI)<sup>42,43</sup>. However, those concepts and governing mechanisms are universally applicable to ferroelectric<sup>28,29</sup>, multiferroic<sup>47</sup>, and 2D van-der-Waals materials<sup>48-51</sup>, as well as to amorphous materials<sup>52-54</sup> with local inversion symmetry breaking. In fact, systems with a locally varying DMI<sup>55,56</sup> or a spontaneous symmetry breaking with respect to spin chirality have been proposed for stabilizing twisted and

---

<sup>a)</sup>Electronic mail: streubel@unl.edu

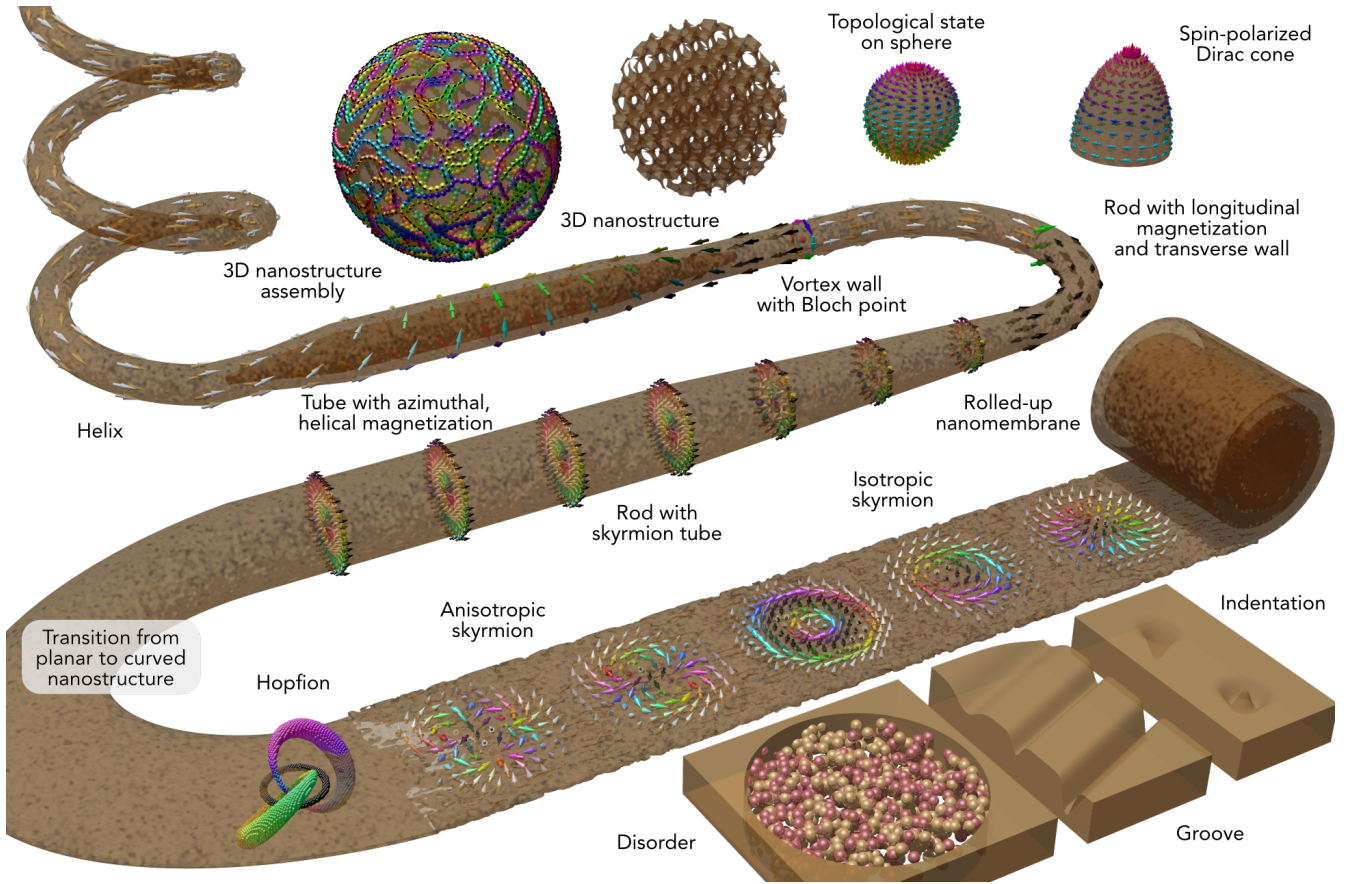


FIG. 1. Magnetism in curved geometries in real, reciprocal and spin space. Magnetic properties and novel functionalities are governed by curvature and short-range order alongside elements and composition. Local inversion symmetry breaking by curvature, strain and short-range order can promote the formation of 3D topological spin textures owing to an emergent local vector exchange interaction (DMI) with prospective applications to microelectronics while offering greater flexibility in materials synthesis. Geometrically confined structures, such as nanorods, nanotubes, and nanohelices, induce a curvature-driven DMI that discriminates between spin chirality and supports the nucleation of chiral and topological states with unprecedented stability upon current excitation. 3D nanostructures synthesized by self-assembly of nanoparticles, nanoprinting or etching enable microrobotics in gaseous and liquid phase, and fundamental studies of 3D spin frustration, and 3D magnetic logic and storage systems.

anisotropic magnetic solitons<sup>16,57</sup>, including topological spin knots referred to as hopfions<sup>14–17,58</sup>. The inherent dilemma of mutually exclusive small topological states and high magnetic ordering temperature, essential to spintronics applications, may be addressed using targeted synthesis of magnetically ordered alloys<sup>59</sup>. The prerequisite non-planar arrangement of atoms of the same element can be interpreted as a curved interface within the solid-state material, opening a completely new direction of exploring curvature as a new design parameter.

A complementary route to break inversion symmetry without impairing intrinsic properties relies on engineering curved nanostructures and tailoring magnetic exchange interactions<sup>60</sup>. Curvature has been employed to design tubular architectures with virtually unlimited magnetic domain wall velocity and unidirectional spin wave propagation owing to curvature-driven magneto-

chirality<sup>61</sup>. Since curvature-driven inversion symmetry breaking is conceptually analogous to an emergent DMI, topological states can be created and manipulated solely by curvature<sup>62</sup> without the need of intrinsic inversion symmetry breaking. To this extent, we envision that curvature will be used as a scientific design principle in the form of rough, curved structural, chemical and magnetic interfaces, gradients, and inhomogeneities/disorder in solid-state materials. This includes, in particular, artificial magneto-electric materials<sup>63</sup>, local DMI to stabilize anisotropic topological states, room-temperature skyrmions spanning a few nanometers, and spin waves emanating from and along non-collinear spin textures, such as chiral domain walls<sup>64,65</sup> and 3D topological states<sup>33</sup> enabling configurable 3D magnonic crystals. The advantage of designing and implementing curved vector fields over structurally predefined curvature opens a new way to tune on-demand the spin wave dispersion, i.e.,

band structure, through twisting and deforming, or altering the topology of the magnetization configuration.

Similar to the recent success of expanding low-dimensional magnetism into 3D nanomagnetism<sup>66–68</sup>, implementing curvature as a design concept into future magnetic materials requires an integrated approach of advanced modeling, synthesis, and characterization to validate the properties and behavior of curved magnetic structures. Recent developments of analytical and numerical frameworks have allowed for quantifying curvature-induced magneto-chirality<sup>61,69</sup>, curvature-driven formation of topological states<sup>62,70</sup>, and vector spin exchange on the atomic scale<sup>71</sup>. Advances in electrochemical deposition<sup>72</sup> and 3D nanoprinting<sup>73–76</sup> enabled the synthesis of tubular, helical and more complex nanostructures with ever-growing quality of magnetic and structural properties. Magnetic properties of planar films have been tailored by interface engineering taking advantage of improved growth capabilities and ab-initio guided synthesis<sup>3</sup>. Magnetic microscopy, tomography and scattering<sup>77–81</sup> at coherent x-ray light sources and aberration-corrected transmission electron microscopy centers have become essential to characterize chemical and structural inhomogeneities within the magnetic material and near interfaces/surfaces, and to visualize 3D magnetization vector fields. Great progress has been made in pushing limits of optical and scanning probe microscopies relying on, e.g., Kerr effect, superconducting quantum interference device magnetometry<sup>82</sup>, and nitrogen-vacancy magnetometry<sup>83</sup>.

Given the enormous scientific opportunities and challenges with adding curvature as a critical parameter to magnetic materials, this perspective provides an overview of recent progress in synthesis, theory and experimental studies, and discusses potential future directions of harnessing curvature for 3D nanomagnetism. In particular, we summarize the current state of 3D nanostructures, curvature effects and their relation to topological magnetic states in Section II. Current and future technological advances in numerical modeling, synthesis and characterization, enabling these scientific breakthroughs, are discussed in Section III. Sections IV and V give a scientific and technological perspective of harnessing curvature for basic sciences and prospective applications of 3D nanomagnetism.

## II. STATE-OF-THE-ART OF CURVATURE-INDUCED EFFECTS

Curved geometries are characterized by the spatial distribution of the local inverse radius, i.e., curvature, that can span a wide range from  $1/\mu\text{m}$  down to  $10/\text{nm}$ . Generally, the upper and lower boundaries are governed by extrinsic properties, including shape and size of 3D nanostructures and structural deformation, and intrinsic properties, such as interfaces, heterogeneity and disorder, respectively (Fig. 1). The unique feature of cur-

vature is its inherent local inversion symmetry breaking which, depending on its origin, leads to a constant or gradually/randomly changing modification to magnetic properties<sup>60,84,85</sup>. The former refers to the special case of a constant curvature and magnetization orientation with respect to the curvature; the latter to the general case of a varying microscopic or nanoscopic curvature. Note that this applies to real, reciprocal and spin space; curved spin geometries in reciprocal and spin space affect mainly spin excitations and electronic transport due to different spin-orbit coupling phenomena. The effect of a locally varying curvature in the form of structural, chemical, electronic and magnetic inhomogeneities and disorder scales with its ratio of magnitude to spatial variation. A sufficiently large ratio can affect magnetic properties and, for instance, stabilize topological spin textures on the corresponding length scale; otherwise, curvature-induced modifications to magnetic interactions will mostly compensate each other. On the other hand, engineering curved nanostructures allows for tailoring magnetic exchange interactions without impairing intrinsic properties. This approach is fundamentally different from traditionally tuning shape and size to modify magnetic dipole energies of nanostructures.

### A. 0D and 1D nanostructures

The most prominent properties of nanostructures are shape and size that alter or even completely suppress magnetism when approaching tens of nanometers. These modifications stem from an increased surface-to-volume ratio that boosts unfavorable magnetic dipole contributions, triggering a high sensitivity to short-range order and location/orientation of the magnetization of adjacent nanoparticles. The latter can be employed to design complex 3D nanostructure assemblies of core-shell and solid magnetic nanoparticles possessing a centered magnetic moment, as well as Janus particles with an off-center magnetic moment in the form of a well-defined in-plane or perpendicular<sup>86–88</sup> magnetization, vortices<sup>89–92</sup> or topological states<sup>93</sup>. Magnetic short-range and even long-range order manifest in clusters with spin frustration (Fig. 2a)<sup>94</sup>, 2D heterostructured colloidal crystals (Fig. 2b)<sup>95</sup> and straight tubular chains with variable diameters<sup>96</sup>. Theoretical studies revealed novel assemblies beyond straight chains<sup>97</sup> and flakes, such as meandering chains<sup>98</sup>, rings with different sizes, shapes and topology (Fig. 2c)<sup>99–101</sup>, and shells (Fig. 2d)<sup>102</sup>.

Physically expanding a spherical nanoparticle along one axis results in cylindrical nanorods with a uniaxial structural and magnetic symmetry. These structures typically stabilize a longitudinal magnetization similar to planar nanowires lacking a magneto-crystalline anisotropy; all other magnetic properties, such as domain wall nucleation and motion, magnetization reversal and spin wave propagation, are fundamentally different due to constant local curvature (circular cross-section). Early

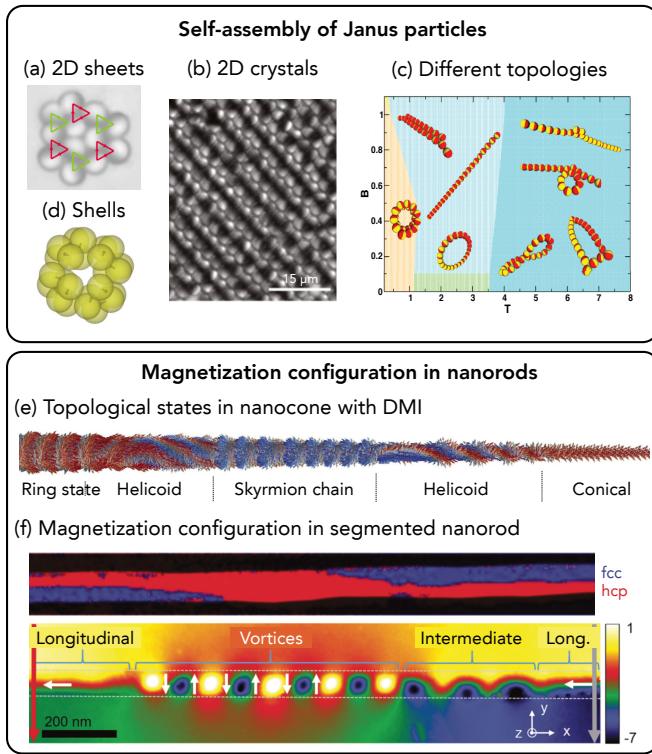


FIG. 2. Magnetization configurations in 0D and 1D nanostructures. (a–d) Self-assembly of magnetic Janus particles into (a,b) 2D arrays with specific symmetry (static), (c) straight chains, closed loops and helices (static, length, temperature and field dependent) and (d) 3D shells (static, electric charge-stabilized). (a) Reproduced with permission from Phys. Rev. E 77, 031407 (2008). Copyright 2008 American Physical Society. (b) Reproduced with permission from Langmuir 35, 6106 (2019). Copyright 2019 American Chemical Society. (c) Reproduced with permission from Phys. Rev. E 97, 022601 (2018). Copyright 2018 American Physical Society. (d) D. Morphew and D. Chakrabarti, Nanoscale 10, 13875 (2018); licensed under a Creative Commons Attribution (CC BY) license. (e) 3D non-collinear spin textures forming in FeGe nanorods with DMI revealing dependence on spatial confinement (diameter). Reproduced with permission from Phys. Rev. B 95, 112 024409 (2017). Copyright 2017 American Physical Society. (f) Magnetization in Co-rich CoNi nanorods with face-centered cubic (fcc) and hexagonal close packed (hcp) crystal structures visualized with electron holography. Reproduced with permission from ACS Nano 14, 1399 (2020). Copyright 2020 American Chemical Society. (a,b,f) and (c–e) are experimental and numerical data, respectively.

theoretical works on domain wall nucleation and propagation in nanorods provided quantitative proof for a suppressed Walker breakdown<sup>103</sup> for transverse walls<sup>104</sup>. The unprecedented large domain wall velocities have only recently been contested by synthetic antiferromagnets and angular moment-compensated ferrimagnets<sup>105,106</sup> with inversion symmetry breaking. The combination of uniaxial symmetry and shape of the nanorods causes, depending on the diameter<sup>107</sup>, either a deterministic nu-

cleation of transverse domain walls or Bloch points at the center of vortex walls<sup>108–110</sup> (Fig. 1). More complex non-collinear spin textures emerge in nanorods with an intrinsic inversion symmetry breaking and resulting Dzyaloshinskii-Moriya interaction (DMI)<sup>42,43</sup>, which reveal a periodic switching between skyrmionic and helical spins for matching and non-matching rod diameter, respectively (Fig. 2e)<sup>111</sup>.

In recent years, tremendous progress has been made in synthesis and visualizing the magnetization configuration<sup>112</sup>, including magnetization reversal process and correlation with local structural and chemical properties. Adopting x-ray photon emission electron microscopy<sup>113</sup> to conduct transmission experiments and analyzing both direct and shadow XMCD contrast enabled the visualization of helical spins in curved nanomembranes<sup>114</sup> and nanorods<sup>115</sup>, and studying 3D printed nanohelices<sup>116</sup>. The correlation between local structural and chemical properties and the magnetization configuration has been addressed with electron holography in nanorods in terms of imperfections<sup>117–119</sup>, such as grains and surface roughness, and engineered chemical/structural segmentation (Fig. 2f)<sup>120–122</sup>. The latter approach allowed for transforming a simple longitudinal magnetization prevailing in elongated nanorods into helical, vortex or transverse configurations, which are strong contenders for novel spin torque nanooscillators. Recently, experimental studies of current-driven domain wall motion in nanorods corroborated the theoretically predicted high velocities<sup>123</sup>.

## B. 2D curved geometries and curvature effects

Nanoparticles (0D) and nanorods (1D) without a magnetic core resemble shell (spherical shell) or ring (nanotube) structures with distinct magnetic properties governed by topology and curvature. Hollow tubular architectures with longitudinal magnetization and vortex domain walls lack, in contrast to nanorods, a Bloch point in the center (Fig. 1). These nanostructures promise virtually unlimited magnetic domain wall velocity (Fig. 3a)<sup>124</sup>, unidirectional spin wave propagation (Fig. 3b)<sup>125–128</sup>, and vortex chirality-dependent standing spin wave spectra<sup>127,129</sup>, owing to curvature-driven magneto-chirality<sup>61,69</sup>. The latter refers to the spin chirality selection in nanotubes due to lifted degeneracy between moving vortex walls with opposite circulation. The spin transfer torque tilts the magnetization within the domain wall inward (outward), depending on its circulation, and enhances (impairs) the stability of the vortex wall by reducing (increasing) its magnetic stray field<sup>125</sup>. In addition to these dynamic modifications, tube diameter or strength of magnetic dipole interactions can be varied to switch between longitudinal, helical and vortex configurations (Fig. 3c)<sup>130</sup>. Engineering systems with unidirectional spin wave propagation is appealing for energy efficient magnonics<sup>34</sup> and creating unidirectional magne-

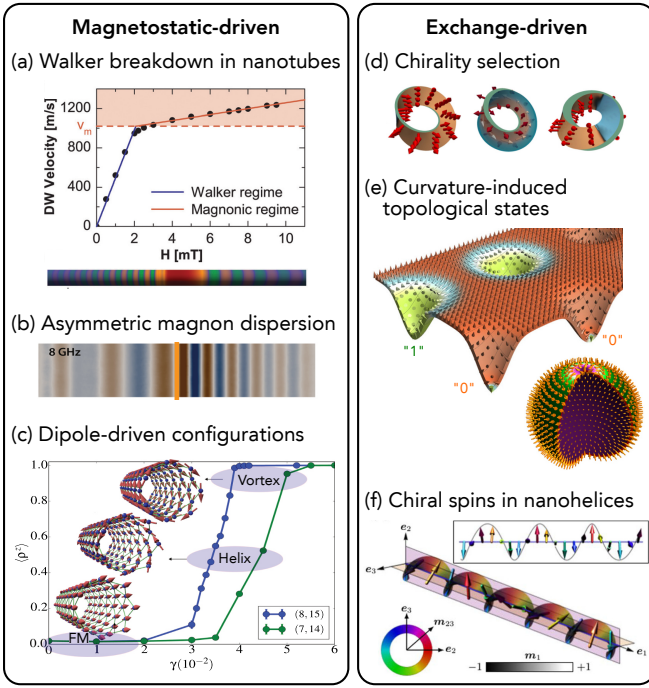


FIG. 3. Numerically predicted curvature effects in 2D curved geometries. (a) Ultra-fast domain wall velocities in nanotubes due to delayed Walker breakdown associated with spin chirality selection. Reproduced from *Appl. Phys. Lett.* 99, 122505 (2011), with the permission of AIP Publishing. (b) Asymmetric magnon dispersion in nanotubes originating from spin chirality selection similar to interfacial DMI in planar systems. Reproduced with permission from *Phys. Rev. Lett.* 117, 227203 (2016). Copyright 2016 American Physical Society. (c) Transformation of magnetic states in nanotubes with magnetic dipole coupling strength. H. D. Salinas, J. Restrepo, and Ò. Iglesias, *Sci. Rep.* 8, 10275 (2018); licensed under a Creative Commons Attribution (CC BY) license. (d) Spin chirality selection in Möbius bands governed by perpendicular magnetic anisotropy. O. V. Pylypovskyi, V. P. Kravchuk, D. D. Sheka, D. Makarov, O. G. Schmidt, and Y. Gaididei, *Phys. Rev. Lett.* 114, 197204 (2015); licensed under a Creative Commons Attribution (CC BY) license. (e) Formation of skyrmions in nanoindentations and spherical surfaces due to emergent DMI associated with local inversion symmetry breaking. Reproduced with permission from *Phys. Rev. Lett.* 120, 067201 (2018). Copyright 2018 American Physical Society. Reproduced with permission from *Phys. Rev. B* 94, 144402 (2016). Copyright 2016 American Physical Society. (f) Helicoidal spin textures in nanohelices reversibly transforming into homogeneous and periodical states upon stretching/compression. O. M. Volkov, D. D. Sheka, Y. Gaididei, V. P. Kravchuk, U. K. Röbler, J. Fassbender, and D. Makarov, *Sci. Rep.* 8, 866 (2018); licensed under a Creative Commons Attribution (CC BY) license.

toacoustic waves<sup>131</sup>. The former has just recently been demonstrated in planar architectures by resonantly exciting non-collinear spin textures, such as vortices<sup>65</sup>, Bloch points<sup>64</sup>, and domain walls<sup>132</sup>, in ferromagnetic and synthetic antiferromagnets. Particularly interesting is the spin wave propagation along curved domain walls<sup>64</sup> and

skyrmion tubes<sup>33</sup> to design 3D reconfigurable magnonic waveguides.

Mathematically, curved geometries can be treated as planar systems following a coordinate transformation. The generalized theory of curvilinear micromagnetism<sup>60</sup> illustrates how local and non-local interactions emerge from curvature, including a magnetic exchange interaction similar to DMI (Fig. 4)<sup>66,84,85</sup>, an easy-surface anisotropy<sup>133</sup>, and, for rough interfaces and surfaces and heterogeneous materials, i.e. local curvature, a spatial distribution of easy-axis, easy-cone or easy-plane anisotropy. The vector spin exchange originates from the local inversion symmetry breaking and causes a local preference for spin chirality if the magnetization and normal vector of the curved surface are not aligned (Fig. 4). For instance, spheres and tubes with radial magnetization do not show a preference. The curvature-driven DMI puts magneto-chirality<sup>69</sup> in a broader context and explains the emergence of chiral and topological spin textures in curved surfaces with cylindrical symmetry<sup>134</sup>, cones<sup>84</sup>, twisted bands<sup>135</sup>, Möbius bands (Fig. 3d)<sup>136</sup>, tori<sup>137</sup>, bent nanotubes<sup>138</sup> and rods<sup>139,140</sup>, nanohelices<sup>63,141,142</sup>, shells<sup>143–146</sup>, and indentations (Fig. 3e)<sup>62,70</sup>. Antiferromagnetic nanohelices support the formation of coherent magnon condensates in the momentum space<sup>142</sup>. Geometrically tailoring the curvature of nanohelices allows for stabilizing topologically distinct chiral spin textures, such as cycloidal and helicoidal configurations as well as collinear single-domain and multi-domain states (Fig. 3f)<sup>63,141</sup>. These states can be transformed into each other by stretching or squeezing the nanohelix, offering a new approach to design magneto-electric materials without external magnetic fields<sup>63</sup>. Similarly, the vortex ground state in ring-shaped nanowires transitions upon deformation into the trivial onion state<sup>147</sup>. These transformations represent an unwinding of chiral, topological spin textures into trivial states, triggered by the curvature-induced DMI.

Nanoscale indentations enable the stabilization and manipulation of topological spin textures, such as skyrmions and skyrmioniums also known as target skyrmions (Fig. 3e)<sup>62,70</sup>, in magnetic materials with otherwise absent inversion symmetry breaking. Relying on exchange instead of magneto-static energies, this mechanism is fundamentally distinct from using thickness gradients to nucleate vortex lattices in percolated non-planar films<sup>148</sup>. Shape, size and topology of the magnetic state can be tailored by adjusting the local curvature. In a broader sense, these theoretical studies infer that local inversion symmetry breaking, due to structural and chemical inhomogeneity, and rough, curved interfaces, causes an inhomogeneous, local DMI in real materials. The challenge is to engineer these curved interfaces to promote the formation of topological spin textures instead of randomly canted spins occurring in frustrated spin systems.

To date, experimental studies of curvature effects are still rare. Magnetic switching in tubular architectures with radial magnetization and nanotubes with longitudi-

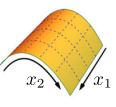
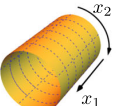
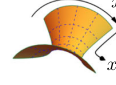
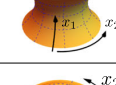
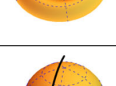
Curved geometry	Anisotropy		Local interactions			Non-local interactions
	Type	$e_a$	$w_A^x$	$w_{\text{DMI}}^x$	$w_{\text{D2}}^x$	
	easy-axis	$\hat{n}, e_2$	✓	–	✓	✓
	hard-axis	$\hat{n}$	✓	–	–	–
	easy-axis	$e_1$	✓	–	–	–
	easy or hard-axis	$e_a$	✓	–	✓	✓
	easy-axis	$\hat{n}$	✓	–	–	✓
	hard-axis	$\mathbf{n}$	✓	–	–	–
	easy-axis	$e_1$	✓	–	–	–
	easy-axis	$e_2$	✓	–	–	–
	easy or hard-axis	$e_a$	✓	✓	✓	–
	easy-axis	$\hat{n}, e_1$	✓	✓	✓	–
	easy or hard-axis	$e_a$	✓	✓	✓	✓
	easy-axis	$\hat{n}$	✓	–	–	✓
	easy or hard-axis	$e_a$	✓	✓	✓	✓
	easy-axis	$\hat{n}$	✓	–	–	✓

FIG. 4. Theory of curvilinear micromagnetism. Non-local magnetic interactions emerge from a curvature-driven DMI in systems where the magnetization is not aligned along the normal vector of the curved surface. D. D. Sheka, O. V. Pylypovskiy, P. Landeros, Y. Gaididei, A. Kákay and D. Makarov, *Commun. Phys.* 3, 128 (2020); licensed under a Creative Commons Attribution (CC BY) license.

nal magnetization were visualized with magnetic force microscopy<sup>149</sup> and superconducting quantum interference device microscopy<sup>82</sup>. These tabletop tools, providing spatial resolution on the sub-100 nm scale, represent a significant advancement compared with earlier works using cantilever magnetometry<sup>150,151</sup>. Azimuthal soft-magnetization configurations<sup>152</sup>, inaccessible in planar geometry, have proven essential to giant magneto-impedance field sensors with unprecedented sensitivity<sup>153</sup>. A first glimpse of the potential of curvature for spintronics was recently given by disentangling spin and charge resistance in aluminum nanowires deposited above a groove<sup>154</sup>. The experiment showed a higher efficiency compared with planar structures which is essential to low-power spin current electronics and 3D microelectronics architectures with curved interconnects.

### C. Topological states

Topological magnetic states are 3D inherently curved magnetization vector fields (Fig. 1) that behave like quasi-particles upon magnetic and electric field excitation<sup>155</sup>. The magnetic properties and electronic transport phenomena<sup>21</sup> are linked via solid-state electromagnetism<sup>18–20</sup>, which sets them apart from chiral domain walls and vortices<sup>12</sup>, and makes them both fundamentally intriguing and relevant to low-power spin-based microelectronics. Since the theoretical prediction of skyrmions<sup>13</sup> and their experimental observation in single-crystals<sup>156,157</sup> and thin films<sup>158</sup>, magnetic skyrmions have been extensively studied in view of current manipulation<sup>159</sup>, current creation<sup>160,161</sup> and electric detection of individual skyrmions via the topological Hall effect<sup>162,163</sup>, associated with the perpendicular deflection of skyrmions<sup>164</sup>, or, more recently, Nernst effect<sup>165,166</sup>. These investigations had mainly been driven by engineering planar interfaces<sup>3</sup> to tailor spin-orbit coupling, essential to DMI<sup>42,43</sup> (formation), topological Hall effect (detection), and spin-orbit torque (manipulation). Synthesizing ultra-thin multilayer stacks with tailored interfacial DMI<sup>71</sup> enabled the stabilization of room-temperature skyrmions in ferromagnets<sup>167</sup> and ferrimagnets<sup>106,168,169</sup>. The latter benefit from significantly enhanced current-driven velocities near angular momentum compensation. Using complex oxide materials to grow epitaxial interface heterostructures with broken inversion symmetry and a large gradient of the electrostatic potential promoted the formation of skyrmions at low temperature<sup>170,171</sup> whose size can be controlled by the ferroelectric polarization<sup>172</sup>.

The smallest room-temperature skyrmionic spin structures ( $< 20$  nm) were stabilized by pseudo-random substitution of Si atoms with Co excess atoms in polycrystalline B20 Co-Si materials<sup>59</sup>. Disorder also exists in multicomponent B20 single-crystals stabilizing topological phases (Fig. 5a)<sup>173</sup>, such as  $\text{Fe}_{1-y}(\text{Co}, \text{Mn})_y(\text{Ge}, \text{Si})$ <sup>59,173–176</sup>, which crystallize as an achiral lattice with an inherent chemical disorder that becomes chiral to the atomic building blocks<sup>177</sup>. A recent theoretical work<sup>178</sup> showed the necessity of spin frustration to explain the experimentally observed transition between different topological phases in B20 structures (Fig. 5b)<sup>173,179</sup>, including magnetic monopoles on the order of 1 nm<sup>179–181</sup>, and rebuked the commonly accepted requirement of large DMI to stabilize small topological states. Atomistic simulations<sup>182</sup> and experimental studies<sup>183,184</sup> of amorphous ferrimagnets confirmed further the persistence of DMI in structurally and chemically disordered materials. In fact, chemical and structural disorder can cause bulk DMI<sup>52,184</sup> and stabilize topological states in amorphous compounds (Fig. 5c)<sup>54</sup>. This is attributed to an increased Anderson localization<sup>185,186</sup> and the suppression of electron transfer between transition metal atoms, that enlarge local density of states and spin-orbit coupling<sup>187</sup>, local DMI, magneto-resistance and Hall effects<sup>188</sup>. However, ob-

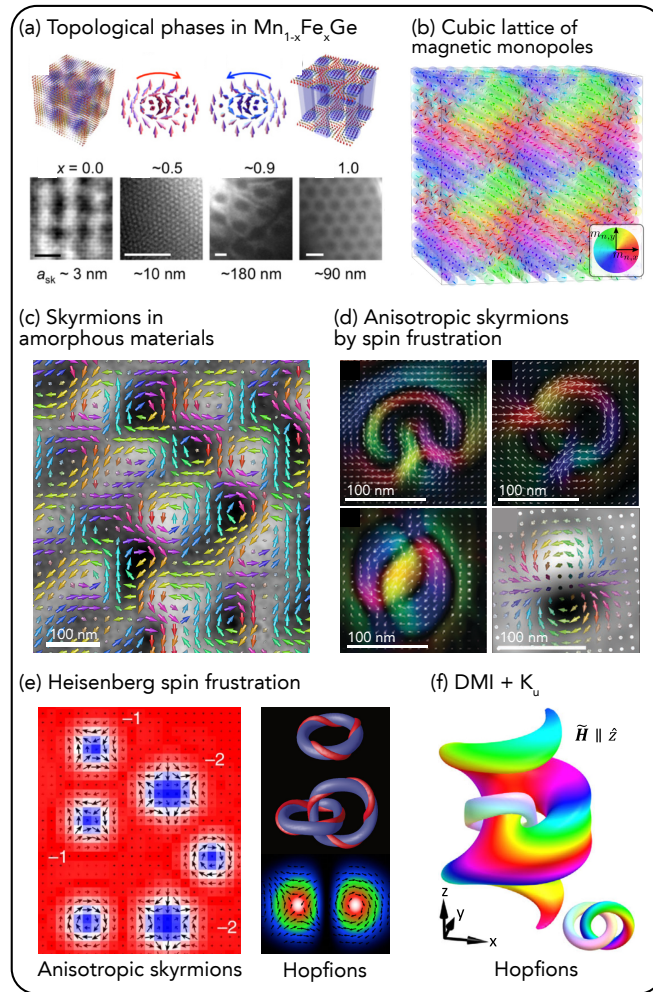


FIG. 5. Topological states stabilized by inversion symmetry breaking and spin frustration. (a) Topological phase transitions between trigonal and cubic skyrmion phases in B20  $\text{Mn}_{1-x}\text{Fe}_x\text{Ge}$  with  $x$  visualized with Lorentz microscopy (electron intensity shown). N. Kanazawa, K. Shibata, and Y. Tokura, *New J. Phys.* 18, 045006 (2016); licensed under a Creative Commons Attribution (CC BY) license. (b) Ab-initio calculations of MnGe based on Heisenberg spin frustration without DMI revealing cubic lattice of skyrmions and magnetic monopoles. Reproduced with permission from *Phys. Rev. B* 103, 024410 (2021). Copyright 2021 American Physical Society. (c) Coexistence of helical spins and skyrmions in amorphous Fe-Ge films visualized with Lorentz microscopy (electron phase and magnetization depicted). Reproduced with permission from *Adv. Mater.* 33, 2004830 (2021). Copyright 2021 John Wiley and Sons. (d) Anisotropic skyrmions in (left)  $\text{La}_{1-x}\text{Sr}_x\text{MnO}_3$ , transforming into each other via field-driven motion of Bloch lines, and (right) amorphous Fe-Ge retrieved from Lorentz microscopy. Reproduced with permission from *Adv. Mater.* 29, 1603958 (2017). Copyright 2017 John Wiley and Sons. Reproduced with permission from *Adv. Mater.* 33, 2004830 (2021). Copyright 2021 John Wiley and Sons. (e) Formation of anisotropic skyrmions and topological knots (hopfions, preimages and cross-section shown) by Heisenberg spin frustration retrieved from micromagnetic simulations. X. Zhang, J. Xia, Y. Zhou, X. Liu, H. Zhang and M. Ezawa, *Nat. Commun.* 8, 1717 (2017); licensed under a Creative Commons Attribution (CC BY) license. Reproduced with permission from *Phys. Rev. Lett.* 118, 247203 (2017). Copyright 2020 American Physical Society. (f) Metastable hopfion relaxed in system with DMI and uniaxial symmetry by micromagnetic simulations (preimages shown). Reproduced with permission from *Phys. Rev. Lett.* 125, 057201 (2020). Copyright 2020 American Physical Society. (a,c,d) and (b,e,f) are experimental and numerical data, respectively.

servicing topological knots in polycrystalline soft-magnetic bulk materials, lacking inversion symmetry breaking, demonstrated a certain degree of randomness in the occurrence of topological objects similar to magnetic vortices in extended soft-magnetic films<sup>58</sup>. The coordination number of the amorphous structure can be tuned by the deposition temperature from a high-coordination-phase

at low temperatures<sup>189</sup> to a lower-coordination-phase at room temperature<sup>190</sup> with a short-range order resembling that of B20 structures. In this context, disorder refers to locally varying DMI due to atomic short-range order and not to randomly distributed pinning sites, which have theoretically been investigated in view of current-driven skyrmion dynamics<sup>191–195</sup>.



Systems with a locally varying DMI<sup>55,56</sup> or a spontaneous symmetry breaking with respect to spin chirality, triggered by spin frustration, have been proposed for stabilizing twisted and anisotropic magnetic solitons<sup>56,57</sup>, including topological spin knots referred to as hopfions<sup>16,17,196</sup> (Fig. 5e), and, in parts, experimentally been observed (Fig. 5d)<sup>54,58,197,198</sup>. The lowest-order hopfion can be pictured as a spin torus which is twisted along its circumference continuously transforming between vortex and antivortex. The increased complexity of hopfions generally hinders a deterministic formation; a recent numerical study proposed to combine spatial confinement with DMI and perpendicular magnetic anisotropy to stabilize hopfion-like spin textures (Fig. 5f)<sup>196</sup>. These higher-order, anisotropic topological states possess a vanishing gyrovector and intrinsically compensate the perpendicular deflection of quasi-particles due to Magnus force promising a straight trajectory at increased velocities (Figs. 11b,c). Examples range from biskyrmions (bound pair of skyrmions with opposite chirality)<sup>199–201</sup> and bilayer skyrmions<sup>202</sup> to antiskyrmions<sup>203,204</sup>, skyrmioniums (biaxial skyrmions)<sup>205–207</sup> and antiskyrmioniums<sup>208</sup> to skyrmion bags<sup>209,210</sup> and hopfions<sup>211,212</sup> as well as antiferromagnetic topological states<sup>213–217</sup>. Moreover, the Magnus force can be suppressed by nanoscale modifications to structural and magnetic properties in the form of tracks and pinning sites<sup>23,218</sup>, or switching to tubular systems with a corresponding helical skyrmion trajectory<sup>219</sup>. Considering topological states in 2D and disordered materials further benefits novel concepts for manipulating magnetic exchange and topological states via curvature (Fig. 3e)<sup>62,70</sup>, voltage<sup>220–225</sup>, strain<sup>226–228</sup>, or pressure<sup>229–231</sup>, which are less effective or even destructive in (poly-)crystalline metallic systems. These alternate routes provide a convenient way to twist and deform, or even alter the topology of 3D curved magnetization vector fields needed to design configurable 3D magnonic crystals<sup>33</sup> or tunable topological magnonics<sup>40,41</sup>.

#### D. Curved spin geometries in reciprocal space

In addition to magnetic exchange manifesting collinear, non-collinear and topological magnetism, spin-orbit coupling enables an efficient charge-to-spin conversion and current-induced spin-orbit torques, mediated by non-trivial spin textures in reciprocal space. The latter originate from inversion symmetry-breaking Dresselhaus<sup>232</sup> and Rashba<sup>233</sup> fields, which impose a spin chirality on the electronic bands (Fig. 6) and generate a non-equilibrium spin polarization. The conversion between charge and spin current relies on the (inverse) Edelstein or (inverse) spin Hall effect, and has experimentally been observed at, e.g., non-magnetic metal interfaces<sup>234,235</sup> and insulating oxide interfaces<sup>236,237</sup>, and in ferroelectric materials<sup>238</sup> and 2D van-der-Waals heterostructures<sup>239</sup>. Topological materi-

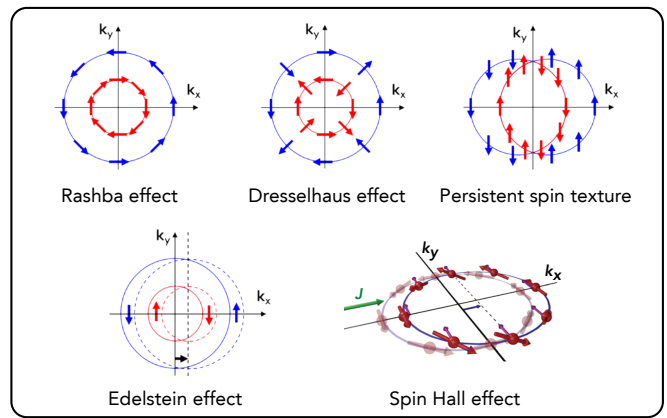


FIG. 6. Spin-orbit coupling phenomena with corresponding spin orientation of the two spin-split electronic sub-bands for systems without inversion symmetry. The Edelstein effect causes a spin accumulation due to shifted Fermi surfaces with an external electric field. An electric current  $J$  displaces the Fermi surface along its flow direction thereby tilting their spins up (down) for  $k_y > 0$  ( $k_y < 0$ ) and creating a spin current in the  $y$ -direction (spin Hall effect). L. L. Tao and E. Y. Tsymlal, Nat. Commun. 9, 2763 (2018); licensed under a Creative Commons Attribution (CC BY) license. Reproduced with permission from Rev. Mod. Phys. 87, 1213 (2015). Copyright 2015 American Physical Society.

als possess a gapless surface state protected by time-reversal symmetry<sup>240</sup>, whose band dispersion features a Dirac cone decorated with electron spins pointing tangential to the surface<sup>241</sup>. This spin texture is dramatically changed upon magnetic doping due to local time-reversal symmetry breaking, that opens a gap at the Dirac point and causes a magnetically induced hedgehog-like spin configuration (Fig. 1)<sup>242</sup>. The latter allows for generating spin currents<sup>243</sup> and producing spin-transfer torques on adjacent ferromagnets<sup>242</sup>. Chiral crystals, that lack inversion, mirror or other rotation-inversion symmetries, stabilize topologically non-trivial spin textures whose spin components parallel to the electron momenta appear around highly symmetric  $k$ -points<sup>244</sup>. Both existence and inverted topology in right- and left-handed crystals were recently observed in chiral tellurium crystals<sup>241</sup>, promising pure spin current generation. In ferroelectric materials, the spin texture is coupled to and can be controlled by the ferroelectric polarization providing a promising platform to explore the coupling between spin, orbital, valley, and lattice degrees of freedom in solids<sup>245</sup>.

One particular benefit of Rashba spin-orbit coupling is its control by a gate voltage across an interface supporting a 2D electron gas in the form of a spin field-effect transistor. Its practical realization is challenging since non-collinear spin textures possess a reduced spin diffusion length owing to an enhanced magnetic impurity and defect scattering of electrons changing their momentum and randomizing the spin<sup>246</sup>. This effect can be circumvented by engineering structures where the magni-

tudes of Rashba and Dresselhaus spin-orbit coupling are equal, resulting in a unidirectional spin-orbit field and a momentum-independent spin configuration, known as the persistent spin texture (Fig. 6). Under these conditions, electron motion is accompanied by spin precession around the unidirectional spin-orbit field, leading to a spatially periodic mode referred to as a persistent spin helix<sup>247</sup>. The latter is robust against spin-independent disorder and offers an infinite spin lifetime. It has experimentally been demonstrated in a 2D electron gas semiconductor quantum-well structure by tuning quantum-well width and doping<sup>247,248</sup>, and theoretically been predicted in bulk oxide materials with a non-symmorphic space group symmetry<sup>249</sup>. Examining the role of local curvature, structural and chemical disorder in view of real-space inversion symmetry breaking and their potential to enhance charge-to-spin conversion and increase critical temperatures is critical particularly to the emergent field of topological amorphous materials<sup>5</sup>.

### III. TECHNOLOGICAL ADVANCES

Scientific advances and future directions are heavily intertwined with technological advances in numerical modeling, synthesis and characterization. Their development throughout the last decade has diversified both original research perspective and scientific community.

#### A. Numerical modeling

Accurate modeling of magnetic systems and magnetic interactions in solid-state materials is more important than ever before to accelerate materials discovery, predict magnetic phase transitions, static and dynamic properties, and refute or corroborate analytical and experimental data. This is mainly because of an increased complexity compared to, e.g., planar ferromagnetic Permalloy ( $\text{Ni}_{80}\text{Fe}_{20}$ ) films, and driven by the use of multiple elements, including transition metal, metalloids, heavy-element, and rare-earth materials, curved nanostructures, disorder, and link to spin-orbit coupling and magneto-transport phenomena. Affordable parallel computing with multi-core central processing units (CPU) and graphics processing units (GPU), as well as inexpensive memory have helped establish numerical simulations as a mainstream technique to address curvature phenomena.

Numerous public-domain finite element/difference method software packages are available to model magnetic materials with DMI, including legacy OOMMF<sup>250</sup>, MuMax3<sup>251</sup>, and Fidimag<sup>252</sup>. Atomistic solvers, such as Vampire<sup>253</sup>, Spirit<sup>254</sup>, and Fidimag<sup>252</sup>, enable a more accurate modeling of singular magnetic spin textures, e.g., Bloch points/lines and skyrmions, antiferro- and ferromagnetism, helimagnets, and frustrated systems as well as 3D curved nanostructures, structural and chemical dis-

order, and temperature effects. Micromagnetic simulations of 3D curved geometries with arbitrary shape can be carried out with Nmag<sup>255</sup>, which is a powerful framework in combination with the HLib library<sup>256</sup>. Future developments will accommodate computational intense calculations of elastic properties and magnetostriction, and time-dependent deformation and motion of realistic multifunctional materials. One leap in this direction has been done by Boris Computational Spintronics<sup>257</sup>, a multi-physics software with incorporated heat flow solver, electronic transport solver, temperature-dependent material parameters, and mechanical stress-strain solver. While these micromagnetic platforms offer insight into magnetic states, magnetization reversal processes, size effects, and current- and field-driven spin excitations, they do rely on physical parameters, such as saturation magnetization, magnetic exchange interactions, magnetic anisotropy, etc., typically retrieved from experiments or ab-initio calculations.

In the wake of interface and curvature engineering, density functional theory is essential to determining the dependence of interface and curvature effects, including DMI and spin-orbit torque, on used elements, and structural and chemical order. Three of the most popular ab-initio frameworks are FLEUR<sup>258</sup>, VASP<sup>259</sup>, and Quantum ESPRESSO<sup>260</sup>, which provide means to model band structures and quantify atomic DMI values. The numerical results of exchange-coupled systems strongly depend on the atomic coordinates, which are typically approximated according to their crystalline structures. However, this presumption is invalid for inhomogeneous and disordered materials. Arguably, the actual coordinates of each individual atom is virtually impossible to determine; the systems can however be approximated according to their short-range order that can be quantified with molecular dynamics simulations using, e.g., LAMMPS<sup>261</sup>. The latter simulates dynamic processes of assembly, nucleation and diffusion during synthesis or upon external stimulation on the atomic scale. This hierarchical approach of modeling will become more important to future studies of real materials with imperfections, disorder and highly inhomogeneous regions, including amorphous materials and interfaces.

#### B. Synthesis

Engineering interfaces has been a focus of recent research on nanomagnetic materials, primarily due to the possibility to harness the spin-orbit coupling induced by symmetry breaking effects at such interfaces<sup>2,3</sup>. These efforts have been guided by ab-initio calculations to identify the best pairing of heavy-element material or oxide and magnetic element in view of largest DMI values<sup>71</sup> to stabilize chiral spin textures and topological states. Magneto-transport properties, such as spin Hall effect and spin-orbit torque, essential to current manipulation of chiral spin textures have typically been phenomenolog-

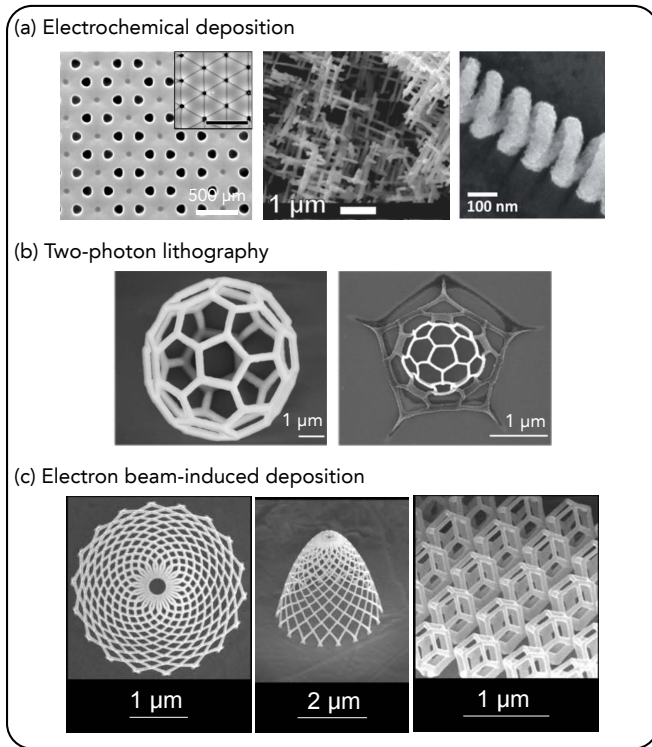


FIG. 7. Synthesis of 3D nanostructures using bottom-up techniques. (a) Electrochemical deposition into porous alumina templates for fabrication of magnetic nanorod arrays, 3D magnetic networks, and nanohelices. Reproduced with permission from *Langmuir* 27, 800 (2011). Copyright 2011 American Chemical Society. M. F. P. Wagner, A. S. Paulus, J. Brötz, W. Sigle, C. Trautmann, K.-O. Voss, F. Völklein, M. E. Toimil-Molaes, *Adv. Electron. Mater.* 7, 2001069 (2021); licensed under a Creative Commons Attribution (CC BY) license. Reproduced with permission from *Nanoscale* 6, 9415 (2014). Copyright 2014 Royal Society of Chemistry. (b) Polymer templates obtained by two-photon lithography (left), and additional etching and pyrolysis (right) revealing significant shrinkage. Reproduced with permission from *Microelectron. Eng.* 191, 25 (2018). Copyright 2018 Elsevier. (c) Nanoprinting of 3D nanostructures utilizing electron beam-induced deposition through dissociation of metal-carbonyl precursor molecules. S. Janbaz, N. Noordzij, D. S. Widyaratih, C. W. Hagen, L. E. Fratila-Apachitei, and A. A. Zadpoor, *Sci. Adv.* 3, eaao1595 (2017); licensed under a Creative Commons Attribution (CC BY) license.

ically optimized and correlated to ab-initio calculations. In conjunction with exploring different classes of materials, including atomic monolayers, epitaxial, polycrystalline and amorphous films as well as 2D materials, this approach has flourished owing to employing both intrinsic and extrinsic (interface) properties, which offers new functionalities and greater flexibility in materials synthesis. The next decade will show to which extent structural and chemical inhomogeneity, disorder and curved interfaces can be harnessed to tailor magnetic exchange interactions and manipulate topological states in solid-state materials.

The synthesis of 3D nanostructures utilizing electrochemical deposition (Fig. 7a)<sup>72,262,263</sup>, two-photon lithography (Fig. 7b)<sup>75,264–267</sup> and focused electron beam-induced deposition (Fig. 7c)<sup>73,74</sup> has seen tremendous progress particularly with respect to controlling shape, roughness, morphology, homogeneity and purity. Electrochemical deposition using porous alumina or gyroid polymer<sup>268</sup> templates enabled the synthesis of nanorods, nanotubes nanohelices, multi-segmented specimens<sup>115,117–122,269</sup> and 3D networks<sup>270–273</sup> with variable diameter ( $< 50$  nm), length ( $\sim 1\mu\text{m}$ ) and metallic materials (Fig. 7a). The default trigonal symmetry of the porous template was circumvented by focused ion beam guided anodization<sup>270</sup>. Focused electron beam-induced deposition has taken the lead in synthesizing 3D nanostructures with virtually any shape and curvature, including nanowires<sup>116,274,275</sup>, networks (Fig. 7c)<sup>276–278</sup>, and topological structures<sup>279</sup>. Relying on the dissociation of adsorbed metal-carbonyl precursor molecules by the electron beam, the printed metallic nanostructures typically incorporate carbon or oxygen impurities of  $\gtrsim 10\%$ , which can be reduced using reactive gases during synthesis or post-growth. In-depth studies of process parameters, such as growth rate, precursor depletion/diffusion and heat load<sup>277,280</sup>, and computer-aided nanofabrication<sup>278,281</sup>, including Monte Carlo simulations of reaction-diffusion processes, have been essential to advancing 3D nanoprinting and investigating curvature and topology effects in 3D nanostructures.

Alternate techniques for 3D nanostructuring are printing polymeric 3D nanotemplates with two-photon lithography and subsequent metal deposition<sup>264</sup>, implosion fabrication harnessing shrinkage and dehydration of hydrogel scaffolds<sup>282</sup>, and self-assembly of nanoparticles on curved liquid-liquid interfaces to structure liquids<sup>283–285</sup> that can be endowed with a remanent magnetization (Fig. 10)<sup>76,286,287</sup>. Nanoindentations with engineered curvature can be carved out via dry etching with ion irradiation prior to non-epitaxial film deposition. Post-growth nanoscale modifications to magnetic exchange, anisotropy and saturation magnetization may be performed with low-current ion irradiation<sup>218</sup>. Another versatile technique with respect to tailored magnetic properties is strain engineering rolled-up nanotech<sup>288–290</sup> that facilitates internal strain gradients to manufacture tubular magnetic geometries with variable diameter/curvature and thickness<sup>152,291,292</sup>. Subsequently, strain engineering has been generalized to synthesize shape-morphing micromachines (Fig. 13)<sup>293–296</sup>, reconfigurable actuators<sup>297,298</sup>, and shape memory polymers<sup>299</sup> with magnetic functionality.

### C. Characterization

Whether 3D nanostructures or topological magnetic states, the challenge with characterizing 3D magnetization vector fields is the complexity and ambiguity

of many characterization techniques due to the lack of knowledge about all three magnetization components and their spatial distribution at a sufficient spatial resolution. Joint studies harnessing multimodal techniques and subsequent detection of remaining components have provided means to identify stable magnetic states. The most advanced tools with respect to resolution and sensitivity are x-ray and electron techniques, complemented by tabletop instruments, such as scanning probe and optical microscopy, magneto-transport, electron spin resonance spectroscopy, and magnetic neutron scattering revealing internal spin structures of nanoparticles<sup>300,301</sup>. Choosing state-of-the-art instrumentation is typically a compromise between high sensitivity, high spatial resolution, temporal resolution, and accessibility. Additional constraints are element specificity, interaction between probe and magnetization, and environment, e.g., applying current/voltage, strain/pressure and magnetic fields or changing temperature and gas/solutions, to create, manipulate and detect magnetic states.

### 1. Advanced electron and x-ray characterization

Electron microscopy<sup>80,81</sup> combines subatomic spatial resolution and beam coherence. One prime example harnessing both quantities is atomic scalar tomography to examine atomic order, internal defects and strain of nanoparticles in vacuum<sup>302–305</sup> and liquid cells<sup>306–308</sup>. An adequate technique to visualize the magnetization on the atomic scale would tremendously benefit the study of antiferromagnets, disordered materials and topological states spanning only a few atoms. Future demonstrations might be accomplished by recording the diffraction pattern using 4D scanning transmission electron microscopy similar to current approaches for strain mapping<sup>304</sup>. For now, 3D magnetization vector fields can be reconstructed on the nanoscale using vector field tomography based on off-axis or in-line electron holography (Fig. 8a)<sup>122,309,310</sup>. Electron holography allows for studying the interaction of electromagnetic waves with 3D nanostructures<sup>117–119,311</sup> or thin films<sup>54,157,183,197,205,312–315</sup> on the nanoscale (Fig. 8b). In-line holography, also known as Fresnel mode Lorentz microscopy, retrieves the electron phase from a focal plane series using transport-of-intensity equation<sup>316</sup> or Gerchberg-Saxton algorithm<sup>317</sup> without the need for a biprism and reference beam. The latter can also be avoided by leveraging differential phase contrast<sup>318–320</sup>. Magnetic (vector) and electrostatic/structural (scalar) contributions to the electron phase can be separated by subtracting the phase of the magnetically saturated state or of the flipped sample. A third option unique to the Gerchberg-Saxton algorithm takes into account different length scales and phase amplitudes<sup>54,183</sup> as well as the slow convergence of low-frequency components of non-electrostatic features during the iterative phase retrieval<sup>321</sup>. The simultaneous detection of both in-plane components of the magnetic induction (two-dimensional

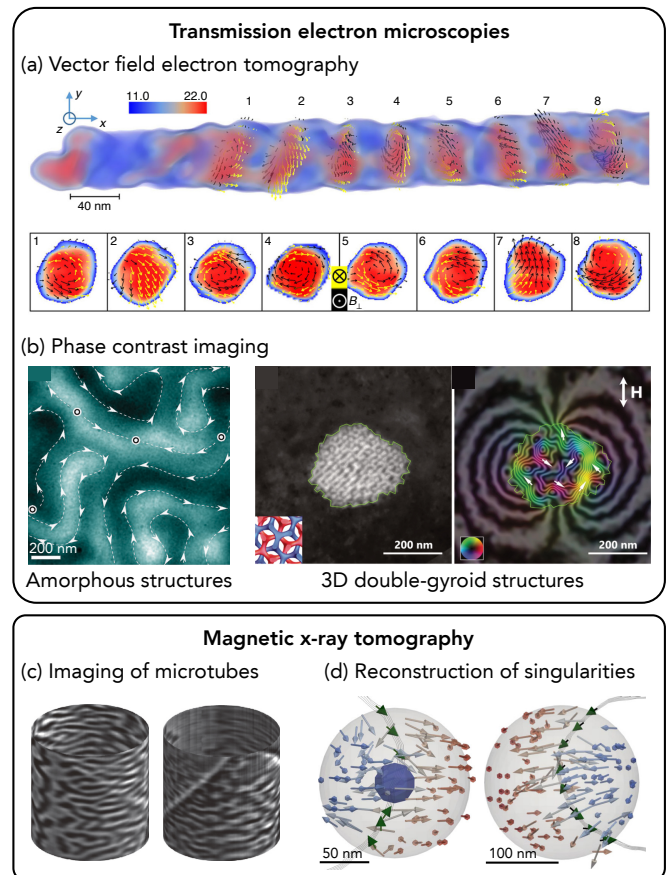


FIG. 8. Advanced electron and x-ray characterization of 3D curved geometries. (a) Magnetization in Co/Cu multilayered nanorods obtained from holographic vector field electron tomography. D. Wolf, N. Biziere, S. Sturm, D. Reyes, T. Wade, T. Niermann, J. Krehl, B. Warot-Fonrose, B. Büchner, E. Snoeck, C. Gatel, and A. Lubk, *Commun. Phys.* 2, 87 (2019); licensed under a Creative Commons Attribution (CC BY) license. (b) Electron phase contrast imaging of (left) chiral ferrimagnetism in amorphous structures and (right) spin frustration in 3D printed nanostructures visualized with Lorentz microscopy and electron holography, respectively. Reproduced with permission from *Adv. Mater.* 30, 1800199 (2018). Copyright 2018 John Wiley and Sons. Reproduced with permission from *Nano Lett.* 20, 3642 (2020). Copyright 2020 American Chemical Society. (c) 3D imaging of radial magnetization in tubular Co/Pd microstructures using soft x-rays. R. Streubel, F. Kronast, P. Fischer, D. Parkinson, O. G. Schmidt, and D. Makarov, *Nat. Commun.* 6, 7612 (2015); licensed under a Creative Commons Attribution (CC BY) license. (d) 3D reconstruction of magnetic singularities in striped domain patterns in  $\text{Ni}_{80}\text{Fe}_{20}/\text{NdCo}_5/\text{Ni}_{80}\text{Fe}_{20}$  films. A. Hierro-Rodríguez, C. Quirós, A. Sorrentino, L. M. Alvarez-Prado, J. I. Martín, J. M. Alameda, S. McVitie, E. Pereiro, M. Vélez, and S. Ferrer, *Nat. Commun.* 11, 6382 (2020); licensed under a Creative Commons Attribution (CC BY) license.

gradient of the electron phase) sets electron microscopy apart from x-ray techniques and is essential to time-resolved studies of the vast majority of magnetic systems.

X-ray spectromicroscopies<sup>79</sup>, harnessing x-ray magnetic circular dichroism or x-ray magnetic linear dichroism as element-specific absorption contrast mechanism, have been a workhorse for quantifying orbital and spin moments<sup>322,323</sup>, and visualizing magnetization configurations and spin excitations on the tens of nanometer scale. Time-resolved measurements concerned thermal spin fluctuations, and current- and magnetic field-driven nucleation and manipulation of chiral domain walls, topological states and magnons. Orbital moments offer insight into the local electron orbital alignment. The limitation to one magnetization component can be overcome, for stable magnetic states, by tilting the sample to access another component or performing vector field tomography. Within the last few years, magnetic x-ray tomography has matured from prototypical demonstration with soft x-rays (Fig. 8c)<sup>292</sup> to full-scale soft and hard x-ray tomography (Fig. 8d)<sup>58,324–326</sup> to stroboscopic tomographic imaging of driven magnetization dynamics<sup>327</sup>. This incredible progress has been possible by algorithm and hardware development at numerous synchrotron facilities. Alternatively, resonant x-ray scattering<sup>328</sup> can be employed to determine periodicity, spin chirality and depth profile of periodic structures, such as skyrmion lattices in magnetic<sup>329,330</sup> and ferroelectric<sup>331</sup> materials. The interference pattern under the magnetic diffraction peak created by coherent x-rays were used to reconstruct aperiodic magnetization vector fields on the nanoscale harnessing ptychography<sup>77,78</sup>, and to study thermal spin fluctuations near, e.g., topological phase transitions on the nanosecond time scale with x-ray photon correlation spectroscopy at free electron laser facilities<sup>332</sup>.

Phase contrast imaging, such as x-ray and electron ptychography, holography and tomography techniques, is based on wave propagation and offers superior sensitivity and contrast compared with conventional microscopy. At synchrotron facilities, a coherent x-ray beam is currently generated by a pinhole smaller than 10  $\mu\text{m}$  that clips more than 90% of the beam. Free electron lasers and field-emission aberration-corrected transmission electron microscopes already provide a coherent x-ray and electron beam, respectively. Ongoing developments of faster, more sensitive detectors, and better optics and sources, e.g., monochromatic, brilliant, smaller and coherent beams, offered by aberration-corrected transmission electron microscopes and next-generation diffraction-limited light sources, will significantly lower data acquisition time, and improve illumination conditions and accessibility to a limited number of high-end instruments. Answering scientific questions concerning the relation between magnetization, structural and chemical order, topology and electric response will strongly rely on advancing operandi and time-resolved capabilities ranging from millisecond (pump-free)<sup>54,333</sup> to picosecond (pump-probe)<sup>334</sup> time scales. The former is limited by the detector, the latter by the pulse width and pulse separation. Nanofabrication advances include developing platforms for current, voltage and piezoelectric strain manip-

ulation, and correlating magneto-transport properties, such as topological Hall effect, with the magnetization configuration of individual topological states. The latter will benefit from increasing the number of aberration-corrected transmission electron microscopes and x-ray beamline endstations with liquid helium cryostat holders and allow for studying topological states in topological insulators and magnetic systems with possible quantum fluctuations. Ambient experiments using, e.g., oxygen and hydrogen gas provide means to modify interface/surface chemistry (spin-orbit coupling) or exchange interaction by reversible hydrogen intercalation. Liquid cells based on amorphous silicon nitride nanomembranes or graphene can be used to control magnetism via chemical means or study self-assembly of nanoparticles.

## 2. *Tabletop instrumentation*

Magneto-optical Kerr effect magnetometry and microscopy<sup>336</sup>, offering sensitivity to either normal, transverse or longitudinal magnetization components of the outer 20 nm, provided means to study magnetization reversal processes and current-driven manipulation of micrometer-sized topological states<sup>161</sup>, and 3D nanostructures by analyzing reflections from different surface regions (Fig. 9a)<sup>291,337–339</sup>. These measurements can be combined with magneto-transport experiments to retrieve magneto-resistance and (topological) Hall coefficient for non-collinear spin textures (Fig. 9b)<sup>181</sup>, or with micro Hall probes to determine the magnetic hysteresis loops for the entire 3D nanostructures (Fig. 9c)<sup>281,340</sup>. Magnetic imaging on the tens of nanometer scale is commonly carried out with magnetic force microscopy<sup>341</sup> by probing the second derivative of the normal stray field. Recent advanced in magnetic tip customization have enabled simultaneous measurements of multiple components<sup>342</sup>, a configurable tip magnetization to track normal and in-plane components<sup>343</sup>, nanotube-based monopole sensors<sup>344</sup>, and a significantly enhanced sensitivity<sup>345</sup>. These steps are essential to quantitative magnetic force microscopy and reconstructing the 3D magnetization vector field. The challenge with magnetic force microscopy is the magnetic dipole interaction between tip and sample that alters the states in soft-magnetic systems or drags magnetic domain walls in relatively hard-magnetic materials. This limitation has been addressed with non-invasive scanning probe microscopies. Superconducting quantum interference device microscopy<sup>82,346</sup> measures the magnetic induction on the nanoscale, which was demonstrated with ferromagnetic nanotubes and nanocubes (Fig. 9d). Nitrogen-vacancy scanning probe microscopy<sup>83,347</sup> emerged as a highly sensitive technique to image non-collinear spin textures at the nanoscale in 2D van-der-Waals materials<sup>348</sup> and antiferromagnets<sup>349</sup>, and reconstruct the full 3D magnetization vector field<sup>350</sup>. Extended magnetic phases were classified with respect to topology and

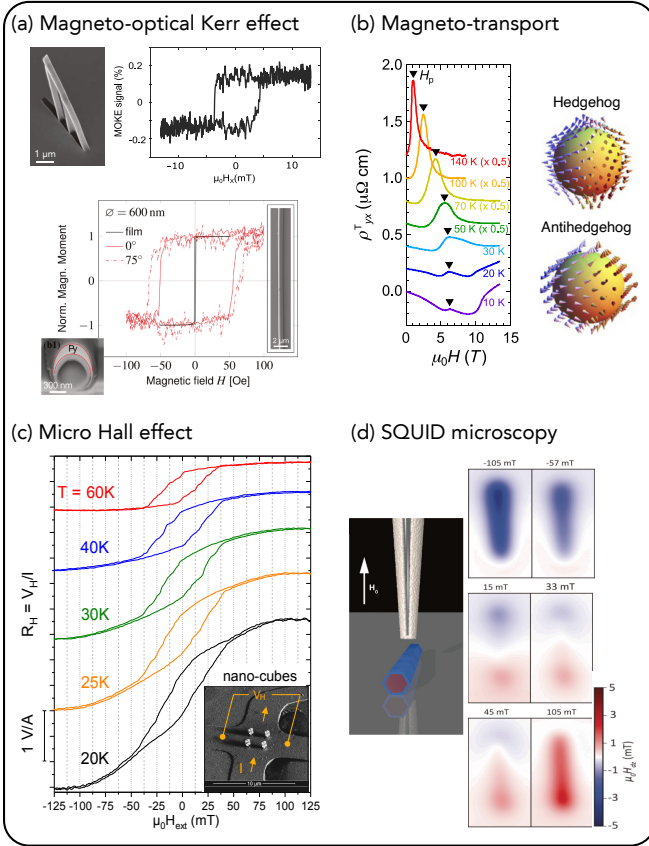


FIG. 9. Tabletop characterization tools for 3D nanomagnetism. (a) Surface-sensitive magneto-optical Kerr effect magnetometry of 3D conduit nanoprinted by focused electron beam-induced deposition of Permalloy, and tubular Permalloy cap structure. Reproduced with permission from ACS Nano 11, 11066 (2017). Copyright 2017 American Chemical Society. Reproduced with permission from Nano Lett. 12, 3961 (2012). Copyright 2012 American Chemical Society. (b) Magneto-transport in B20 MnGe single-crystal showing temperature-dependent topological Hall effect due to emergence of topological states, including magnetic monopoles shown on the right. Reproduced with permission from Phys. Rev. Lett. 125, 137202 (2020). Copyright 2020 American Physical Society. (c) Micro Hall effect measurements on CoFe nanocube frames printed by focused electron beam-induced deposition. M. Al Mamoori, L. Keller, J. Pieper, S. Barth, R. Winkler, H. Plank, J. Müller, and M. Huth, Materials 11, 289 (2018); licensed under a Creative Commons Attribution (CC BY) license. (d) Superconducting quantum interference device microscopy visualizing the magnetization reversal process in ferromagnetic nanotubes. Reproduced with permission from Nano Lett. 18, 964 (2018). Copyright 2018 American Chemical Society. All techniques can be applied to 3D curved geometries.

chirality of the 3D spin textures using electron spin resonance spectroscopy<sup>231,351,352</sup>. The latter also allows for quantifying magnetic exchange stiffness and damping. Leveraging the magnon dispersion in inversion symmetry-broken systems, Brillouin light scattering provided means to quantify DMI near the interface, including spin chirality inversion in ferrimagnets<sup>184</sup>.

## IV. SCIENTIFIC PERSPECTIVE

Growing expertise and capabilities in modeling, synthesis and characterization will enable researchers to explore rich sciences not only in magnetism and condensed matter physics, but also in close conjunction with engineering, biology and chemistry where the magnetization is either of central importance or a mean to improve functionality. In 3D nanomagnetism, this is reflected in an increasing number of theoretical and experimental works that harness curvature in 3D nanostructures and real, disordered materials to manipulate topological states.

### A. 3D nanostructures

We anticipate three major research directions concerning assemblies of nanoparticles, spin frustration in 3D nanostructures, and magnetization vector fields and spin excitations in curved geometries.

#### 1. Nanoparticle assembly

Experimental investigation of theoretically predicted nanoparticle assemblies with non-trivial geometries, such as shells, rings, helices and nanopatterns with different sizes, shapes and topology will face challenges with the inherent size and shape distribution of nanoparticles that cause disorder and deformation of the assembly. Numerical modeling will need to account for these experimental limitations to provide better insight into the self-assembly and its application potential. Disordered particle crystals and curved dipole-coupled systems can be used to explore disorder and curvature effects, and to determine to which extent dipole systems resemble exchange-coupled materials.

Whereas the vast majority of experimental and theoretical studies of nanoparticle assembly in solution<sup>353</sup> has relied on magnetic dipole interactions there is ample opportunity to employ mechanical (gravity, surface tension) and chemical (pH, ligands) means. One prominent example is the assembly and jamming of nanoparticles at inversion symmetry broken liquid-liquid interfaces, which provide a reversible structural transformation between liquid and glassy states (Figs. 10a,d)<sup>76,354</sup>. The glassy state can be pictured as a skeleton enclosing the liquid core with potentially highly anisotropic, non-equilibrium shape. In combination with superparamagnetic nanoparticles, this approach enables a transition between paramagnetic ferrofluid and ferromagnetic liquid housing 2D ferromagnetism on the curved liquid interface<sup>76,286,287,355</sup>. With each nanoparticle acting as a uniformly magnetized macrospin, thermal spin excitations, magnetic short-range and long-range order depend on the structural short-range order of adjacent nanoparticles (Fig. 10b)<sup>286</sup>, similar to XY macrospins in planar systems<sup>356,357</sup>. These systems have the potential

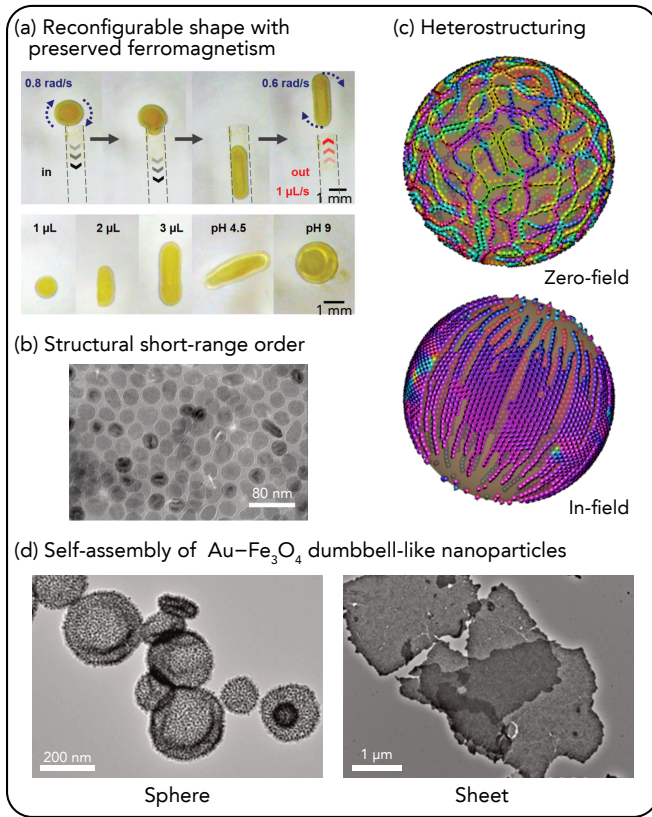


FIG. 10. Self-assembly of nanoparticle building blocks into 3D hierarchical systems in liquid environment. (a) Interfacial jamming of superparamagnetic nanoparticles at liquid-liquid interfaces forming ferromagnetic liquid droplets with reconfigurable shape and preserved magnetization observed in hydrodynamics experiments. Reproduced with permission from Science 365, 264 (2019). Copyright 2019 American Association for the Advancement of Science. (b) Isotropic elastic and magnetic properties stemming from structural short-range order of jammed nanoparticles imaged with transmission electron microscopy in their dried state. Reproduced with permission from Proc. Natl. Acad. Sci. USA 118, e2017355118 (2021). Copyright 2021 National Academy of Sciences. (c) In-field and zero-field assembly of nanoparticles from a mixture of dispersed superparamagnetic and non-magnetic nanoparticles revealing distinct heterostructures with enhanced magnetic anisotropy and remanent magnetization. The depicted states are modeled with molecular dynamics and micromagnetic simulations and leave out non-magnetic nanoparticles. (d) Self-assembly of Au-Fe<sub>3</sub>O<sub>4</sub> dumbbell-like nanoparticles with packing parameter of (left) 0.63, and (right) 0.84 visualized with transmission electron microscopy. Reproduced with permission from Nano Lett. 20, 8773 (2020). Copyright 2020 American Chemical Society.

to become a versatile platform to investigate spin liquid to spin glass transitions in planar and curved geometries which can be controlled by chemical properties, such as pH and ligands, stress and strain, electric and magnetic fields. The pH affects the screening of electrostatic charges and thus the separation between negatively charged nanoparticles jammed at the interface.

Jamming mixtures of non-magnetic and superparamagnetic nanoparticles in the presence of an external magnetic field provides a route to adaptive reconfigurable 3D printing and heterostructuring (Fig. 10c), as known from 2D ferrofluids<sup>358</sup>. Long chains<sup>359–361</sup> and lattices<sup>362</sup> form at liquid-liquid and liquid-air interfaces in alternating in-plane magnetic fields where the balance between viscous and magnetic torque, and magnetic attraction and hydrodynamic repulsion govern the stability and mechanical response of the dynamically stable, ordered structures. Jamming these assemblies will inhibit the mobility of individual particles, producing a locked remanent magnetization of the entire droplet. This novel approach stimulates to reimagine magnetism and microbotics from the perspective of liquids with solid-state functionalities<sup>355</sup> and prospective applications to viscosity engineering, magnetically functionalized liquid-crystalline and plastic-crystalline phases<sup>363–365</sup>, organic synthesis in living cells<sup>366</sup>, and encapsulation and triggered release of cargo<sup>354,361</sup>.

## 2. 3D spin frustration

The expansion of frustrated dipole systems from planar artificial spin ice structures into 3D space will be essential to the resemblance of inherently 3D, frustrated exchange-coupled materials<sup>367</sup>. Although providing valuable insight into spin frustration, the current approach is restricted to 2D planar systems and improperly scaled nearest and next-nearest neighbor interactions due to the finite size of nanoislands. Advances in focused electron beam induced deposition, two-photon lithography and electrochemical deposition will allow for synthesizing single- and multi-component nanostructures where magnetic moments are confined to vertices or connecting segments. This bottom up approach enables a pathway to design 3D geometrically frustrated heterostructures with various symmetry and geometry of isotropic lattices, 2D layered structures, and deliberately disordered systems. Tailoring shape and size (extrinsic) or anisotropy, exchange and Curie temperature (intrinsic) of multi-component heterostructures translates to an ensemble of magnetically harder and softer materials. While single-component nanostructures are simpler to manufacture, they are less realistic since exchange interactions affect thermal spin fluctuations and local ground states. Multi-component materials with different thermal expansion coefficients will open a path to reversibly transform isotropic into anisotropic spin frustrated systems by changing dipole interactions which is particularly impactful for isotropic macrospins with negligible energy barrier, such as XY, Kitaev spins and spin glasses. The realization of these complex transitions is unique to macrospin incorporated into a nanostructure matrix and not feasible to achieve in a conventional way, e.g., changing temperature and studying systems with various lattice parameters. While the primary interest in 3D

frustrated heterostructures relies in basic science, they may also find application in random number generation or magnetic dipole logic<sup>368</sup>.

### 3. *Non-collinear spin textures in 3D nanostructures*

The accumulated knowledge of and advances in synthesis, characterization and numerical modeling of 3D nanostructures, will help boost research efforts to manufacture 3D networks for spintronics (race track memory), magnonics (spin wave excitation), and neuromorphic computing (spin oscillator). These prospective applications require high metal purity and minimal interface roughness to guarantee adequate magnetic exchange interactions, and spin-transfer or spin-orbit torque. The current manipulation of spin textures is not only essential with respect to application, but also a critical need as structural complexity prevents an effective control by external magnetic fields. We envision two routes going forward addressing domain wall manipulation in 3D networks, and more complex non-collinear spin textures and topological states in nanostructures. There are numerous challenges to overcome before realizing microelectronics based on topological states in 3D networks.

The coherent, synchronized motion of domain walls via spin-transfer or spin-orbit torque necessitates replica of domain walls with the same chirality, type, magnetic moment, width and thickness. Since domain wall shape and type are governed by extrinsic (shape, thickness, curvature) and intrinsic (exchange, saturation magnetization, anisotropy) properties, particular attention will be devoted to architectures of multiple components, i.e., vertices and connecting segments, bent and modulated nanostructures that affect both kinetics and dynamics of domain walls. To some extent, slightly different domain wall velocities can be compensated using shift registration in the form of periodic pinning sites. Similarly important is to ensure compatibility with planar systems, which demands a mean to effectively couple chiral spin textures into and out of the 3D networks<sup>337</sup>. Alternatively, new ways to nucleate and manipulate chiral domain walls in 3D networks are needed, taking advantage of, e.g., local stray fields predefining domain wall chirality, and varying cross-section to alter current density beyond the nucleation threshold. A combination of strain and temperature manipulation of local magnetic exchange and anisotropy could enable logical operations in the form of gates and splitters. Even considering the most ideal case of an amorphous metallic network without grain boundary pinning, questions remain about contact resistance, heat dissipation, pinning at corners, and curvature effects. The challenge will be to harness rather than to compensate these effects.

The multitude of physical parameters influencing magnetization vector fields and spin excitations in 3D networks makes the study and optimization of individual components essential, particularly, in view of more com-

plex non-collinear spin textures and topological states. A major milestone is the synthesis of 3D nanostructures with inversion symmetry breaking to stabilize and retain chiral, non-collinear spin textures. The common approach of single-crystals with inversion symmetry-broken unit cells is impossible to achieve with the vast majority of bottom-up nanofabrication techniques, and impractical in view of 3D networks and application. This leaves curvature, interfaces, and short-range order in amorphous materials. Biaxial 3D networks provide interfacial and curvature-induced inversion symmetry breaking, while enabling spin-orbit torque manipulation. It is unclear, though, how non-collinear spin textures wrapping the magnetic shell would transition at vertices and intersections due to changes of topology. Switching from magnetic shell to magnetic core allows free navigation through the 3D network at the expense of compensated inversion symmetry breaking. These symmetry arguments underline the essence of local variations in curvature, interfaces and short-range order to consolidate a sizable DMI.

Current efforts to synthesize and investigate cylindrical and tubular nanostructures in view of magnetic states and magnetization reversal process will expand to include domain wall dynamics, spin excitations, and 3D imaging of the magnetization vector field as well as its correlation with local structural and chemical properties in terms of imperfections and engineered chemical/structural segmentation. The latter allows for stabilizing non-collinear spin textures, such as helices, skyrmions and skyrmioniums, which may serve as novel 3D spin oscillators or magnonic crystals for, e.g., speech and pattern recognition. Structural transformation by virtue of thinning (conical shape) or bending (curvature) will further provide means to localize non-collinear spin textures and transition regions between states with distinct topology. This includes reversible switching between collinear and non-collinear spin textures in bent nanostructures, such as helices and rings, harnessing strain-mediated curvature modifications to the magnetic exchange without magnetostriction, magnetic fields and current flow. While a first demonstration can be given by mechanical stretching and compression, designing artificial magnetoelectric materials<sup>63</sup> will involve incorporating nanostructures in, e.g., piezoelectric sol-gel lead zirconate titanate matrices<sup>369</sup>. 3D magnonic crystals will likely be realized using cylindrical or tubular nanostructures with longitudinal and azimuthal magnetization configurations owing to a profound theoretical understanding and significant advances in synthesis capabilities. The emanation of magnetic spin waves from domain walls separating uniformly magnetized domains simplifies analysis, and addresses the fundamental question of curvature-driven magneto-chirality selection of vortex domain walls and a unidirectional spin wave propagation in tubular geometries that can be tuned by magnetic fields, strain and curvature. A more challenging subject are spin waves emanating from non-collinear, topological spin textures in



3D nanostructures, and their dependence on both structural and magnetic properties, including, in particular, chirality, topology, and periodicity. This close relationship makes them highly appealing from the perspective of quantum materials for non-volatile, analog information processing.

### B. Topological states stabilized by curvature and short-range order

The research on topological solitons in condensed matter will diversify with a strong emphasis on expanding the zoo of topological magnetization vector fields in homogeneous and inhomogeneous materials, and harnessing curvature, disorder, strain and voltage to tailor type, strength and inhomogeneity of magnetic exchange interactions on the nano and atomic scale. Overcoming physical and technological limitations of ferromagnetic Néel and Bloch type skyrmions will be addressed by exploring ferrimagnetic, antiferromagnetic and multiferroic isotropic and anisotropic topological states, such as higher-order skyrmions and hopfions. These studies will thrive on multimodal investigations combining magneto-resistance measurements with magnetic imaging of individual and ensembles of topological states with different chirality, topological charge and dimensions. We anticipate similar procedures for dynamic experiments of spin excitations, such as current-, voltage- and strain-driven motion, nucleation and spin wave propagation (Fig. 11). Reconstructing thermally stable 3D magnetization vector field with magnetic tomography will provide unambiguous evidence of its topology. Synthesis and experiment will be guided by numerical modeling of the most realistic possible configurations relying on molecular dynamics, ab-initio, micromagnetic and Monte Carlo simulations. A more detailed discussion of technological advances is given in Section III.

Symmetry and order are regarded essential to quantum materials ranging from superconductors to topological insulators to topological magnetic and polar states. Vector spin exchange, i.e., DMI, is an indirect magnetic exchange interaction mediated by conduction electrons of adjacent atoms that reveals, similar to RKKY exchange coupling<sup>370–372</sup>, a spatial oscillatory behavior of both sign and magnitude, and is highly sensitive to structural and chemical order<sup>373</sup>. The corresponding local DMI can be homogeneous, inhomogeneous or random on the microscale, and ideally requires a sub-atomically accurate placement of elements and atoms to tailor topological objects and their current-induced motion (Figs. 11a,b)<sup>56,212</sup>. However, this is experimentally impractical in view of both efforts and materials synthesis. Instead, we envision that research will focus on structural and chemical disorder in the form of random substitution/intercalation of atoms, rough interfaces, and amorphicity to tailor interatomic exchange on the atomic and nanoscale. Recent theoretical and

experimental works have shown promise of these alternate, unconventional means, and reinforced the need for a profound understanding of fundamental mechanisms. This ranges from probing and understanding to engineering and harnessing curvature, structural and chemical short-range order in exchange-coupled systems to stabilize topologically non-trivial states with unprecedented small feature sizes and tailored symmetry. Room-temperature skyrmions spanning a few nanometers are currently futuristic but may be realized by enlarging the mean distance between spin-polarized atoms via pseudo-random atom substitution in inversion symmetry-broken systems that leaves the exchange stiffness and DMI exchange constant unaffected<sup>59</sup>.

Amorphous magnetic materials exhibit, due to suppressed electron transfer between transition metal atoms and enlarged local density of states and spin-orbit coupling<sup>187</sup>, increased magneto-resistance and Hall effects, and provide greater flexibility in materials synthesis and manipulations via current, voltage, strain and curvature. In contrast to single-crystals and epitaxial films, they can be grown on virtually any planar, curved or modulated substrate, and will allow for exploring compositions and phases inaccessible in crystalline form due to, e.g., phase segregation. Minimal magneto-crystalline anisotropy and sensitivity to short-range order make amorphous materials ideal prototypical systems to examine curvature-driven DMI, local inversion symmetry breaking and spin chirality selection in terms of stabilized topological magnetic states and magneto-transport phenomena (Fig. 3). This includes, in particular, the visualization of topological states with different shape, size and topology, stabilized by isotropic and anisotropic nanoscale indentations and sculptures, and quantification of anisotropic exchange interactions and magneto-transport properties along, e.g., grooves. Selective release from the substrate and mechanical manipulation of free-standing films in the form of local curvature, bending, tensile and compressive strain and pressure are additional intriguing routes to alter magnetic exchange, and nucleate and switch topological states. Electric voltage can be used to manipulate magnetic exchange and anisotropy via modifications to the electron density of states near the Fermi level (Fig. 11d)<sup>221</sup> and strain-mediated coupling (Fig. 11f)<sup>228</sup>, altering both degree of inversion symmetry breaking and magneto-resistance. The high sensitivity to short-range order of amorphous materials on the verge between conductors and insulators will enable strain tuning of DMI far exceeding the values for polycrystalline films of one order of magnitude using 0.1% in-plane deformation<sup>228</sup>. The spatial variations in voltage consolidate a reconfigurable curved interface with respect to magnetic exchange that, in principle, can resemble mechanical curvature and induce a local DMI. These efforts can be combined with helium ion irradiation to tailor magnetic exchange, anisotropy and magnetic moment on the nanoscale (Fig. 11g)<sup>218</sup>. The latter allows for writing tracks for skyrmion nucle-

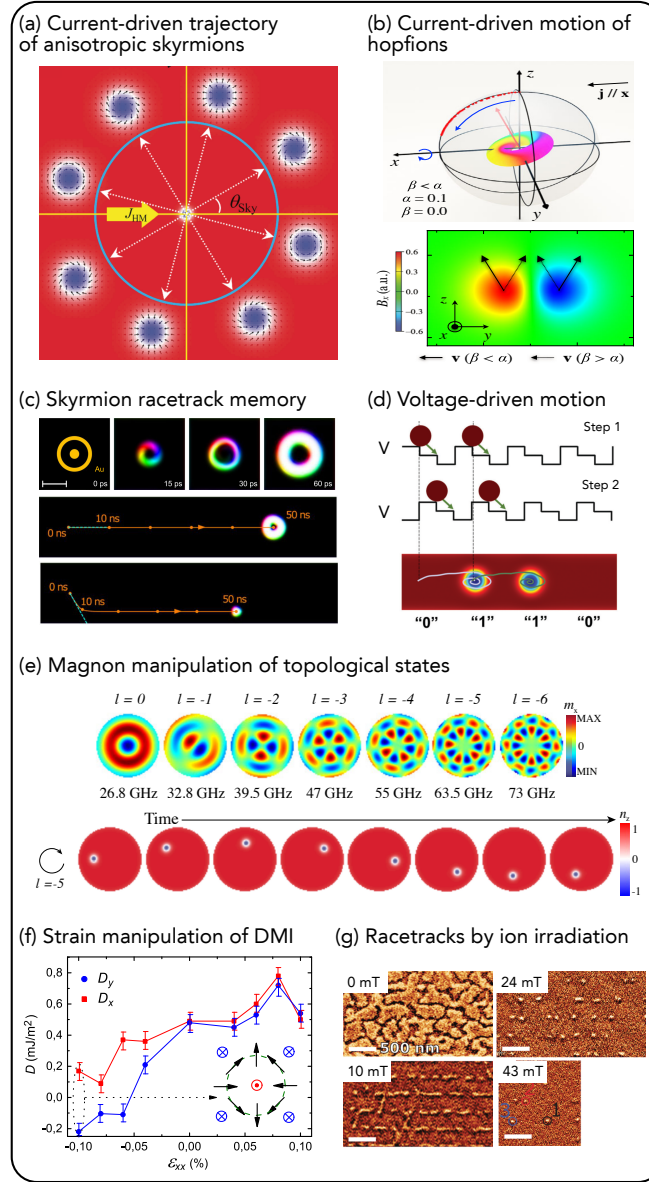


FIG. 11. Manipulation strategies for topological magnetic states, excluding curvature-induced effects discussed in Figure 3. (a) Spin Hall effect-induced motion of anisotropic skyrmions. Reproduced from Appl. Phys. Lett. 114, 192401 (2019), with the permission of AIP Publishing. (b) Current-driven motion of hopfions by spin-transfer torque revealing rotation and expansion or shrinking depending on spin damping  $\alpha$  and non-adiabatic coefficient  $\beta$ . Bottom image shows cross-sectional view of emergent magnetic field with velocities for vortex and antivortex configuration. Reproduced with permission from Phys. Rev. Lett. 124, 127204 (2020). Copyright 2020 American Physical Society. (c) Optically induced current pulse nucleation and current-driven displacement by spin-orbit torque of skyrmionium as compared with skyrmion. B. Göbel, A. F. Schäffer, J. Berakdar, I. Mertig, and S. S. P. Parkin, Sci. Rep. 9, 12119 (2019); licensed under a Creative Commons Attribution (CC BY) license. (d) Voltage control of magnetic anisotropy mediated by adjacent dielectric layer for directional motion of topological states. Reproduced with permission from Nanoscale 10, 222733 (2018). Copyright 2018 Royal Society of Chemistry. (e) Magnetic trapping of magnetic skyrmion by vertical magnons with large orbital angular momentum. Reproduced with permission from Phys. Rev. Lett. 124, 217204 (2020). Copyright 2020 American Physical Society. (f) Strain manipulation of magnetic exchange interaction in Co/Pt multilayers. Reproduced with permission from Phys. Rev. Lett. 124, 157202 (2020). Copyright 2020 American Physical Society. (g) Formation of skyrmions by helium ion irradiation-induced modifications to magnetic anisotropy and exchange in Pt/Co/MgO. Reproduced with permission from Nano Lett. 21, 2989 (2021). Copyright 2021 American Chemical Society. (a–e) and (f,g) are numerical and experimental data, respectively.

ation and motion preventing deflection due to the Magnus force (Fig. 11c)<sup>207</sup>. Since voltage manipulation of the electronic structures and magnetic exchange is typ-

ically limited to insulators and ultra-thin materials due to screening effects in conductors, it will be highly interesting to see experimental studies on the potential of

amorphous materials.

Initial investigations will concern extended and nanopatterned homogeneous systems whose compositions are chosen according to their crystalline B20 counterparts with sizable DMI. In long-term, heterogeneous and individually optimized layered structures with continuously varying composition, elements, morphology and magnetic properties may emerge, enabling, e.g., the formation of topological knots with unique current-driven motion (Fig. 11b)<sup>212</sup>. This includes different types and strengths of exchange interactions, magnetic anisotropy and transition temperatures as well as multifunctional films with, e.g., magnetic and ferro-/piezoelectric properties. These materials have been synthesized as layered heterostructures or single-crystals, and been subject to compatibility limitations. The latter are lifted in amorphous media requiring only short-range order. Multifunctional materials promise voltage, strain and curvature control of topological magnetism, antiferromagnetism and multiferroism, magnetic control of polar topological states, and amorphous topological insulators and superconductors<sup>6,374</sup> whose properties can be locally configured by topological magnetic states. An alternate route will focus on atomic layered structures to host topological states spanning a few atoms while taking advantage of negligible damping/pinning due to hybridization of ordered  $p$ -orbitals. Both characteristics make 2D van-der-Waals materials exceptionally susceptible to disorder and voltage, and enable a selective release from the substrate to examine curvature and strain effects all-electrically and via magnetic imaging<sup>48–51</sup>.

Discovering new materials and means to manipulate individual topological states can, in long-term, be accompanied by investigations of collective behavior and spin excitations. This pertains to both magnetization dynamics and phase transitions between topologically distinct states, and their relation to structural and chemical short-range order, and local DMI. Spin waves are interesting with respect to disorder-induced topological magnonics<sup>7</sup>, and their lateral and particularly vertical propagation along, e.g., skyrmion tubes, which is critical to envisioning configurable 3D magnonic crystals. Vertical magnons with large orbital angular momentum provide further means to manipulate topological states (Fig. 11e)<sup>375</sup>. The advantage of designing and implementing curved vector fields over structurally predefined curvature is a new way to tune on-demand the spin wave dispersion, i.e., band structure and topology, through twisting and deforming, or altering the topology of the magnetization configuration. In contrast to topological states confined to 3D nanostructures, extended films offer further collective behavior and potentially a route to design 3D networks of topological states and (topological) spin wave guides.

## V. TECHNOLOGICAL PERSPECTIVE

Despite a strong focus on basic sciences and the early stage of research and development, numerous technological applications of curved magnetic geometries have been proposed and, in parts, been realized. They differentiate themselves from planar technologies by an enhanced performance, novel functionality and/or higher efficiency (lower power consumption). Similar to scientific advances, structural properties have taken the lead in both sensing and microrobotics applications. We anticipate a growing interest in tailoring structural, chemical, magnetic and electronic curved geometries in quantum materials to manipulate chiral and topological states for novel sensing and microelectronics based on spintronics. The fundamental aspects of adding curvature as a critical parameter to magnetic materials were discussed in detail in Sections II and IV.

### A. Sensing

One of the earliest and most tangible beneficiaries of curved magnetic geometries are flexible and stretchable magneto-resistive sensors (Fig. 12)<sup>376</sup>, which can be synthesized by conventional thin film deposition directly onto a flexible and/or stretchable polymeric substrate or via selective release and subsequent transfer onto virtually any surface. The high-quality structural, chemical and magnetic properties enable sensing capabilities, comparable with rigid specimens on, e.g., silicon wafers, relying on giant magnetic resistance and impedance<sup>153,377,378</sup>, Hall effect, and giant stress resistance and impedance<sup>379</sup>. While functional multilayer stacks placed either in the neutral plane or onto micrometer-thick foils experience minimal impact from strain and stress, films on thicker substrates suffer magnetostriction which benefits giant stress impedance measurements in the form of an altered magnetic susceptibility and anisotropy. These characteristics provide the foundation for sensing fluid and gas flow (bending), thermal and mechanical expansions of planar and curved geometries (interfacial strain), and the physical orientation within a constant magnetic field or of a variable magnetic field as an inexpensive and thin alternative to semiconductor Hall probes. The latter will empower contactless position sensing for magnetic bearings, 3D "touch" screen and wearable navigation devices (position and movement in 3D), and on-skin interactive electronics for, e.g., augmented and virtual reality applications<sup>376,380–383</sup>. Switching from extended films to 3D nanostructures, such as nanopillars, tubes and helices, will offer spatially resolved sensing capabilities<sup>384–386</sup> on the submicrometer scale and an improved sensitivity to both magnetic field and stress. Magneto-resistive vector field sensing could be realized with 3D networks of nanostructures. Given that the magnetic anisotropy and susceptibility of superparam-

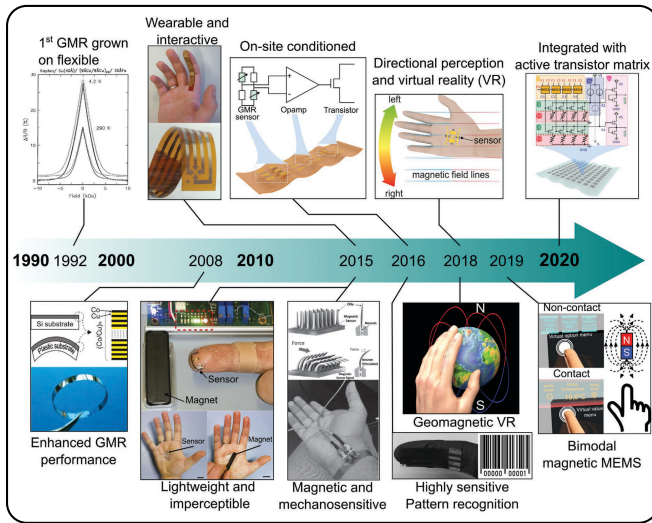


FIG. 12. Development of magnetosensitive e-skins based on magneto-resistive sensing. G. S. Canon Bermudez and D. Makarov, *Adv. Funct. Mater.* 2007788 (2021); licensed under a Creative Commons Attribution (CC BY) license.

magnetic nanoparticle coatings is highly dependent on the assemblies' short-range order, they can be used to monitor and detect thermal and mechanical expansions as well as cracks in and twists of conducting wires based on impedance changes. Similarly, local magnetic fields in liquids can be probed by analyzing self-assembly of superparamagnetic nanoparticles. The magnetic phase transition from paramagnetism to ferromagnetism of superparamagnetic nanoparticles upon jamming in liquid environment could be adapted to sensing pH with biocompatible hydrogels<sup>387,388</sup>. The latter are highly sensitive to small changes in pH leading to a hysteresis-free shrinkage and expansion, which will affect the mean distance between embedded nanoparticles and their remanent magnetization, and boost sensitivity<sup>389,390</sup>.

## B. Microrobotics

Magnetic nano and microstructures dispersed in liquid and in gaseous environments are strong contenders for microrobotics because of a high susceptibility to external magnetic fields, which enables remote control of translational and rotational motion, orientation and direction, and the selection of different modi of operation. Mechanical actuation and selective transformation of shape-morphing micromachines with distinct local magnetic and elastic properties<sup>294–296</sup> can be realized by chemically, temperature or magnetic field-driven structural deformation, and adapted to complex origami (Figs. 13a,b)<sup>295,297,391</sup>, cargo delivery in liquid<sup>293,294,298,354,361</sup> and gaseous<sup>294</sup> environment, viscosity/turbulence engineering (microfluidics)<sup>359,361</sup>, and surface roughness/modulation (optics). The magnetic functionality is typically given by ferromagnetic nanopar-

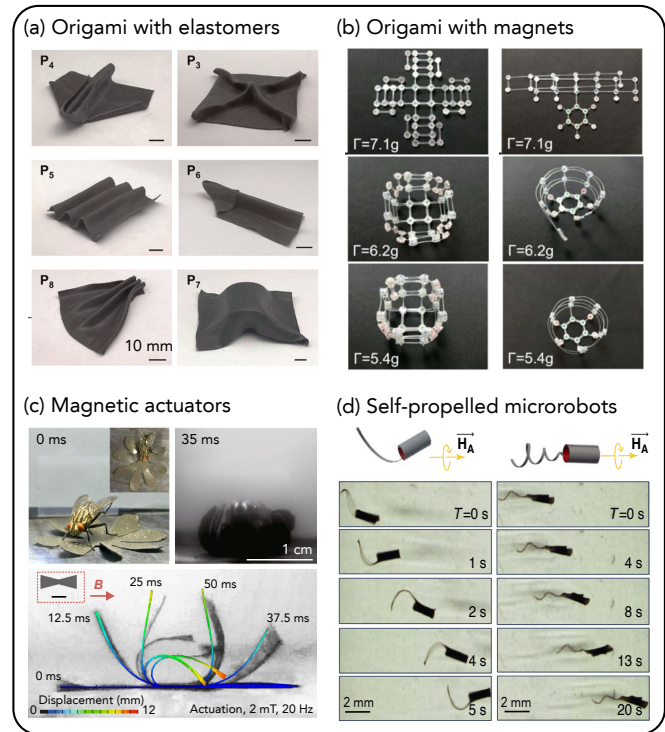


FIG. 13. Shape-morphing magnetic materials in gaseous and liquid environment. (a) Magnetic nanoparticles incorporated into elastomer matrix whose short-range order and magnetic anisotropy can be tuned at elevated temperatures in a magnetic field. Depicted shapes emerge from planar sheet in the presence of a magnetic field. Reproduced with permission from *Nano Lett.* 20, 5185 (2020). Copyright 2020 American Chemical Society. (b) Programmed self-assembly of frames equipped with multipole permanent magnets. R. Niu, C. X. Du, E. Esposito, J. Ng, M. P. Brenner, P. L. McEuen, and I. Cohen, *Proc. Natl. Acad. Sci. USA* 116, 24402 (2019); licensed under a Creative Commons Attribution (CC BY) license. (c) Millisecond actuation based on perpendicular magnetized films exposed to linear AC magnetic field. X. Wang, G. Mao, J. Ge, M. Drack, G. S. Cañón Bermúdez, D. Wirthl, R. Illing, T. Kosub, L. Bischoff, C. Wang, J. Fass-bender, M. Kaltenbrunner, and D. Makarov, *Commun. Mater.* 1, 67 (2020); licensed under a Creative Commons Attribution (CC BY) license. (d) Bio-inspired flagellated micromachines with magnetization stemming from embedded aligned ferromagnetic nanoparticles driven by a rotating magnetic field in liquid environment. H.-W. Huang, M. S. Sakar, A. J. Petruska, S. Pané, and B. J. Nelson, *Nat. Commun.* 7, 12263 (2016); licensed under a Creative Commons Attribution (CC BY) license.

ticles, embedded in elastic films or magnetic films with tailored magnetic properties, and the mechanical response to a rotating or constant magnetic field. The latter offers quasi-static<sup>297</sup> and dynamic (millisecond time scale, Fig. 13c)<sup>298</sup> actuation, including microrobots that walk, crawl, roll, and climb in air and liquid environment<sup>294</sup>, bio-inspired flagellated micromachines (Fig. 13d)<sup>293</sup>, and printing of complex 3D structures that emerge from 2D planar films<sup>295</sup>. These develop-

ments pave the way toward prospective applications in life sciences and engineering, such as drug and cargo delivery, directional tissue growth, microsurgery and artificial fertilization as well as functional and reconfigurable microfluidic channels, adaptive optical elements, viscosity engineering, local magnetic field sensing and generation, and actuation<sup>9–11</sup>. The reconfigurable magnetization of ferromagnetic liquid droplets provides a mean to promote magnetically aligned cell differentiation and proliferation, which is particularly appealing for blood vessels, cartilage, and nerve tissue regeneration in living cells<sup>366</sup>. In-field assembly and jamming of mixed phases of non-magnetic and superparamagnetic nanoparticles on liquid-liquid interfaces will enable reversible magnetic field-sensitive nanopatterning and designing birefringent, refractive, diffractive and potentially chiral liquid optical components. Choosing ligands with the potential to significantly reduce interfacial tension will provide means to generate micrometer, potentially, sub-micron, droplets from parent specimens owing to spontaneous emulsification. A magnetic field promoting the assembly and agglomeration of nanoparticles at the interface will enable a stimulated emulsification in the form of an explosive release of ferromagnetic microdroplets. The viscosity of lubricating liquids can be enhanced by DC magnetic field-induced assembly of superparamagnetic nanoparticles into chains, tubes, flakes, or rings, which decelerates translational and rotational motion of motors; disassembling may occur naturally at remanence or within an AC magnetic field.

### C. Microelectronics

Compared with sensing and microrobotics, realizing low-power microelectronics by harnessing curved geometries is a long-term effort that requires substantial scientific, technological and, to some extent, conceptual advances regarding, in particular, implementation and integration. Examples range from more conventional mechanisms, such as dipole spin frustration and current manipulation, to voltage, curvature and topology control. Spin frustration in 3D heterogeneous nanostructures may find application in random number generation and magnetic dipole logic. Current-driven domain wall manipulation and propagation in 3D networks provide a path toward 3D racetrack memory devices and domain wall logic, as recently demonstrated in 2D<sup>368</sup>, with superior storage density owing to minimal footprint. Incorporating curved nanorods in piezoelectric matrices enables voltage-induced switching between collinear and non-collinear spin textures with distinct magnetoresistance; this approach allows for designing artificial non-volatile magneto-electric materials based on strain-mediated curvature modifications to the magnetic exchange without magnetostriction, magnetic fields and current flow. Thickness-modulated low-damping materials, such as yttrium iron garnet, or 3D networks thereof

can be explored in reference to their capability to serve as tunable ferromagnetic oscillators with multiple independent narrow resonances. These efforts will help launch 5G cellular communication services in the originally intended high-frequency band of (24 ~ 28) GHz to bolster future demand in bandwidth and rate, which is prevented by the currently employed complementary metal-oxide-semiconductor (CMOS) voltage-controlled oscillators.

Novel 3D spin oscillators and magnonic crystals for, e.g., speech and pattern recognition can be realized with non-collinear spin textures, such as chiral domain walls, vortices, helices, and topological states, formed in segments of 3D networks or individual cylindrical nanostructures. The close relation between spin wave excitation and spin chirality, topology, and periodicity as well as structural properties offers a significantly larger parameter space than conventional nanospin oscillators and magnonics based on a uniform magnetization. These devices will take advantage of spatial confinement and directionality of the spin excitation (higher efficiency), and a distinct dispersion relation with potential topological features. Prototypical systems may be based on reconfigurable vortices in non-planar antidot arrays, domain walls pinned at corners of bent planar and 3D nanostructures, and domain walls separating uniformly magnetized domains in cylindrical or tubular nanostructures with longitudinal and azimuthal magnetization configurations. Harnessing chiral spin textures in 3D nanostructures and extended films has the advantage of designing and implementing curved magnetization vector fields over structurally predefined curvature, and opens a new way to tune on-demand the spin wave dispersion through twisting and deforming, or altering the topology of the magnetization configuration. Extended films offer further collective behavior and a route to design 3D networks of topological states and topological spin wave guides, which is intriguing from the perspective of novel quantum materials. A potential commercialization demands an all-electric characterization of the spin oscillators and magnonic materials probing the transmitted current signal as a fingerprint of thermal and radiofrequency spin wave excitations.

A greater flexibility in materials synthesis of quantum materials and correlated electron systems can be accomplished in the form of amorphous and polycrystalline materials with local inversion symmetry breaking. Focusing on the short-range order instead of global symmetry will allow for designing multifunctional materials which are typically incompatible due to mismatching lattice constants, symmetry and phase segregation. These materials offer voltage, strain and curvature control of topological magnetism, antiferromagnetism and multiferroism, magnetic control of polar topological states, and amorphous topological insulators and superconductors whose properties can be tuned by local decoration with topological magnetic states. Local voltage applications will provide a mean to consolidate a reconfigurable curved interface with respect to magnetic exchange, and

to alter local DMI. The latter is envisioned to promote the formation of complex 3D magnetization vector fields all-electrically, e.g., creating and deleting skyrmioniums and antiskyrmioniums as well as anisotropic solitons like topological knots, which is essential to post-CMOS microelectronics.

## VI. CONCLUSION

Harnessing curvature as a design parameter to tailor and manipulate magnetic properties of non-collinear and topological states as well as of 3D magnetic nanostructures is a vital emergent field with ample opportunity for basic and applied sciences. Despite its primary focus on basic sciences and early stage of research and development, a multitude of prospective applications have emerged, including magnetic field and stress sensing, microrobotics, and information processing and storage. Their realization requires advances in and an integrated approach of modeling, synthesis, and characterization across multiple length scales. This perspective presented recent advances in basic and applied sciences, and technology in context of ongoing research efforts which we hope will guide and stimulate future directions.

## VII. AUTHOR'S CONTRIBUTIONS

R.S. wrote the manuscript with suggestions from E.Y.T. and P.F.

## VIII. ACKNOWLEDGEMENT

This work was supported by the Laboratory Directed Research and Development Program of Lawrence Berkeley National Laboratory under U.S. Department of Energy Contract No. DE-AC02-05-CH11231, and Nebraska EPSCoR under the FIRST Award #OIA-1557417.

## IX. DATA AVAILABILITY

The data that support the findings of this study are available from the corresponding author upon reasonable request.

- <sup>1</sup>A. Manchon, H. C. Koo, J. Nitta, S. M. Frolov, and R. A. Duine, "New perspectives for Rashba spin-orbit coupling," *Nat. Mater.* **14**, 871 (2015).
- <sup>2</sup>A. Soumyanarayanan, N. Reyren, A. Fert, and C. Panagopoulos, "Emergent phenomena induced by spin-orbit coupling at surfaces and interfaces," *Nature* **539**, 509 (2016).
- <sup>3</sup>F. Hellman, A. Hoffmann, Y. Tserkovnyak, G. S. D. Beach, E. E. Fullerton, C. Leighton, A. H. MacDonald, D. C. Ralph, D. A. Arena, H. A. Dürr, P. Fischer, J. Grollier, J. P. Heremans, T. Jungwirth, A. V. Kimel, B. Koopmans, I. N. Krivorotov, S. J. May, A. K. Petford-Long, J. M. Rondinelli, N. Samarth, I. K. Schuller, A. N. Slavin, M. D. Stiles, O. Tchernyshyov,

- A. Thiaville, and B. L. Zink, "Interface-induced phenomena in magnetism," *Rev. Mod. Phys.* **89**, 025006 (2017).
- <sup>4</sup>E. Y. Tsybal and I. Zutic, *Spintronics Handbook: Spin Transport and Magnetism*, Vol. 3 (CRC press, 2019).
- <sup>5</sup>Y.-B. Yang, T. Qin, D.-L. Deng, L.-M. Duan, and Y. Xu, "Topological amorphous metals," *Phys. Rev. Lett.* **123**, 076401 (2019).
- <sup>6</sup>K. Ienaga, T. Hayashi, Y. Tamoto, S. Kaneko, and S. Okuma, "Quantum criticality inside the anomalous metallic state of a disordered superconducting thin film," *Phys. Rev. Lett.* **125**, 257001 (2020).
- <sup>7</sup>X. S. Wang, A. Brataas, and R. E. Troncoso, "Bosonic bott index and disorder-induced topological transitions of magnons," *Phys. Rev. Lett.* **125**, 217202 (2020).
- <sup>8</sup>E. Vedmedenko, R. Kawakami, D. Sheka, P. Gambardella, A. Kirilyuk, A. Hirohata, C. Binek, O. Chubykalo-Fesenko, S. Sanvito, B. Kirby, J. Grollier, K. Everschor-Sitte, T. Kampfrath, C.-Y. You, and A. Berger, "The 2020 magnetism roadmap," *J. Phys. D: Appl. Phys.* **53**, 453001 (2020).
- <sup>9</sup>B. Wang, K. Kostarelos, B. J. Nelson, and L. Zhang, "Trends in micro-/nanorobotics: Materials development, actuation, localization, and system integration for biomedical applications," *Adv. Mater.* **33**, 2002047 (2021).
- <sup>10</sup>H. Zhou, C. C. Mayorga-Martinez, S. Pané, L. Zhang, and M. Pumera, "Magnetically driven micro and nanorobots," *Chem. Rev.* (2021), 10.1021/acs.chemrev.0c01234.
- <sup>11</sup>N. Ebrahimi, C. Bi, D. J. Cappelleri, G. Ciuti, A. T. Conn, D. Faivre, N. Habibi, A. Hošovský, V. Iacovacci, I. S. M. Khalil, V. Magdanz, S. Misra, C. Pawashe, R. Rashidifar, P. E. D. Soto-Rodriguez, Z. Fekete, and A. Jafari, "Magnetic actuation methods in bio/soft robotics," *Adv. Funct. Mater.* **31**, 2005137 (2021).
- <sup>12</sup>Y. Zheng and W. Chen, "Characteristics and controllability of vortices in ferromagnetics, ferroelectrics, and multiferroics," *Rep. Prog. Phys.* **80**, 086501 (2017).
- <sup>13</sup>A. N. Bogdanov and D. A. Yablonskii, "Thermodynamically stable "vortices" in magnetically ordered crystals. the mixed state of magnets," *Sov. Phys. JETP* **68**, 101 (1989).
- <sup>14</sup>I. Bogolubsky, "Three-dimensional topological solitons in the lattice model of a magnet with competing interactions," *Phys. Lett. A* **126**, 511 – 514 (1988).
- <sup>15</sup>P. J. Ackerman and I. I. Smalyukh, "Static three-dimensional topological solitons in fluid chiral ferromagnets and colloids," *Nat. Mater.* **16**, 426 (2016).
- <sup>16</sup>P. Sutcliffe, "Skyrmion knots in frustrated magnets," *Phys. Rev. Lett.* **118**, 247203 (2017).
- <sup>17</sup>P. Sutcliffe, "Hopfions," in *Ludwig Faddeev Memorial Volume* (World Scientific Publishing, 2018) p. 539.
- <sup>18</sup>N. Nagaosa, J. Sinova, S. Onoda, A. H. MacDonald, and N. P. Ong, "Anomalous hall effect," *Rev. Mod. Phys.* **82**, 1539–1592 (2010).
- <sup>19</sup>N. Nagaosa and Y. Tokura, "Emergent electromagnetism in solids," *Phys. Scr.* **T146**, 014020 (2012).
- <sup>20</sup>W. Han, S. Maekawa, and X.-C. Xie, "Spin current as a probe of quantum materials," *Nat. Mater.* **19**, 139–152 (2020).
- <sup>21</sup>A. Soumyanarayanan, M. Raju, A. L. Gonzalez Oyarce, A. K. C. Tan, M.-Y. Im, A. P. Petrović, P. Ho, K. H. Khoo, M. Tran, C. K. Gan, F. Ernult, and C. Panagopoulos, "Tunable room-temperature magnetic skyrmions in Ir/Fe/Co/Pt multilayers," *Nat. Mater.* **16**, 898 (2017).
- <sup>22</sup>N. Nagaosa and Y. Tokura, "Topological properties and dynamics of magnetic skyrmions," *Nat. Nanotech.* **8**, 899–911 (2013).
- <sup>23</sup>R. Wiesendanger, "Nanoscale magnetic skyrmions in metallic films and multilayers: a new twist for spintronics," *Nat. Rev. Mater.* **1**, 16044 (2016).
- <sup>24</sup>A. Fert, N. Reyren, and V. Cros, "Magnetic skyrmions: advances in physics and potential applications," *Nat. Rev. Mater.* **2**, 17031 (2017).
- <sup>25</sup>N. Kanazawa, S. Seki, and Y. Tokura, "Noncentrosymmetric magnets hosting magnetic skyrmions," *Adv. Mater.* **29**, 1603227

- (2017).
- <sup>26</sup>K. Everschor-Sitte, J. Masell, R. M. Reeve, and M. Kläui, “Perspective: Magnetic skyrmions—overview of recent progress in an active research field,” *J. Appl. Phys.* **124**, 240901 (2018).
  - <sup>27</sup>X. Zhang, Y. Zhou, K. M. Song, T.-E. Park, J. Xia, M. Ezawa, X. Liu, W. Zhao, G. Zhao, and S. Woo, “Skyrmion-electronics: writing, deleting, reading and processing magnetic skyrmions toward spintronic applications,” *J. Phys.: Condens. Matter* **32**, 143001 (2020).
  - <sup>28</sup>A. K. Yadav, C. T. Nelson, S. L. Hsu, Z. Hong, J. D. Clarkson, C. M. Schlepütz, A. R. Damodaran, P. Shafer, E. Arenholz, L. R. Dedon, D. Chen, A. Vishwanath, A. M. Minor, L. Q. Chen, J. F. Scott, L. W. Martin, and R. Ramesh, “Observation of polar vortices in oxide superlattices,” *Nature* **530**, 198 (2016).
  - <sup>29</sup>S. Das, Y. L. Tang, Z. Hong, M. A. P. Gonçalves, M. R. McCarter, C. Klewe, K. X. Nguyen, F. Gómez-Ortiz, P. Shafer, E. Arenholz, V. A. Stoica, S. L. Hsu, B. Wang, C. Ophus, J. F. Liu, C. T. Nelson, S. Saremi, B. Prasad, A. B. Mei, D. G. Schlom, J. Iñiguez, P. García-Fernández, D. A. Muller, L. Q. Chen, J. Junquera, L. W. Martin, and R. Ramesh, “Observation of room-temperature polar skyrmions,” *Nature* **568**, 368 (2019).
  - <sup>30</sup>A. Fert, V. Cros, and J. Sampaio, “Skyrmions on the track,” *Nat. Nanotech.* **8**, 152–156 (2013).
  - <sup>31</sup>J. Sampaio, V. Cros, S. Rohart, A. Thiaville, and A. Fert, “Nucleation, stability and current-induced motion of isolated magnetic skyrmions in nanostructures,” *Nat. Nanotech.* **8**, 839–844 (2013).
  - <sup>32</sup>S. Parkin and S.-H. Yang, “Memory on the racetrack,” *Nat. Nanotech.* **10**, 195–198 (2015).
  - <sup>33</sup>X. Xing, Y. Zhou, and H. Braun, “Magnetic skyrmion tubes as nonplanar magnonic waveguides,” *Phys. Rev. Applied* **13**, 034051 (2020).
  - <sup>34</sup>A. V. Chumak, V. I. Vasyuchka, A. A. Serga, and B. Hillebrands, “Magnon spintronics,” *Nat. Phys.* **11**, 453 (2015).
  - <sup>35</sup>Y. Huang, W. Kang, X. Zhang, Y. Zhou, and W. Zhao, “Magnetic skyrmion-based synaptic devices,” *Nanotechnology* **28**, 08LT02 (2017).
  - <sup>36</sup>A. Kurenkov, S. DuttaGupta, C. Zhang, S. Fukami, Y. Horio, and H. Ohno, “Artificial neuron and synapse realized in an antiferromagnet/ferromagnet heterostructure using dynamics of spin-orbit torque switching,” *Adv. Mater.* **31**, 1900636 (2019).
  - <sup>37</sup>J. Grollier, D. Querlioz, K. Y. Camsari, K. Everschor-Sitte, S. Fukami, and M. D. Stiles, “Neuromorphic spintronics,” *Nat. Electron.* **3**, 360–370 (2020).
  - <sup>38</sup>S. Zhang and Y. Tserkovnyak, “Antiferromagnet-based neuromorphics using dynamics of topological charges,” *Phys. Rev. Lett.* **125**, 207202 (2020).
  - <sup>39</sup>J. Závorka, F. Jakobs, D. Heinze, N. Keil, S. Kromin, S. Jaiswal, K. Litzius, G. Jakob, P. Virnau, D. Pinna, K. Everschor-Sitte, L. Rózsa, A. Donges, U. Nowak, and M. Kläui, “Thermal skyrmion diffusion used in a reshuffler device,” *Nat. Nanotech.* **14**, 658–661 (2019).
  - <sup>40</sup>S. A. Díaz, J. Klinovaja, and D. Loss, “Topological magnons and edge states in antiferromagnetic skyrmion crystals,” *Phys. Rev. Lett.* **122**, 187203 (2019).
  - <sup>41</sup>S. A. Díaz, T. Hirosawa, J. Klinovaja, and D. Loss, “Chiral magnonic edge states in ferromagnetic skyrmion crystals controlled by magnetic fields,” *Phys. Rev. Research* **2**, 013231 (2020).
  - <sup>42</sup>I. E. Dzyaloshinskii, “Thermodynamic theory of weak ferromagnetism in antiferromagnetic substances,” *Sov. Phys. JETP* **5**, 1259 (1957).
  - <sup>43</sup>T. Moriya, “Anisotropic superexchange interaction and weak ferromagnetism,” *Phys. Rev.* **120**, 91–98 (1960).
  - <sup>44</sup>A. Fert and P. M. Levy, “Role of anisotropic exchange interactions in determining the properties of spin-glasses,” *Phys. Rev. Lett.* **44**, 1538–1541 (1980).
  - <sup>45</sup>A. N. Bogdanov and U. K. Röbber, “Chiral symmetry breaking in magnetic thin films and multilayers,” *Phys. Rev. Lett.* **87**, 037203 (2001).
  - <sup>46</sup>K.-W. Kim, H.-W. Lee, K.-J. Lee, and M. D. Stiles, “Chirality from interfacial spin-orbit coupling effects in magnetic bilayers,” *Phys. Rev. Lett.* **111**, 216601 (2013).
  - <sup>47</sup>S. Seki, X. Z. Yu, S. Ishiwata, and Y. Tokura, “Observation of skyrmions in a multiferroic material,” *Science* **336**, 198–201 (2012).
  - <sup>48</sup>M.-G. Han, J. A. Garlow, Y. Liu, H. Zhang, J. Li, D. DiMarzio, M. W. Knight, C. Petrovic, D. Jariwala, and Y. Zhu, “Topological magnetic-spin textures in two-dimensional van der Waals  $\text{Cr}_2\text{Ge}_2\text{Te}_6$ ,” *Nano Lett.* **19**, 7859–7865 (2019).
  - <sup>49</sup>B. Ding, Z. Li, G. Xu, H. Li, Z. Hou, E. Liu, X. Xi, F. Xu, Y. Yao, and W. Wang, “Observation of magnetic skyrmion bubbles in a van der Waals ferromagnet  $\text{Fe}_3\text{GeTe}_2$ ,” *Nano Lett.* **20**, 868–873 (2020).
  - <sup>50</sup>Y. Wu, S. Zhang, J. Zhang, W. Wang, Y. L. Zhu, J. Hu, G. Yin, K. Wong, C. Fang, C. Wan, X. Han, Q. Shao, T. Taniguchi, K. Watanabe, J. Zang, Z. Mao, X. Zhang, and K. L. Wang, “Néel-type skyrmion in  $\text{WTe}_2/\text{Fe}_3\text{GeTe}_2$  van der Waals heterostructure,” *Nat. Commun.* **11**, 3860 (2020).
  - <sup>51</sup>M. Yang, Q. Li, R. V. Chopdekar, R. Dhall, J. Turner, J. D. Carlström, C. Ophus, C. Klewe, P. Shafer, A. T. N’Diaye, J. W. Choi, G. Chen, Y. Z. Wu, C. Hwang, F. Wang, and Z. Q. Qiu, “Creation of skyrmions in van der Waals ferromagnet  $\text{Fe}_3\text{GeTe}_2$  on  $(\text{Co}/\text{Pd})_n$  superlattice,” *Sci. Adv.* **6**, eabb5157 (2020).
  - <sup>52</sup>D.-H. Kim, M. Haruta, H.-W. Ko, G. Go, H.-J. Park, T. Nishimura, D.-Y. Kim, T. Okuno, Y. Hirata, Y. Futakawa, H. Yoshikawa, W. Ham, S. Kim, H. Kurata, A. Tsukamoto, Y. Shiota, T. Moriyama, S.-B. Choe, K.-J. Lee, and T. Ono, “Bulk dzyaloshinskii-moriya interaction in amorphous ferrimagnetic alloys,” *Nat. Mater.* **18**, 685–690 (2019).
  - <sup>53</sup>A. Haim, R. Ilan, and J. Alicea, “Quantum anomalous parity hall effect in magnetically disordered topological insulator films,” *Phys. Rev. Lett.* **123**, 046801 (2019).
  - <sup>54</sup>R. Streubel, D. S. Bouma, F. Bruni, X. Chen, P. Ercius, J. Ciston, A. T. N’Diaye, S. Roy, S. Kevan, P. Fischer, and F. Hellman, “Chiral spin textures in amorphous iron-germanium thick films,” *Adv. Mater.* **33**, 2004830 (2021).
  - <sup>55</sup>M. Hoffmann, B. Zimmermann, G. P. Müller, D. Schürhoff, N. S. Kiselev, C. Melcher, and S. Blügel, “Antiskyrmions stabilized at interfaces by anisotropic dzyaloshinskii-moriya interactions,” *Nat. Commun.* **8**, 308 (2017).
  - <sup>56</sup>C. Jin, C. Zhang, C. Song, J. Wang, H. Xia, Y. Ma, J. Wang, Y. Wei, J. Wang, and Q. Liu, “Current-induced motion of twisted skyrmions,” *Appl. Phys. Lett.* **114**, 192401 (2019).
  - <sup>57</sup>X. Zhang, J. Xia, Y. Zhou, X. Liu, H. Zhang, and M. Ezawa, “Skyrmion dynamics in a frustrated ferromagnetic film and current-induced helicity locking-unlocking transition,” *Nat. Commun.* **8**, 1717 (2017).
  - <sup>58</sup>C. Donnelly, K. L. Metlov, V. Scagnoli, M. Guizar-Sicairos, M. Holler, N. S. Bingham, J. Raabe, L. J. Heyderman, N. R. Cooper, and S. Gliga, “Experimental observation of vortex rings in a bulk magnet,” *Nat. Phys.* **17**, 316–321 (2021).
  - <sup>59</sup>B. Balasubramanian, P. Manchanda, R. Pahari, Z. Chen, W. Zhang, S. R. Valloppilly, X. Li, A. Sarella, L. Yue, A. Ullah, P. Dev, D. A. Muller, R. Skomski, G. C. Hadjipanayis, and D. J. Sellmyer, “Chiral magnetism and high-temperature skyrmions in B20-ordered Co-Si,” *Phys. Rev. Lett.* **124**, 057201 (2020).
  - <sup>60</sup>D. D. Sheka, O. V. Pylypovskiy, P. Landeros, Y. Gaididei, A. Kákay, and D. Makarov, “Nonlocal chiral symmetry breaking in curvilinear magnetic shells,” *Commun. Phys.* **3**, 128 (2020).
  - <sup>61</sup>R. Hertel, “Ultrafast domain wall dynamics in magnetic nanotubes and nanowires,” *J. Phys.: Condens. Matter* **28**, 483002 (2016).
  - <sup>62</sup>V. P. Kravchuk, D. D. Sheka, A. Kákay, O. M. Volkov, U. K. Röbber, J. van den Brink, D. Makarov, and Y. Gaididei, “Multiple of skyrmion states on a curvilinear defect: Reconfigurable skyrmion lattices,” *Phys. Rev. Lett.* **120**, 067201 (2018).

- <sup>63</sup>O. Volkov, U. Röbber, J. Fassbender, and D. Makarov, “Concept of artificial magnetoelectric materials via geometrically controlling curvilinear helimagnets,” *J. Phys. D: Appl. Phys.* **52**, 345001 (2019).
- <sup>64</sup>V. Sluka, T. Schneider, R. A. Gallardo, A. Kákay, M. Weigand, T. Warnatz, R. Mattheis, A. Roldán-Molina, P. Landeros, V. Tiberkevich, A. Slavin, G. Schütz, A. Erbe, A. Deac, J. Lindner, J. Raabe, J. Fassbender, and S. Wintz, “Emission and propagation of 1d and 2d spin waves with nanoscale wavelengths in anisotropic spin textures,” *Nat. Nanotech.* **14**, 328–333 (2019).
- <sup>65</sup>G. Dieterle, J. Förster, H. Stoll, A. S. Semisalova, S. Finizio, A. Gangwar, M. Weigand, M. Noske, M. Fähnle, I. Bykova, J. Gräfe, D. A. Bozhko, H. Y. Musiienko-Shmarova, V. Tiberkevich, A. N. Slavin, C. H. Back, J. Raabe, G. Schütz, and S. Wintz, “Coherent excitation of heterosymmetric spin waves with ultrashort wavelengths,” *Phys. Rev. Lett.* **122**, 117202 (2019).
- <sup>66</sup>R. Streubel, P. Fischer, F. Kronast, V. P. Kravchuk, D. D. Sheka, Y. Gaididei, O. G. Schmidt, and D. Makarov, “Magnetism in curved geometries,” *J. Phys. D: Appl. Phys.* **49**, 363001 (2016).
- <sup>67</sup>A. Fernández-Pacheco, R. Streubel, O. Fruchart, R. Hertel, P. Fischer, and R. P. Cowburn, “Three-dimensional nanomagnetism,” *Nat. Commun.* **8**, 15756 (2017).
- <sup>68</sup>P. Fischer, D. Sanz-Hernández, R. Streubel, and A. Fernández-Pacheco, “Launching a new dimension with 3d magnetic nanostructures,” *APL Materials* **8**, 010701 (2020).
- <sup>69</sup>R. Hertel, “Curvature-induced magnetochirality,” *SPIN* **03**, 1340009 (2013).
- <sup>70</sup>O. V. Pylypovskyi, D. Makarov, V. P. Kravchuk, Y. Gaididei, A. Saxena, and D. D. Sheka, “Chiral skyrmion and skyrmionium states engineered by the gradient of curvature,” *Phys. Rev. Applied* **10**, 064057 (2018).
- <sup>71</sup>A. Belabbes, G. Bihlmayer, F. Bechstedt, S. Blügel, and A. Manchon, “Hund’s rule-driven dzyaloshinskii-moriya interaction at  $3d-5d$  interfaces,” *Phys. Rev. Lett.* **117**, 247202 (2016).
- <sup>72</sup>M. Stano and O. Fruchart, “Magnetic nanowires and nanotubes,” in *Handbook of Magnetic Materials*, edited by E. Bruck (Elsevier, 2018) Chap. 3, p. 155.
- <sup>73</sup>J. De Teresa, A. Fernández-Pacheco, R. Córdoba, L. Serrano-Ramón, S. Sangiao, and M. Ibarra, “Review of magnetic nanostructures grown by focused electron beam induced deposition (FEBID),” *J. Phys. D: Appl. Phys.* **49**, 243003 (2016).
- <sup>74</sup>R. Winkler, J. Fowlkes, P. Rack, and H. Plank, “3d nanoprinting via focused electron beams,” *J. Appl. Phys.* **125**, 210901 (2019).
- <sup>75</sup>G. Williams, M. Hunt, B. Boehm, A. May, M. Taverne, D. Ho, S. Giblin, D. Read, J. Rarity, R. Allenspach, and S. Ladak, “Two-photon lithography for 3d magnetic nanostructure fabrication,” *Nano Res.* **11**, 845 (2018).
- <sup>76</sup>X. Liu, N. Kent, A. Ceballos, R. Streubel, Y. Jiang, Y. Chai, P. Y. Kim, J. Forth, F. Hellman, S. Shi, D. Wang, B. A. Helms, P. D. Ashby, P. Fischer, and T. P. Russell, “Reconfigurable ferromagnetic liquid droplets,” *Science* **365**, 264 (2019).
- <sup>77</sup>F. Pfeiffer, “X-ray ptychography,” *Nat. Photon.* **12**, 9–17 (2018).
- <sup>78</sup>X. Shi, N. Burdet, B. Chen, G. Xiong, R. Streubel, R. Harder, and I. K. Robinson, “X-ray ptychography on low-dimensional hard-condensed matter materials,” *Appl. Phys. Rev.* **6**, 011306 (2019).
- <sup>79</sup>C. Donnelly and V. Scagnoli, “Imaging three-dimensional magnetic systems with x-rays,” *J. Phys.: Condens. Matter* **32**, 213001 (2020).
- <sup>80</sup>P. A. Midgley and R. E. Dunin-Borkowski, “Electron tomography and holography in materials science,” *Nat. Mater.* **8**, 1476–1122 (2009).
- <sup>81</sup>D. Wolf, A. Lubk, F. Röder, and H. Lichte, “Electron holographic tomography,” *Curr. Opin. Solid State Mater. Sci.* **17**, 126 – 134 (2013).
- <sup>82</sup>D. Vasyukov, L. Ceccarelli, M. Wyss, B. Gross, A. Schwarb, A. Mehlin, N. Rossi, G. Tütüncüoğlu, F. Heimbach, R. R. Zamani, A. Kovács, A. Fontcuberta i Morral, D. Grundler, and M. Poggio, “Imaging stray magnetic field of individual ferromagnetic nanotubes,” *Nano Lett.* **18**, 964–970 (2018).
- <sup>83</sup>F. Casola, T. van der Sar, and A. Yacoby, “Probing condensed matter physics with magnetometry based on nitrogen-vacancy centres in diamond,” *Nat. Rev. Mater.* **3**, 17088 (2018).
- <sup>84</sup>Y. Gaididei, V. P. Kravchuk, and D. D. Sheka, “Curvature effects in thin magnetic shells,” *Phys. Rev. Lett.* **112**, 257203 (2014).
- <sup>85</sup>D. D. Sheka, V. P. Kravchuk, and Y. Gaididei, “Curvature effects in statics and dynamics of low dimensional magnets,” *J. Phys. A: Math. Theor.* **48**, 125202 (2015).
- <sup>86</sup>M. Albrecht, G. Hu, I. L. Guhr, T. C. Ulbrich, J. Boneberg, P. Leiderer, and G. Schatz, “Magnetic multilayers on nanospheres,” *Nat. Mater.* **4**, 203 (2005).
- <sup>87</sup>T. C. Ulbrich, D. Makarov, G. Hu, I. L. Guhr, D. Suess, T. Schrefl, and M. Albrecht, “Magnetization reversal in a novel gradient nanomaterial,” *Phys. Rev. Lett.* **96**, 077202 (2006).
- <sup>88</sup>L. Baraban, D. Makarov, R. Streubel, I. Mönch, D. Grimm, S. Sanchez, and O. G. Schmidt, “Catalytic janus motors on microfluidic chip: Deterministic motion for targeted cargo delivery,” *ACS Nano* **6**, 3383–3389 (2012).
- <sup>89</sup>R. Streubel, D. Makarov, F. Kronast, V. Kravchuk, M. Albrecht, and O. G. Schmidt, “Magnetic vortices on closely packed spherically curved surfaces,” *Phys. Rev. B* **85**, 174429 (2012).
- <sup>90</sup>R. Streubel, V. P. Kravchuk, D. D. Sheka, D. Makarov, F. Kronast, O. G. Schmidt, and Y. Gaididei, “Equilibrium magnetic states in individual hemispherical permalloy caps,” *Appl. Phys. Lett.* **101**, 132419 (2012).
- <sup>91</sup>D. Nissen, D. Mitin, O. Klein, S. S. P. K. Arekapudi, S. Thomas, M.-Y. Im, P. Fischer, and M. Albrecht, “Magnetic coupling of vortices in a two-dimensional lattice,” *Nanotechnology* **26**, 465706 (2015).
- <sup>92</sup>R. Streubel, F. Kronast, C. F. Reiche, T. Mühl, A. U. B. Wolter, O. G. Schmidt, and D. Makarov, “Vortex circulation and polarity patterns in closely packed cap arrays,” *Appl. Phys. Lett.* **108**, 042407 (2016).
- <sup>93</sup>R. Streubel, L. Han, M.-Y. Im, F. Kronast, U. K. Röbber, F. Radu, R. Abrudan, G. Lin, O. G. Schmidt, P. Fischer, and D. Makarov, “Manipulating topological states by imprinting non-collinear spin textures,” *Sci. Rep.* **5**, 8787 (2015).
- <sup>94</sup>L. Baraban, D. Makarov, M. Albrecht, N. Rivier, P. Leiderer, and A. Erbe, “Frustration-induced magic number clusters of colloidal magnetic particles,” *Phys. Rev. E* **77**, 031407 (2008).
- <sup>95</sup>A. Tsyrenova, K. Miller, J. Yan, E. Olson, S. M. Anthony, and S. Jiang, “Surfactant-mediated assembly of amphiphilic janus spheres,” *Langmuir* **35**, 6106–6111 (2019).
- <sup>96</sup>J. Yan, M. Bloom, S. C. Bae, E. Luijten, and S. Granick, “Linking synchronization to self-assembly using magnetic janus colloids,” *Nature* **491**, 578–581 (2012).
- <sup>97</sup>T. W. Long, U. M. Córdova-Figueroa, and I. Kretzschmar, “Measuring, modeling, and predicting the magnetic assembly rate of 2d-staggered janus particle chains,” *Langmuir* **35**, 8121–8130 (2019).
- <sup>98</sup>F. Deifenbeck, H. Löwen, and E. C. Oğuz, “Ground state of dipolar hard spheres confined in channels,” *Phys. Rev. E* **97**, 052608 (2018).
- <sup>99</sup>J. G. Donaldson, P. Linse, and S. S. Kantorovich, “How cube-like must magnetic nanoparticles be to modify their self-assembly?” *Nanoscale* **9**, 6448–6462 (2017).
- <sup>100</sup>J. Hernández-Rojas and F. Calvo, “Temperature- and field-induced structural transitions in magnetic colloidal clusters,” *Phys. Rev. E* **97**, 022601 (2018).
- <sup>101</sup>Q. Xie and J. Harting, “Controllable capillary assembly of magnetic ellipsoidal janus particles into tunable rings, chains and hexagonal lattices,” *Adv. Mater.* **33**, 2006390 (2021).
- <sup>102</sup>D. Morphew and D. Chakrabarti, “Programming hierarchical self-assembly of colloids: matching stability and accessibility,” *Nanoscale* **10**, 13875–13882 (2018).
- <sup>103</sup>N. L. Schryer and L. R. Walker, “The motion of  $180^\circ$  domain walls in uniform dc magnetic fields,” *J. Appl. Phys.* **45**,



- 5406–5421 (1974).
- <sup>104</sup>M. Yan, A. Kákay, S. Gliga, and R. Hertel, “Beating the walker limit with massless domain walls in cylindrical nanowires,” *Phys. Rev. Lett.* **104**, 057201 (2010).
- <sup>105</sup>S. Woo, K. M. Song, X. Zhang, Y. Zhou, M. Ezawa, X. Liu, S. Finizio, J. Raabe, N. J. Lee, S.-I. Kim, S.-Y. Park, Y. Kim, J.-Y. Kim, D. Lee, O. Lee, J. W. Choi, B.-C. Min, H. C. Koo, and J. Chang, “Current-driven dynamics and inhibition of the skyrmion hall effect of ferrimagnetic skyrmions in GdFeCo films,” *Nat. Commun.* **9**, 959 (2018).
- <sup>106</sup>L. Caretta, M. Mann, F. Büttner, K. Ueda, B. Pfau, C. M. Günther, P. Hession, A. Churikova, C. Klose, M. Schneider, D. Engel, C. Marcus, D. Bono, K. Bagschik, S. Eisebitt, and G. S. D. Beach, “Fast current-driven domain walls and small skyrmions in a compensated ferrimagnet,” *Nat. Nanotech.* **13**, 1154 (2018).
- <sup>107</sup>N. Biziere, C. Gatel, R. Lassalle-Balier, M. C. Clochard, J. E. Wegrowe, and E. Snoeck, “Imaging the fine structure of a magnetic domain wall in a Ni nanocylinder,” *Nano Lett.* **13**, 2053–2057 (2013).
- <sup>108</sup>S. Da Col, S. Jamet, N. Rougemaille, A. Locatelli, T. O. Mentès, B. S. Burgos, R. Afid, M. Darques, L. Cagnon, J. C. Toussaint, and O. Fruchart, “Observation of bloch-point domain walls in cylindrical magnetic nanowires,” *Phys. Rev. B* **89**, 180405 (2014).
- <sup>109</sup>M. Charilaou, H.-B. Braun, and J. F. Löffler, “Monopole-induced emergent electric fields in ferromagnetic nanowires,” *Phys. Rev. Lett.* **121**, 097202 (2018).
- <sup>110</sup>A. Wartelle, B. Trapp, M. Staño, C. Thirion, S. Bochmann, J. Bachmann, M. Foerster, L. Aballe, T. O. Mentès, A. Locatelli, A. Sala, L. Cagnon, J.-C. Toussaint, and O. Fruchart, “Bloch-point-mediated topological transformations of magnetic domain walls in cylindrical nanowires,” *Phys. Rev. B* **99**, 024433 (2019).
- <sup>111</sup>M. Charilaou and J. F. Löffler, “Skyrmion oscillations in magnetic nanorods with chiral interactions,” *Phys. Rev. B* **95**, 024409 (2017).
- <sup>112</sup>M. Poggio, “Determining magnetization configurations and reversal of individual magnetic nanotubes,” in *Magnetic Nano- and Microwires*, Woodhead Publishing Series in Electronic and Optical Materials, edited by M. Vazquez (Woodhead Publishing, 2020) second edition ed., Chap. 17, p. 491.
- <sup>113</sup>A. Scholl, H. Ohldag, F. Nolting, J. Stöhr, and H. A. Padmore, “X-ray photoemission electron microscopy, a tool for the investigation of complex magnetic structures (invited),” *Rev. Sci. Instrum.* **73**, 1362–1366 (2002).
- <sup>114</sup>R. Streubel, L. Han, F. Kronast, A. A. Ünal, O. G. Schmidt, and D. Makarov, “Imaging of buried 3d magnetic rolled-up nanomembranes,” *Nano Lett.* **14**, 3981–3986 (2014).
- <sup>115</sup>S. Ruiz-Gómez, M. Foerster, L. Aballe, M. P. Proenca, I. Lucas, J. Prieto, A. Mascaraque, J. de la Figuera, A. Quesada, and L. Pérez, “Observation of a topologically protected state in a magnetic domain wall stabilized by a ferromagnetic chemical barrier,” *Sci. Rep.* **8**, 16695 (2018).
- <sup>116</sup>A. Wartelle, J. Pablo-Navarro, M. Staño, S. Bochmann, S. Pairis, M. Rioult, C. Thirion, R. Belkhou, J. de Teresa, C. Magén, and O. Fruchart, “Transmission XMCD-PEEM imaging of an engineered vertical FEBID cobalt nanowire with a domain wall,” *Nanotechnology* **29**, 045704 (2017).
- <sup>117</sup>Y. P. Ivanov, A. Chuvilin, S. Lopatin, and J. Kosel, “Modulated magnetic nanowires for controlling domain wall motion: Toward 3d magnetic memories,” *ACS Nano* **10**, 5326–5332 (2016).
- <sup>118</sup>G. L. Drisko, C. Gatel, P.-F. Fazzini, A. Ibarra, S. Mourdikoudis, V. Bley, K. Fajerwerg, P. Fau, and M. Kahn, “Air-stable anisotropic monocrystalline nickel nanowires characterized using electron holography,” *Nano Letters* **18**, 1733–1738 (2018).
- <sup>119</sup>I. M. Andersen, L. A. Rodríguez, C. Bran, C. Marcelot, S. Joulie, T. Hungria, M. Vazquez, C. Gatel, and E. Snoeck, “Exotic transverse-vortex magnetic configurations in conical nanowires,” *ACS Nano* **14**, 1399–1405 (2020).
- <sup>120</sup>D. Reyes, N. Biziere, B. Warot-Fonrose, T. Wade, and C. Gatel, “Magnetic configurations in co/cu multilayered nanowires: Evidence of structural and magnetic interplay,” *Nano Letters* **16**, 1230–1236 (2016).
- <sup>121</sup>C. Bran, E. Berganza, J. A. Fernandez-Roldan, E. M. Palmero, J. Meier, E. Calle, M. Jaafar, M. Foerster, L. Aballe, A. Fraile Rodríguez, R. P. del Real, A. Asenjo, O. Chubykalo-Fesenko, and M. Vazquez, “Magnetization ratchet in cylindrical nanowires,” *ACS Nano* **12**, 5932–5939 (2018).
- <sup>122</sup>D. Wolf, N. Biziere, S. Sturm, D. Reyes, T. Wade, T. Niermann, J. Krehl, B. Warot-Fonrose, B. Büchner, E. Snoeck, C. Gatel, and A. Lubk, “Holographic vector field electron tomography of three-dimensional nanomagnets,” *Commun. Phys.* **2**, 87 (2019).
- <sup>123</sup>M. Schöbitz, A. De Riz, S. Martin, S. Bochmann, C. Thirion, J. Vogel, M. Foerster, L. Aballe, T. O. Mentès, A. Locatelli, F. Genuzio, S. Le-Denmat, L. Cagnon, J. C. Toussaint, D. Gusakova, J. Bachmann, and O. Fruchart, “Fast domain wall motion governed by topology and cersted fields in cylindrical magnetic nanowires,” *Phys. Rev. Lett.* **123**, 217201 (2019).
- <sup>124</sup>M. Yan, C. Andreas, A. Kákay, F. García-Sánchez, and R. Hertel, “Fast domain wall dynamics in magnetic nanotubes: Suppression of walker breakdown and cherenkov-like spin wave emission,” *Appl. Phys. Lett.* **99**, 122505 (2011).
- <sup>125</sup>M. Yan, C. Andreas, A. Kákay, F. García-Sánchez, and R. Hertel, “Chiral symmetry breaking and pair-creation mediated walker breakdown in magnetic nanotubes,” *Appl. Phys. Lett.* **100**, 252401 (2012).
- <sup>126</sup>M. Yan, A. Kákay, C. Andreas, and R. Hertel, “Spin-cherenkov effect and magnonic mach cones,” *Phys. Rev. B* **88**, 220412 (2013).
- <sup>127</sup>J. A. Otálora, M. Yan, H. Schultheiss, R. Hertel, and A. Kákay, “Curvature-induced asymmetric spin-wave dispersion,” *Phys. Rev. Lett.* **117**, 227203 (2016).
- <sup>128</sup>J. A. Otálora, M. Yan, H. Schultheiss, R. Hertel, and A. Kákay, “Asymmetric spin-wave dispersion in ferromagnetic nanotubes induced by surface curvature,” *Phys. Rev. B* **95**, 184415 (2017).
- <sup>129</sup>J. Yang, J. Kim, B. Kim, Y.-J. Cho, J.-H. Lee, and S.-K. Kim, “Vortex-chirality-dependent standing spin-wave modes in soft magnetic nanotubes,” *J. Appl. Phys.* **123**, 033901 (2018).
- <sup>130</sup>H. D. Salinas, J. Restrepo, and Ö. Iglesias, “Change in the magnetic configurations of tubular nanostructures by tuning dipolar interactions,” *Sci. Rep.* **8**, 10275 (2018).
- <sup>131</sup>M. Küß, M. Heigl, L. Flacke, A. Hörner, M. Weiler, M. Albrecht, and A. Wixforth, “Nonreciprocal dzyaloshinskii-moriya magnetoacoustic waves,” *Phys. Rev. Lett.* **125**, 217203 (2020).
- <sup>132</sup>E. Albisetti, S. Tacchi, R. Silvani, G. Scaramuzzi, S. Finizio, S. Wintz, C. Rinaldi, M. Cantoni, J. Raabe, G. Carlotti, R. Bertacco, E. Riedo, and D. Petti, “Optically inspired nanomagnetics with nonreciprocal spin waves in synthetic antiferromagnets,” *Adv. Mater.* **32**, 1906439 (2020).
- <sup>133</sup>O. A. Tretiakov, M. Morini, S. Vasylyevych, and V. Slastikov, “Engineering curvature-induced anisotropy in thin ferromagnetic films,” *Phys. Rev. Lett.* **119**, 077203 (2017).
- <sup>134</sup>V. L. Carvalho-Santos, F. A. Apolonio, and N. M. Oliveira-Neto, “On geometry-dependent vortex stability and topological spin excitations on curved surfaces with cylindrical symmetry,” *Phys. Lett. A* **377**, 1308–1316 (2013).
- <sup>135</sup>K. V. Yershov, V. P. Kravchuk, D. D. Sheka, J. van den Brink, and Y. Gaididei, “Spontaneous deformation of flexible ferromagnetic ribbons induced by dzyaloshinskii-moriya interaction,” *Phys. Rev. B* **100**, 140407 (2019).
- <sup>136</sup>O. V. Pylypovskiy, V. P. Kravchuk, D. D. Sheka, D. Makarov, O. G. Schmidt, and Y. Gaididei, “Coupling of chiralities in spin and physical spaces: The möbius ring as a case study,” *Phys. Rev. Lett.* **114**, 197204 (2015).
- <sup>137</sup>A. W. Teixeira, S. Castillo-Sepúlveda, S. Vojkovic, J. M. Fonseca, D. Altbir, Á. S. Núñez, and V. L. Carvalho-Santos, “Analysis on the stability of in-surface magnetic configurations in toroidal nanoshells,” *J. Magn. Magn. Mater.* **478**, 253–259 (2019).

- <sup>138</sup>D. Mancilla-Almonacid, M. Castro, J. Fonseca, D. Altbir, S. Alende, and V. Carvalho-Santos, "Magnetic ground states for bent nanotubes," *J. Magn. Magn. Mater.* **507**, 166754 (2020).
- <sup>139</sup>R. Moreno, V. L. Carvalho-Santos, A. P. Espejo, D. Laroze, O. Chubykalo-Fesenko, and D. Altbir, "Oscillatory behavior of the domain wall dynamics in a curved cylindrical magnetic nanowire," *Phys. Rev. B* **96**, 184401 (2017).
- <sup>140</sup>R. Cacilhas, C. I. L. de Araujo, V. L. Carvalho-Santos, R. Moreno, O. Chubykalo-Fesenko, and D. Altbir, "Controlling domain wall oscillations in bent cylindrical magnetic wires," *Phys. Rev. B* **101**, 184418 (2020).
- <sup>141</sup>O. M. Volkov, D. D. Sheka, Y. Gaididei, V. P. Kravchuk, U. K. Röbler, J. Fassbender, and D. Makarov, "Mesoscale dzyaloshinskii-moriya interaction: geometrical tailoring of the magnetochirality," *Sci. Rep.* **8**, 866 (2018).
- <sup>142</sup>O. V. Pylypovskiy, D. Y. Kononenko, K. V. Yershov, U. K. Röbler, A. V. Tomilo, J. Fassbender, J. van den Brink, D. Makarov, and D. D. Sheka, "Curvilinear one-dimensional antiferromagnets," *Nano Lett.* **20**, 8157–8162 (2020).
- <sup>143</sup>V. Slastikov, "Micromagnetism of thin shells," *Math. Mod. Meth. Appl. Sci.* **15**, 1469–1487 (2005).
- <sup>144</sup>V. P. Kravchuk, D. D. Sheka, R. Streubel, D. Makarov, O. G. Schmidt, and Y. Gaididei, "Out-of-surface vortices in spherical shells," *Phys. Rev. B* **85**, 144433 (2012).
- <sup>145</sup>V. P. Kravchuk, U. K. Röbler, O. M. Volkov, D. D. Sheka, J. van den Brink, D. Makarov, H. Fuchs, H. Fangohr, and Y. Gaididei, "Topologically stable magnetization states on a spherical shell: Curvature-stabilized skyrmions," *Phys. Rev. B* **94**, 144402 (2016).
- <sup>146</sup>G. Di Fratta, "Micromagnetics of curved thin films," *Z. Angew. Math. Phys.* **71**, 111 (2020).
- <sup>147</sup>Y. Gaididei, K. V. Yershov, D. D. Sheka, V. P. Kravchuk, and A. Saxena, "Magnetization-induced shape transformations in flexible ferromagnetic rings," *Phys. Rev. B* **99**, 014404 (2019).
- <sup>148</sup>R. Streubel, F. Kronast, U. K. Röbler, O. G. Schmidt, and D. Makarov, "Reconfigurable large-area magnetic vortex circulation patterns," *Phys. Rev. B* **92**, 104431 (2015).
- <sup>149</sup>N. Puwenberg, C. F. Reiche, R. Streubel, M. Khan, D. Mukherjee, I. V. Soldatov, M. Melzer, O. G. Schmidt, B. Büchner, and T. Mühl, "Magnetization reversal and local switching fields of ferromagnetic co/pd microtubes with radial magnetization," *Phys. Rev. B* **99**, 094438 (2019).
- <sup>150</sup>D. P. Weber, D. Ruffer, A. Buchter, F. Xue, E. Russo-Averchi, R. Huber, P. Berberich, J. Arbiol, A. Fontcuberta i Morral, D. Grundler, and M. Poggio, "Cantilever magnetometry of individual Ni nanotubes," *Nano Lett.* **12**, 6139–6144 (2012).
- <sup>151</sup>A. Buchter, J. Nagel, D. Ruffer, F. Xue, D. P. Weber, O. F. Kieler, T. Weimann, J. Kohlmann, A. B. Zorin, E. Russo-Averchi, R. Huber, P. Berberich, A. Fontcuberta i Morral, M. Kemmler, R. Kleiner, D. Koelle, D. Grundler, and M. Poggio, "Reversal mechanism of an individual Ni nanotube simultaneously studied by torque and squid magnetometry," *Phys. Rev. Lett.* **111**, 067202 (2013).
- <sup>152</sup>R. Streubel, J. Lee, D. Makarov, M.-Y. Im, D. Karnaushenko, L. Han, R. Schäfer, P. Fischer, S.-K. Kim, and O. G. Schmidt, "Magnetic microstructure of rolled-up single-layer ferromagnetic nanomembranes," *Adv. Mater.* **26**, 316–323 (2014).
- <sup>153</sup>D. Karnaushenko, D. D. Karnaushenko, D. Makarov, S. Bau-nack, R. Schäfer, and O. G. Schmidt, "Self-assembled on-chip-integrated giant magneto-impedance sensorics," *Adv. Mater.* **27**, 6582 (2015).
- <sup>154</sup>K. S. Das, D. Makarov, P. Gentile, M. Cuoco, B. J. van Wees, C. Ortix, and I. J. Vera-Marun, "Independent geometrical control of spin and charge resistances in curved spintronics," *Nano Lett.* **19**, 6839 (2019).
- <sup>155</sup>S.-Z. Lin, C. Reichhardt, C. D. Batista, and A. Saxena, "Particle model for skyrmions in metallic chiral magnets: Dynamics, pinning, and creep," *Phys. Rev. B* **87**, 214419 (2013).
- <sup>156</sup>S. Mühlbauer, B. Binz, F. Jonietz, C. Pfleiderer, A. Rosch, A. Neubauer, R. Georgii, and P. Böni, "Skyrmion lattice in a chiral magnet," *Science* **323**, 915–919 (2009).
- <sup>157</sup>X. Z. Yu, Y. Onose, N. Kanazawa, J. H. Park, J. H. Han, Y. Matsui, N. Nagaosa, and Y. Tokura, "Real-space observation of a two-dimensional skyrmion crystal," *Nature* **465**, 901–904 (2010).
- <sup>158</sup>S. Heinze, K. von Bergmann, M. Menzel, J. Brede, A. Kubetzka, R. Wiesendanger, G. Bihlmayer, and S. Blugel, "Spontaneous atomic-scale magnetic skyrmion lattice in two dimensions," *Nat. Phys.* **7**, 713–718 (2011).
- <sup>159</sup>F. Jonietz, S. Mühlbauer, C. Pfleiderer, A. Neubauer, W. Münzer, A. Bauer, T. Adams, R. Georgii, P. Böni, R. A. Duine, K. Everschor, M. Garst, and A. Rosch, "Spin transfer torques in mnsi at ultralow current densities," *Science* **330**, 1648–1651 (2010).
- <sup>160</sup>N. Romming, C. Hanneken, M. Menzel, J. E. Bickel, B. Wolter, K. von Bergmann, A. Kubetzka, and R. Wiesendanger, "Writing and deleting single magnetic skyrmions," *Science* **341**, 636–639 (2013).
- <sup>161</sup>W. Jiang, P. Upadhyaya, W. Zhang, G. Yu, M. B. Jungfleisch, F. Y. Fradin, J. E. Pearson, Y. Tserkovnyak, K. L. Wang, O. Heinonen, S. G. E. te Velthuis, and A. Hoffmann, "Blowing magnetic skyrmion bubbles," *Science* **349**, 283–286 (2015).
- <sup>162</sup>D. Maccariello, W. Legrand, N. Reyren, K. Garcia, K. Bouze-houane, S. Collin, V. Cros, and A. Fert, "Electrical detection of single magnetic skyrmions in metallic multilayers at room temperature," *Nat. Nanotech.* **13**, 233–237 (2018).
- <sup>163</sup>K. Zeissler, S. Finizio, K. Shahbazi, J. Massey, F. A. Ma'Mari, D. M. Bracher, A. Kleibert, M. C. Rosamond, E. H. Linfield, T. A. Moore, J. Raabe, G. Burnell, and C. H. Marrows, "Discrete hall resistivity contribution from néel skyrmions in multilayer nanodiscs," *Nat. Nanotech.* **13**, 1161–1166 (2018).
- <sup>164</sup>W. Jiang, X. Zhang, G. Yu, W. Zhang, X. Wang, M. Benjamin Jungfleisch, J. E. Pearson, X. Cheng, O. Heinonen, K. L. Wang, Y. Zhou, A. Hoffmann, and S. G. E. te Velthuis, "Direct observation of the skyrmion hall effect," *Nat. Phys.* **13**, 162–169 (2017).
- <sup>165</sup>Z. Wang, M. Guo, H.-A. Zhou, L. Zhao, T. Xu, R. Tomasello, H. Bai, Y. Dong, S.-G. Je, W. Chao, H.-S. Han, S. Lee, K.-S. Lee, Y. Yao, W. Han, C. Song, H. Wu, M. Carpentieri, G. Finocchio, M.-Y. Im, S.-Z. Lin, and W. Jiang, "Thermal generation, manipulation and thermoelectric detection of skyrmions," *Nat. Electron.* **3**, 672–679 (2020).
- <sup>166</sup>A. Fernández Scarioni, C. Barton, H. Corte-León, S. Sievers, X. Hu, F. Ajejas, W. Legrand, N. Reyren, V. Cros, O. Kazakova, and H. W. Schumacher, "Thermoelectric signature of individual skyrmions," *Phys. Rev. Lett.* **126**, 077202 (2021).
- <sup>167</sup>C. Moreau-Luchaire, C. Moutafis, N. Reyren, J. Sampaio, C. A. F. Vaz, N. Van Horne, K. Bouzehouane, K. Garcia, C. Deranlot, P. Warnicke, P. Wöhlhüter, J.-M. George, M. Weigand, J. Raabe, V. Cros, and A. Fert, "Additive interfacial chiral interaction in multilayers for stabilization of small individual skyrmions at room temperature," *Nat. Nanotech.* **11**, 444–448 (2016).
- <sup>168</sup>S. Woo, K. M. Song, X. Zhang, M. Ezawa, Y. Zhou, X. Liu, M. Weigand, S. Finizio, J. Raabe, M.-C. Park, K.-Y. Lee, J. W. Choi, B.-C. Min, H. C. Koo, and J. Chang, "Deterministic creation and deletion of a single magnetic skyrmion observed by direct time-resolved x-ray microscopy," *Nat. Electron.* **1**, 288–296 (2018).
- <sup>169</sup>I. Lemesch, K. Litzius, M. Böttcher, P. Bassirian, N. Kerber, D. Heinze, J. Zázvorka, F. Büttner, L. Caretta, M. Mann, M. Weigand, S. Finizio, J. Raabe, M.-Y. Im, H. Stoll, G. Schütz, B. Dupé, M. Kläui, and G. S. D. Beach, "Current-induced skyrmion generation through morphological thermal transitions in chiral ferromagnetic heterostructures," *Adv. Mater.* **30**, 1805461 (2018).
- <sup>170</sup>J. Matsuno, N. Ogawa, K. Yasuda, F. Kagawa, W. Koshibae, N. Nagaosa, Y. Tokura, and M. Kawasaki, "Interface-driven topological hall effect in srro3-srro3 bilayer," *Sci. Adv.* **2**, e1600304 (2016).

- <sup>171</sup>L. Wang, Q. Feng, Y. Kim, R. Kim, K. H. Lee, S. D. Pollard, Y. J. Shin, H. Zhou, W. Peng, D. Lee, W. Meng, H. Yang, J. H. Han, M. Kim, Q. Lu, and T. W. Noh, "Ferroelectrically tunable magnetic skyrmions in ultrathin oxide heterostructures," *Nat. Mater.* **17**, 1087 (2018).
- <sup>172</sup>E. Y. Tsymlal and C. Panagopoulos, "Whirling spins with a ferroelectric," *Nat. Mater.* **17**, 1054–1055 (2018).
- <sup>173</sup>N. Kanazawa, K. Shibata, and Y. Tokura, "Variation of spin-orbit coupling and related properties in skyrmionic system  $Mn_{1-x}Fe_xGe$ ," *New J. Phys.* **18**, 045006 (2016).
- <sup>174</sup>C. S. Spencer, J. Gayles, N. A. Porter, S. Sugimoto, Z. Aslam, C. J. Kinane, T. R. Charlton, F. Freimuth, S. Chadov, S. Langridge, J. Sinova, C. Felser, S. Blügel, Y. Mokrousov, and C. H. Marrows, "Helical magnetic structure and the anomalous and topological hall effects in epitaxial  $b20 Fe_{1-y}Co_yGe$  films," *Phys. Rev. B* **97**, 214406 (2018).
- <sup>175</sup>J. Gayles, F. Freimuth, T. Schena, G. Lani, P. Mavropoulos, R. A. Duine, S. Blügel, J. Sinova, and Y. Mokrousov, "Dzyaloshinskii-moriya interaction and hall effects in the skyrmion phase of  $Mn_{1-x}Fe_xGe$ ," *Phys. Rev. Lett.* **115**, 036602 (2015).
- <sup>176</sup>K. Shibata, X. Z. Yu, T. Hara, D. Morikawa, N. Kanazawa, K. Kimoto, S. Ishiwata, Y. Matsui, and Y. Tokura, "Towards control of the size and helicity of skyrmions in helimagnetic alloys by spin-orbit coupling," *Nat. Nanotech.* **8**, 723 (2013).
- <sup>177</sup>A. Ullah, B. Balamurugan, W. Zhang, S.-X. Valloppilly, Li, R. Pahari, L.-P. Yue, A. Sokolov, D. Sellmyer, and R. Skomski, "Crystal structure and dzyaloshinski-moriya micromagnetics," *IEEE Trans. Magn.* **55**, 1–5 (2019).
- <sup>178</sup>E. Mendive-Tapia, M. dos Santos Dias, S. Grytsiuk, J. B. Staunton, S. Blügel, and S. Lounis, "Short period magnetization texture of B20-MnGe explained by thermally fluctuating local moments," *Phys. Rev. B* **103**, 024410 (2021).
- <sup>179</sup>T. Tanigaki, K. Shibata, N. Kanazawa, X. Yu, Y. Onose, H. S. Park, D. Shindo, and Y. Tokura, "Real-space observation of short-period cubic lattice of skyrmions in mnge," *Nano Lett.* **15**, 5438–5442 (2015).
- <sup>180</sup>N. Kanazawa, Y. Nii, X. X. Zhang, A. S. Mishchenko, G. De Filippis, F. Kagawa, Y. Iwasa, N. Nagaosa, and Y. Tokura, "Critical phenomena of emergent magnetic monopoles in a chiral magnet," *Nat. Commun.* **7**, 11622 (2016).
- <sup>181</sup>N. Kanazawa, A. Kitaori, J. S. White, V. Ukleev, H. M. Rønnow, A. Tsukazaki, M. Ichikawa, M. Kawasaki, and Y. Tokura, "Direct observation of the statics and dynamics of emergent magnetic monopoles in a chiral magnet," *Phys. Rev. Lett.* **125**, 137202 (2020).
- <sup>182</sup>C. T. Ma, Y. Xie, H. Sheng, A. W. Ghosh, and S. J. Poon, "Robust formation of ultrasmall room-temperature neél skyrmions in amorphous ferrimagnets from atomistic simulations," *Sci. Rep.* **9**, 9964 (2019).
- <sup>183</sup>R. Streubel, C. Lambert, N. Kent, P. Ercius, A. T. N'Diaye, C. Ophus, S. Salahuddin, and P. Fischer, "Experimental evidence of chiral ferrimagnetism in amorphous GdCo films," *Adv. Mater.* **30**, 1800199 (2018).
- <sup>184</sup>C. Kim, S. Lee, H.-G. Kim, J.-H. Park, K.-W. Moon, J. Y. Park, J. M. Yuk, K.-J. Lee, B.-G. Park, S. K. Kim, K.-J. Kim, and C. Hwang, "Distinct handedness of spin wave across the compensation temperatures of ferrimagnets," *Nat. Mater.* **19**, 980–985 (2020).
- <sup>185</sup>P. W. Anderson, "Absence of diffusion in certain random lattices," *Phys. Rev.* **109**, 1492 (1958).
- <sup>186</sup>E. Abrahams, P. W. Anderson, D. C. Licciardello, and T. V. Ramakrishnan, "Scaling theory of localization: Absence of quantum diffusion in two dimensions," *Phys. Rev. Lett.* **42**, 673–676 (1979).
- <sup>187</sup>V. I. Anisimov, R. Hlubina, M. A. Korotin, V. V. Mazurenko, T. M. Rice, A. O. Shorikov, and M. Sigrist, "First-order transition between a small gap semiconductor and a ferromagnetic metal in the isoelectronic alloy  $FeSi_{1-x}Ge_x$ ," *Phys. Rev. Lett.* **89**, 257203 (2002).
- <sup>188</sup>D. S. Bouma, Z. Chen, B. Zhang, F. Bruni, M. E. Flatté, A. Ceballos, R. Streubel, L.-W. Wang, R. Q. Wu, and F. Hellman, "Itinerant ferromagnetism and intrinsic anomalous hall effect in amorphous iron-germanium," *Phys. Rev. B* **101**, 014402 (2020).
- <sup>189</sup>H. Daver and O. Massenet, "Short range order in amorphous FeGe alloys," *Solid State Commun.* **23**, 393 (1977).
- <sup>190</sup>H. S. Randhawa, L. K. Malhotra, H. K. Sehgal, and K. L. Chopra, "Structural transformations in a-Ge alloy films," *phys. status solidi a* **37**, 313–320 (1976).
- <sup>191</sup>C. Reichhardt and C. Olson Reichhardt, "Noise fluctuations and drive dependence of the skyrmion hall effect in disordered systems," *New J. Phys.* **18**, 095005 (2016).
- <sup>192</sup>W. Koshibae and N. Nagaosa, "Theory of current-driven skyrmions in disordered magnets," *Sci. Rep.* **8**, 6328 (2018).
- <sup>193</sup>C. Reichhardt and C. Olson Reichhardt, "Nonlinear transport, dynamic ordering, and clustering for driven skyrmions on random pinning," *Phys. Rev. B* **99**, 104418 (2019).
- <sup>194</sup>C. Reichhardt and C. J. Olson Reichhardt, "Shear banding, intermittency, jamming, and dynamic phases for skyrmions in inhomogeneous pinning arrays," *Phys. Rev. B* **101**, 054423 (2020).
- <sup>195</sup>L. Xiong, B. Zheng, M. Jin, and N. Zhou, "Anisotropic critical behavior of current-driven skyrmion dynamics in chiral magnets with disorder," *New J. Phys.* **22**, 033043 (2020).
- <sup>196</sup>R. Voinescu, J.-S. B. Tai, and I. I. Smalyukh, "Hopf solitons in helical and conical backgrounds of chiral magnetic solids," *Phys. Rev. Lett.* **125**, 057201 (2020).
- <sup>197</sup>X. Yu, Y. Tokunaga, Y. Taguchi, and Y. Tokura, "Variation of topology in magnetic bubbles in a colossal magnetoresistive manganite," *Adv. Mater.* **29**, 1603958 (2017).
- <sup>198</sup>N. Kent, N. Reynolds, D. Raftrey, I. T. G. Campbell, S. Viraawmy, S. Dhuey, R. V. Chopdekar, A. Hierro-Rodriguez, A. Sorrentino, E. Pereiro, S. Ferrer, F. Hellman, P. Sutcliffe, and P. Fischer, "Creation and observation of hopfions in magnetic multilayer systems," *Nat. Commun.* **12**, 1562 (2021).
- <sup>199</sup>X. Z. Yu, Y. Tokunaga, Y. Kaneko, W. Z. Zhang, K. Kimoto, Y. Matsui, Y. Taguchi, and Y. Tokura, "Biskyrmion states and their current-driven motion in a layered manganite," *Nat. Commun.* **5**, 3198 (2014).
- <sup>200</sup>J. C. T. Lee, J. J. Chess, S. A. Montoya, X. Shi, N. Tamura, S. K. Mishra, P. Fischer, B. J. McMorrin, S. K. Sinha, E. E. Fullerton, S. D. Kevan, and S. Roy, "Synthesizing skyrmion bound pairs in fe-gd thin films," *Appl. Phys. Lett.* **109**, 022402 (2016).
- <sup>201</sup>R. Takagi, X. Z. Yu, J. S. White, K. Shibata, Y. Kaneko, G. Tatara, H. M. Rønnow, Y. Tokura, and S. Seki, "Low-field bi-skyrmion formation in a noncentrosymmetric chimney ladder ferromagnet," *Phys. Rev. Lett.* **120**, 037203 (2018).
- <sup>202</sup>X. Zhang, Y. Zhou, and M. Ezawa, "Magnetic bilayer-skyrmions without skyrmion hall effect," *Nat. Commun.* **7**, 10293 (2016).
- <sup>203</sup>A. K. Nayak, V. Kumar, T. Ma, P. Werner, E. Pippel, R. Sahoo, F. Damay, U. K. Röbber, C. Felser, and S. S. P. Parkin, "Magnetic antiskyrmions above room temperature in tetragonal heusler materials," *Nature* **548**, 561 (2017).
- <sup>204</sup>J. Jena, R. Stinshoff, R. Saha, A. K. Srivastava, T. Ma, H. Deniz, P. Werner, C. Felser, and S. S. P. Parkin, "Observation of magnetic antiskyrmions in the low magnetization ferrimagnet  $mn_2rh_0.95ir_0.05sn$ ," *Nano Lett.* **20**, 59–65 (2020).
- <sup>205</sup>F. Zheng, H. Li, S. Wang, D. Song, C. Jin, W. Wei, A. Kovács, J. Zang, M. Tian, Y. Zhang, H. Du, and R. E. Dunin-Borkowski, "Direct imaging of a zero-field target skyrmion and its polarity switch in a chiral magnetic nanodisk," *Phys. Rev. Lett.* **119**, 197205 (2017).
- <sup>206</sup>S. Zhang, F. Kronast, G. van der Laan, and T. Hesjedal, "Real-space observation of skyrmionium in a ferromagnetic-topological insulator heterostructure," *Nano Lett.* **18**, 1057–1063 (2018).
- <sup>207</sup>B. Göbel, A. F. Schäffer, J. Berakdar, I. Mertig, and S. S. P. Parkin, "Electrical writing, deleting, reading, and moving of magnetic skyrmioniums in a racetrack device," *Sci. Rep.* **9**, 12119 (2019).

- <sup>208</sup>S. K. Panigrahy, C. Singh, and A. K. Nayak, “Current-induced nucleation, manipulation, and reversible switching of anti-skyrmioniums,” *Appl. Phys. Lett.* **115**, 182403 (2019).
- <sup>209</sup>F. N. Rybakov and N. S. Kiselev, “Chiral magnetic skyrmions with arbitrary topological charge,” *Phys. Rev. B* **99**, 064437 (2019).
- <sup>210</sup>Z. Zeng, C. Zhang, C. Jin, J. Wang, C. Song, Y. Ma, Q. Liu, and J. Wang, “Dynamics of skyrmion bags driven by the spin-orbit torque,” *Appl. Phys. Lett.* **117**, 172404 (2020).
- <sup>211</sup>X. S. Wang, A. Qaiumzadeh, and A. Brataas, “Current-driven dynamics of magnetic hopfions,” *Phys. Rev. Lett.* **123**, 147203 (2019).
- <sup>212</sup>Y. Liu, W. Hou, X. Han, and J. Zang, “Three-dimensional dynamics of a magnetic hopfion driven by spin transfer torque,” *Phys. Rev. Lett.* **124**, 127204 (2020).
- <sup>213</sup>J. Barker and O. A. Tretiakov, “Static and dynamical properties of antiferromagnetic skyrmions in the presence of applied current and temperature,” *Phys. Rev. Lett.* **116**, 147203 (2016).
- <sup>214</sup>X. Zhang, Y. Zhou, and M. Ezawa, “Antiferromagnetic skyrmion: Stability, creation and manipulation,” *Sci. Rep.* **6**, 24795 (2016).
- <sup>215</sup>W. Legrand, D. Maccariello, F. Ajejas, S. Collin, A. Vecchiola, K. Bouzehouane, N. Reyren, V. Cros, and A. Fert, “Room-temperature stabilization of antiferromagnetic skyrmions in synthetic antiferromagnets,” *Nat. Mater.* **19**, 34–42 (2020).
- <sup>216</sup>V. P. Kravchuk, O. Gomonay, D. D. Sheka, D. R. Rodrigues, K. Everschor-Sitte, J. Sinova, J. van den Brink, and Y. Gaididei, “Spin eigenexcitations of an antiferromagnetic skyrmion,” *Phys. Rev. B* **99**, 184429 (2019).
- <sup>217</sup>H. Jani, J.-C. Lin, J. Chen, J. Harrison, F. Maccherozzi, J. Schad, S. Prakash, C.-B. Eom, A. Ariando, T. Venkatesan, and P. G. Radaelli, “Antiferromagnetic half-skyrmions and bimerons at room temperature,” *Nature* **590**, 74–79 (2021).
- <sup>218</sup>R. Juge, K. Bairagi, K. G. Rana, J. Vogel, M. Sall, D. Mailly, V. T. Pham, Q. Zhang, N. Sisodia, M. Foerster, L. Aballe, M. Belmeguenai, Y. Roussigné, S. Auffret, L. D. Buda-Prejbeanu, G. Gaudin, D. Ravelosona, and O. Boulle, “Helium ions put magnetic skyrmions on the track,” *Nano Lett.* **21**, 2989 (2021).
- <sup>219</sup>X. Wang, X. Wang, C. Wang, H. Yang, Y. Cao, and P. Yan, “Current-induced skyrmion motion on magnetic nanotubes,” *J. Phys. D: Appl. Phys.* **52**, 225001 (2019).
- <sup>220</sup>W. Kang, Y. Huang, C. Zheng, W. Lv, N. Lei, Y. Zhang, X. Zhang, Y. Zhou, and W. Zhao, “Voltage controlled magnetic skyrmion motion for racetrack memory,” *Sci. Rep.* **6**, 23164 (2016).
- <sup>221</sup>X. Wang, W. L. Gan, J. C. Martinez, F. N. Tan, M. B. A. Jalil, and W. S. Lew, “Efficient skyrmion transport mediated by a voltage controlled magnetic anisotropy gradient,” *Nanoscale* **10**, 733 (2018).
- <sup>222</sup>Y. Liu, N. Lei, C. Wang, X. Zhang, W. Kang, D. Zhu, Y. Zhou, X. Liu, Y. Zhang, and W. Zhao, “Voltage-driven high-speed skyrmion motion in a skyrmion-shift device,” *Phys. Rev. Applied* **11**, 014004 (2019).
- <sup>223</sup>H. Imamura, T. Nozaki, S. Yuasa, and Y. Suzuki, “Deterministic magnetization switching by voltage control of magnetic anisotropy and dzyaloshinskii-moriya interaction under an in-plane magnetic field,” *Phys. Rev. Applied* **10**, 054039 (2018).
- <sup>224</sup>R. Tomasello, S. Komineas, G. Siracusano, M. Carpentieri, and G. Finocchio, “Chiral skyrmions in an anisotropy gradient,” *Phys. Rev. B* **98**, 024421 (2018).
- <sup>225</sup>X. Xu, X.-L. Li, Y. G. Semenov, and K. W. Kim, “Creation and destruction of skyrmions via electrical modulation of local magnetic anisotropy in magnetic thin films,” *Phys. Rev. Applied* **11**, 024051 (2019).
- <sup>226</sup>N. Mehmood, X. Song, G. Tian, Z. Hou, D. Chen, Z. Fan, M. Qin, X. Gao, and J.-M. Liu, “Strain-mediated electric manipulation of magnetic skyrmion and other topological states in geometric confined nanodiscs,” *J. Phys. D: Appl. Phys.* **53**, 014007 (2019).
- <sup>227</sup>R. Yanes, F. Garcia-Sanchez, R. Luis, E. Martinez, V. Raposo, L. Torres, and L. Lopez-Diaz, “Skyrmion motion induced by voltage-controlled in-plane strain gradients,” *Appl. Phys. Lett.* **115**, 132401 (2019).
- <sup>228</sup>N. S. Gusev, A. V. Sadovnikov, S. A. Nikitov, M. V. Sapozhnikov, and O. G. Udalov, “Manipulation of the dzyaloshinskii-moriya interaction in Co/Pt multilayers with strain,” *Phys. Rev. Lett.* **124**, 157202 (2020).
- <sup>229</sup>V. A. Sidorov, A. E. Petrova, P. S. Berdonosov, V. A. Dolgikh, and S. M. Stishov, “Comparative study of helimagnets mnsi and  $\text{Cu}_2\text{OSeO}_3$  at high pressures,” *Phys. Rev. B* **89**, 100403 (2014).
- <sup>230</sup>I. Levatić, P. Popčević, V. Šurija, A. Kruchkov, H. Berger, A. Magrez, J. S. White, H. M. Rønnow, and I. Živković, “Dramatic pressure-driven enhancement of bulk skyrmion stability,” *Sci. Rep.* **6**, 21347 (2016).
- <sup>231</sup>S. Seki, Y. Okamura, K. Shibata, R. Takagi, N. D. Khanh, F. Kagawa, T. Arima, and Y. Tokura, “Stabilization of magnetic skyrmions by uniaxial tensile strain,” *Phys. Rev. B* **96**, 220404 (2017).
- <sup>232</sup>G. Dresselhaus, “Spin-orbit coupling effects in zinc blende structures,” *Phys. Rev.* **100**, 580–586 (1955).
- <sup>233</sup>E. Rashba, “Properties of semiconductors with an extremum loop. 1. cyclotron and combinational resonance in a magnetic field perpendicular to the plane of the loop,” *Sov. Phys. Solid State* **2**, 1109 (1960).
- <sup>234</sup>J. C. R. Sánchez, L. Vila, G. Desfonds, S. Gambarelli, J. P. Attané, J. M. De Teresa, C. Magén, and A. Fert, “Spin-to-charge conversion using Rashba coupling at the interface between non-magnetic materials,” *Nat. Commun.* **4**, 2944 (2013).
- <sup>235</sup>M. Isasa, M. C. Martínez-Velarte, E. Villamor, C. Magén, L. Morellón, J. M. De Teresa, M. R. Ibarra, G. Vignale, E. V. Chulkov, E. E. Krasovskii, L. E. Hueso, and F. Casanova, “Origin of inverse Rashba-Edelstein effect detected at the Cu/Bi interface using lateral spin valves,” *Phys. Rev. B* **93**, 014420 (2016).
- <sup>236</sup>E. Lesne, Y. Fu, S. Oyarzun, J. C. Rojas-Sánchez, D. C. Vaz, H. Naganuma, G. Sicoli, J. P. Attané, M. Jamet, E. Jacquet, J. M. George, A. Barthélémy, H. Jaffrès, A. Fert, M. Bibes, and L. Vila, “Highly efficient and tunable spin-to-charge conversion through Rashba coupling at oxide interfaces,” *Nat. Mater.* **15**, 1261 (2016).
- <sup>237</sup>Q. Song, H. Zhang, T. Su, W. Yuan, Y. Chen, W. Xing, J. Shi, J. Sun, and W. Han, “Observation of inverse edelstein effect in Rashba-split 2DEG between  $\text{SrTiO}_3$  and  $\text{LaAlO}_3$  at room temperature,” *Sci. Adv.* **3**, e1602312 (2017).
- <sup>238</sup>P. Noël, F. Trier, L. M. Vicente Arche, J. Bréhin, D. C. Vaz, V. Garcia, S. Fusil, A. Barthélémy, L. Vila, M. Bibes, and J.-P. Attané, “Non-volatile electric control of spin-charge conversion in a  $\text{SrTiO}_3$  Rashba system,” *Nature* **580**, 483 (2020).
- <sup>239</sup>T. S. Ghiasi, A. A. Kaverzin, P. J. Blah, and B. J. van Wees, “Charge-to-spin conversion by the Rashba-Edelstein effect in two-dimensional van der Waals heterostructures up to room temperature,” *Nano Lett.* **19**, 5959 (2019).
- <sup>240</sup>J. E. Moore, “The birth of topological insulators,” *Nature* **464**, 194 (2010).
- <sup>241</sup>S.-Y. Xu, M. Neupane, C. Liu, D. Zhang, A. Richardella, L. Andrew Wray, N. Alidoust, M. Leandersson, T. Balasubramanian, J. Sánchez-Barriga, O. Rader, G. Landolt, B. Slomski, J. Hugo Dil, J. Osterwalder, T.-R. Chang, H.-T. Jeng, H. Lin, A. Bansil, N. Samarth, and M. Zahid Hasan, “Hedgehog spin texture and Berry’s phase tuning in a magnetic topological insulator,” *Nat. Phys.* **8**, 616 (2012).
- <sup>242</sup>A. R. Mellnik, J. S. Lee, A. Richardella, J. L. Grab, P. J. Mintun, M. H. Fischer, A. Vaezi, A. Manchon, E. A. Kim, N. Samarth, and D. C. Ralph, “Spin-transfer torque generated by a topological insulator,” *Nature* **511**, 449 (2014).
- <sup>243</sup>H. Wang, J. Kally, J. S. Lee, T. Liu, H. Chang, D. R. Hickey, K. A. Mkhoyan, M. Wu, A. Richardella, and N. Samarth, “Surface-state-dominated spin-charge current conversion in topological-insulator-ferromagnetic-insulator het-

- erstructures,” *Phys. Rev. Lett.* **117**, 076601 (2016).
- <sup>244</sup>G. Chang, B. J. Wieder, F. Schindler, D. S. Sanchez, I. Belopolski, S.-M. Huang, B. Singh, D. Wu, T.-R. Chang, T. Neupert, S.-Y. Xu, H. Lin, and M. Z. Hasan, “Topological quantum properties of chiral crystals,” *Nat. Mater.* **17**, 978 (2018).
- <sup>245</sup>L. Tao and E. Y. Tsymbal, “Perspectives of spin-textured ferroelectrics,” *J. Phys. D: Appl. Phys.* **54**, 113001 (2021).
- <sup>246</sup>M. I. Dyakonov and V. I. Perel, “Spin relaxation of conduction electrons in noncentrosymmetric semiconductors,” *Sov. Phys. Solid State* **13**, 3023 (1972).
- <sup>247</sup>M. P. Walsler, C. Reichl, W. Wegscheider, and G. Salis, “Direct mapping of the formation of a persistent spin helix,” *Nat. Phys.* **8**, 757–762 (2012).
- <sup>248</sup>J. D. Koralek, C. P. Weber, J. Orenstein, B. A. Bernevig, S.-C. Zhang, S. Mack, and D. D. Awschalom, “Emergence of the persistent spin helix in semiconductor quantum wells,” *Nature* **458**, 610 (2009).
- <sup>249</sup>L. L. Tao and E. Y. Tsymbal, “Persistent spin texture enforced by symmetry,” *Nat. Commun.* **9**, 2763 (2018).
- <sup>250</sup>M. Donahue and D. Porter, “OOMMF user’s guide, version 1.0,” Interagency Report NISTIR , 6376 (1999).
- <sup>251</sup>A. Vansteenkiste, J. Leliaert, M. Dvornik, M. Helsen, F. Garcia-Sanchez, and B. Van Waeyenberge, “The design and verification of MuMax3,” *AIP Advances* **4**, 107133 (2014).
- <sup>252</sup>M.-A. Bisotti, D. Cortés-Ortuño, R. Pepper, W. Wang, M. Beg, T. Kluyver, and H. Fangohr, “Fidimag – a finite difference atomistic and micromagnetic simulation package,” *J. Open Res. Softw.* **6**, 22 (2018).
- <sup>253</sup>R. Evans, W. Fan, P. Chureemart, T. Ostler, M. Ellis, and R. Chantrell, “Atomistic spin model simulations of magnetic nanomaterials,” *J. Phys.: Condens. Matter* **26**, 103202 (2014).
- <sup>254</sup>G. P. Müller, M. Hoffmann, C. Dißelkamp, D. Schürhoff, S. Mavros, M. Sallermann, N. S. Kiselev, H. Jónsson, and S. Blügel, “Spirit: Multifunctional framework for atomistic spin simulations,” *Phys. Rev. B* **99**, 224414 (2019).
- <sup>255</sup>T. Fischbacher, F. Matteo, G. Bordignon, and H. Fangohr, “A systematic approach to multiphysics extensions of finite-element-based micromagnetic simulations: Nmag,” *IEEE Trans. Magn.* **43**, 2896 (2007).
- <sup>256</sup>W. Hackbusch, *Hierarchische Matrizen: Algorithmen und Analysis* (Springer, 2009).
- <sup>257</sup>S. Lepadatu, “Boris computational spintronics—high performance multi-mesh magnetic and spin transport modeling software,” *J. Appl. Phys.* **128**, 243902 (2020).
- <sup>258</sup>P. Kurz, F. Förster, L. Nordström, G. Bihlmayer, and S. Blügel, “Ab initio treatment of noncollinear magnets with the full-potential linearized augmented plane wave method,” *Phys. Rev. B* **69**, 024415 (2004).
- <sup>259</sup>G. Kresse and J. Hafner, “Ab initio molecular dynamics for liquid metals,” *Phys. Rev. B* **47**, 558 (1993).
- <sup>260</sup>P. Giannozzi, S. Baroni, N. Bonini, M. Calandra, R. Car, C. Cavazzoni, D. Ceresoli, G. L. Chiarotti, M. Cococcioni, I. Dabo, A. Dal Corso, S. de Gironcoli, S. Fabris, G. Fratesi, R. Gebauer, U. Gerstmann, C. Gougoussis, A. Kokalj, M. Lazzeri, L. Martin-Samos, N. Marzari, F. Mauri, R. Mazzarello, S. Paolini, A. Pasquarello, L. Paulatto, C. Sbraccia, S. Scandolo, G. Sclauzero, A. P. Seitsonen, A. Smogunov, P. Umari, and R. M. Wentzcovitch, “QUANTUM ESPRESSO: a modular and open-source software project for quantum simulations of materials,” *J. Phys. Condens. Matter* **21**, 395502 (2009).
- <sup>261</sup>S. Plimpton, “Fast parallel algorithms for short-range molecular dynamics,” *J. Comp. Phys.* **117**, 1 (1995).
- <sup>262</sup>J. Fernandez-Roldan, D. Chrischon, L. Dorneles, O. Chubykalo-Fesenko, M. Vazquez, and C. Bran, “Comparative study of magnetic properties of large diameter Co nanowires and nanotubes,” *Nanomaterials* **8**, 692 (2018).
- <sup>263</sup>A. Ruiz-Clavijo, O. Caballero-Calero, and M. Martín-González, “Revisiting anodic alumina templates: from fabrication to applications,” *Nanoscale* **13**, 2227–2265 (2021).
- <sup>264</sup>C. Donnelly, M. Guizar-Sicairos, V. Scagnoli, M. Holler, T. Huthwelker, A. Menzel, I. Vartiainen, E. Müller, E. Kirk, S. Gliga, J. Raabe, and L. J. Heyderman, “Element-specific x-ray phase tomography of 3d structures at the nanoscale,” *Phys. Rev. Lett.* **114**, 115501 (2015).
- <sup>265</sup>G. Seniutinas, A. Weber, C. Padeste, I. Sakellari, M. Farsari, and C. David, “Beyond 100nm resolution in 3d laser lithography – post processing solutions,” *Microelectron. Eng.* **191**, 25 (2018).
- <sup>266</sup>D. Gräfe, S. L. Walden, J. Blinco, M. Wegener, E. Blasco, and C. Barner-Kowollik, “It’s in the fine print: Erasable three-dimensional laser-printed micro- and nanostructures,” *Angew. Chem. Int. Ed.* **59**, 2 (2020).
- <sup>267</sup>M. Hunt, M. Taverne, J. Askey, A. May, A. Van Den Berg, Y.-L. Ho, J. Rarity, and S. Ladak, “Harnessing multi-photon absorption to produce three-dimensional magnetic structures at the nanoscale,” *Materials* **13**, 761 (2020).
- <sup>268</sup>J. A. Dolan, K. Korzeb, R. Dehmel, K. C. Gödel, M. Stefik, U. Wiesner, T. D. Wilkinson, J. J. Baumberg, B. D. Wilts, U. Steiner, and I. Gunkel, “Controlling self-assembly in gyroid terpolymer films by solvent vapor annealing,” *Small* **14**, 1802401 (2018).
- <sup>269</sup>J. Li, S. Sattayasamitsathit, R. Dong, W. Gao, R. Tam, X. Feng, S. Ai, and J. Wang, “Template electrosynthesis of tailored-made helical nanoswimmers,” *Nanoscale* **6**, 9415–9420 (2014).
- <sup>270</sup>B. Chen, K. Lu, and Z. Tian, “Novel patterns by focused ion beam guided anodization,” *Langmuir* **27**, 800–808 (2011).
- <sup>271</sup>A. Ruiz-Clavijo, S. Ruiz-Gomez, O. Caballero-Calero, L. Perez, and M. Martin-Gonzalez, “Tailoring magnetic anisotropy at will in 3d interconnected nanowire networks,” *Phys. Status Solidi-R* **13**, 1900263 (2019).
- <sup>272</sup>J. Llandro, D. M. Love, A. Kovács, J. Caron, K. N. Vyas, A. Kákay, R. Salikhov, K. Lenz, J. Fassbender, M. R. J. Scherer, C. Cimorra, U. Steiner, C. H. W. Barnes, R. E. Dunin-Borkowski, S. Fukami, and H. Ohno, “Visualizing magnetic structure in 3d nanoscale Ni-Fe gyroid networks,” *Nano Lett.* **20**, 3642–3650 (2020).
- <sup>273</sup>M. F. P. Wagner, A. S. Paulus, J. Brötz, W. Sigle, C. Trautmann, K.-O. Voss, F. Völklein, and M. E. Toimil-Molares, “Effects of size reduction on the electrical transport properties of 3d bi nanowire networks,” *Adv. Electron. Mater.* **7**, 2001069 (2021).
- <sup>274</sup>A. Fernández-Pacheco, L. Serrano-Ramón, J. M. Michalik, M. R. Ibarra, J. De Teresa, L. O’Brien, D. Petit, J. Lee, and R. P. Cowburn, “Three dimensional magnetic nanowires grown by focused electron-beam induced deposition,” *Sci. Rep.* **3**, 1492 (2013).
- <sup>275</sup>J. M. De Teresa and A. Fernández-Pacheco, “Present and future applications of magnetic nanostructures grown by febid,” *Appl. Phys. A* **117**, 1645–1658 (2014).
- <sup>276</sup>S. Janbaz, N. Noordzij, D. S. Widyaratih, C. W. Hagen, L. E. Fratila-Apachitei, and A. A. Zadpoor, “Origami lattices with free-form surface ornaments,” *Sci. Adv.* **3**, eaao1595 (2017).
- <sup>277</sup>R. Winkler, B. B. Lewis, J. D. Fowlkes, P. D. Rack, and H. Plank, “High-fidelity 3d-nanoprinting via focused electron beams: Growth fundamentals,” *ACS Applied Nano Materials* **1**, 1014 (2018).
- <sup>278</sup>J. D. Fowlkes, R. Winkler, B. B. Lewis, A. Fernández-Pacheco, L. Skoric, D. Sanz-Hernández, M. G. Stanford, E. Mutunga, P. D. Rack, and H. Plank, “High-fidelity 3d-nanoprinting via focused electron beams: Computer-aided design (3bid),” *ACS Appl. Nano Mater.* **1**, 1028 (2018).
- <sup>279</sup>L. Skoric, D. Sanz-Hernández, F. Meng, C. Donnelly, S. Merino-Aceituno, and A. Fernández-Pacheco, “Layer-by-layer growth of complex-shaped three-dimensional nanostructures with focused electron beams,” *Nano Lett.* **20**, 184 (2020).
- <sup>280</sup>E. Mutunga, R. Winkler, J. Sattelkow, P. D. Rack, H. Plank, and J. D. Fowlkes, “Impact of electron-beam heating during 3d nanoprinting,” *ACS Nano* **13**, 5198 (2019).
- <sup>281</sup>L. Keller, M. K. I. Al Mamoori, J. Pieper, C. Gspan, I. Stockem, C. Schröder, S. Barth, R. Winkler, H. Plank, M. Pohlitz,

- J. Müller, and M. Huth, “Direct-write of free-form building blocks for artificial magnetic 3d lattices,” *Sci. Rep.* **8**, 6160 (2018).
- <sup>282</sup>D. Oran, S. G. Rodrigues, R. Gao, S. Asano, M. A. Skylar-Scott, F. Chen, P. W. Tillberg, A. H. Marblestone, and E. S. Boyden, “3d nanofabrication by volumetric deposition and controlled shrinkage of patterned scaffolds,” *Science* **362**, 1281 (2018).
- <sup>283</sup>S. Shi and T. P. Russell, “Nanoparticle assembly at liquid–liquid interfaces: From the nanoscale to mesoscale,” *Adv. Mater.* **30**, 1800714 (2018).
- <sup>284</sup>J. Forth, X. Liu, J. Hasnain, A. Toor, K. Miszta, S. Shi, P. L. Geissler, T. Emrick, B. A. Helms, and T. P. Russell, “Reconfigurable printed liquids,” *Adv. Mater.* **30**, e1707603 (2018).
- <sup>285</sup>J. Forth, P. Y. Kim, G. Xie, X. Liu, B. A. Helms, and T. P. Russell, “Building reconfigurable devices using complex liquid–fluid interfaces,” *Adv. Mater.* **31**, 1806370 (2019).
- <sup>286</sup>X. Wu, R. Streubel, X. Liu, P. Y. Kim, Y. Chai, Q. Hu, D. Wang, P. Fischer, and T. P. Russell, “Ferromagnetic liquid droplets with adjustable magnetic properties,” *Proc. Natl. Acad. Sci. USA* **118**, e2017355118 (2021).
- <sup>287</sup>X. Liu, Y. Tian, and L. Jiang, “Manipulating dispersions of magnetic nanoparticles,” *Nano Lett.* **0**, null (0).
- <sup>288</sup>V. Y. Prinz, V. A. Seleznev, A. K. Gutakovskiy, A. V. Chehovskiy, V. V. Preobrazhenskii, M. A. Putyato, and T. A. Gavrilova, “Free-standing and overgrown InGaAs/GaAs nanotubes, nanohelices and their arrays,” *Physica E* **6**, 828–831 (2000).
- <sup>289</sup>O. G. Schmidt and K. Eberl, “Thin solid films roll up into nanotubes,” *Nature* **410**, 168 (2001).
- <sup>290</sup>C. Deneke, C. Müller, N. Y. Jin-Phillipp, and O. G. Schmidt, “Diameter scalability of rolled-up In(Ga)As/GaAs nanotubes,” *Semicond. Sci. Technol.* **17**, 1278 (2002).
- <sup>291</sup>R. Streubel, D. J. Thurmer, D. Makarov, F. Kronast, T. Kosub, V. Kravchuk, D. D. Sheka, Y. Gaididei, R. Schäfer, and O. G. Schmidt, “Magnetically capped rolled-up nanomembranes,” *Nano Lett.* **12**, 3961–3966 (2012).
- <sup>292</sup>R. Streubel, F. Kronast, P. Fischer, D. Parkinson, O. G. Schmidt, and D. Makarov, “Retrieving spin textures on curved magnetic thin films with full-field soft x-ray microscopies,” *Nat. Commun.* **6**, 7612 (2015).
- <sup>293</sup>H.-W. Huang, M. S. Sakar, A. J. Petruska, S. Pané, and B. J. Nelson, “Soft micromachines with programmable motility and morphology,” *Nat. Commun.* **7**, 12263 (2016).
- <sup>294</sup>W. Hu, G. Z. Lum, M. Mastrangeli, and M. Sitti, “Small-scale soft-bodied robot with multimodal locomotion,” *Nature* **554**, 81 (2018).
- <sup>295</sup>Y. Kim, H. Yuk, R. Zhao, S. A. Chester, and X. Zhao, “Printing ferromagnetic domains for untethered fast-transforming soft materials,” *Nature* **558**, 274 (2018).
- <sup>296</sup>J. Cui, T.-Y. Huang, Z. Luo, P. Testa, H. Gu, X.-Z. Chen, B. J. Nelson, and L. J. Heyderman, “Nanomagnetic encoding of shape-morphing micromachines,” *Nature* **575**, 164 (2019).
- <sup>297</sup>H. Song, H. Lee, J. Lee, J. K. Choe, S. Lee, J. Y. Yi, S. Park, J.-W. Yoo, M. S. Kwon, and J. Kim, “Reprogrammable ferromagnetic domains for reconfigurable soft magnetic actuators,” *Nano Lett.* **20**, 5185–5192 (2020).
- <sup>298</sup>X. Wang, G. Mao, J. Ge, M. Drack, G. S. Cañón Bermúdez, D. Wirthl, R. Illing, T. Kosub, L. Bischoff, C. Wang, J. Fassbender, M. Kaltenbrunner, and D. Makarov, “Untethered and ultrafast soft-bodied robots,” *Commun. Mater.* **1**, 67 (2020).
- <sup>299</sup>Q. Ze, X. Kuang, S. Wu, J. Wong, S. M. Montgomery, R. Zhang, J. M. Kovitz, F. Yang, H. J. Qi, and R. Zhao, “Magnetic shape memory polymers with integrated multifunctional shape manipulation,” *Adv. Mater.* **32**, 1906657 (2020).
- <sup>300</sup>L. G. Vivas, R. Yanes, D. Berkov, S. Erokhin, M. Bersweiler, D. Honecker, P. Bender, and A. Michels, “Toward understanding complex spin textures in nanoparticles by magnetic neutron scattering,” *Phys. Rev. Lett.* **125**, 117201 (2020).
- <sup>301</sup>D. Zákutná, D. Nižňanský, L. C. Barnsley, E. Babcock, Z. Salhi, A. Feoktystov, D. Honecker, and S. Disch, “Field dependence of magnetic disorder in nanoparticles,” *Phys. Rev. X* **10**, 031019 (2020).
- <sup>302</sup>R. Xu, C.-C. Chen, L. Wu, M. C. Scott, W. Theis, C. Ophus, M. Bartels, Y. Yang, H. Ramezani-Dakhel, M. R. Sawaya, H. Heinz, L. D. Marks, P. Ercius, and J. Miao, “Three-dimensional coordinates of individual atoms in materials revealed by electron tomography,” *Nat. Mater.* **14**, 1099–1103 (2015).
- <sup>303</sup>J. Miao, P. Ercius, and S. J. L. Billinge, “Atomic electron tomography: 3d structures without crystals,” *Science* **353**, aaf2157 (2016).
- <sup>304</sup>Y. Yang, C.-C. Chen, M. C. Scott, C. Ophus, R. Xu, A. Pryor, L. Wu, F. Sun, W. Theis, J. Zhou, M. Eisenbach, P. R. C. Kent, R. F. Sabirianov, H. Zeng, P. Ercius, and J. Miao, “Deciphering chemical order/disorder and material properties at the single-atom level,” *Nature* **542**, 75–79 (2017).
- <sup>305</sup>J. Zhou, Y. Yang, Y. Yang, D. S. Kim, A. Yuan, X. Tian, C. Ophus, F. Sun, A. K. Schmid, M. Nathanson, H. Heinz, Q. An, H. Zeng, P. Ercius, and J. Miao, “Observing crystal nucleation in four dimensions using atomic electron tomography,” *Nature* **570**, 500–503 (2019).
- <sup>306</sup>J. Park, H. Elmlund, P. Ercius, J. M. Yuk, D. T. Limmer, Q. Chen, K. Kim, S. H. Han, D. A. Weitz, A. Zettl, and A. P. Alivisatos, “3d structure of individual nanocrystals in solution by electron microscopy,” *Science* **349**, 290–295 (2015).
- <sup>307</sup>T.-H. Kim, H. Zhao, B. Xu, B. A. Jensen, A. H. King, M. J. Kramer, C. Nan, L. Ke, and L. Zhou, “Mechanisms of skyrmion and skyrmion crystal formation from the conical phase,” *Nano Lett.* **20**, 4731–4738 (2020).
- <sup>308</sup>Z. Ou, Z. Wang, B. Luo, E. Luijten, and Q. Chen, “Kinetic pathways of crystallization at the nanoscale,” *Nat. Mater.* **19**, 450–455 (2020).
- <sup>309</sup>C. Phatak, A. K. Petford-Long, and M. De Graef, “Three-dimensional study of the vector potential of magnetic structures,” *Phys. Rev. Lett.* **104**, 253901 (2010).
- <sup>310</sup>T. Tanigaki, Y. Takahashi, T. Shimakura, T. Akashi, R. Tsuneta, A. Sugawara, and D. Shindo, “Three-dimensional observation of magnetic vortex cores in stacked ferromagnetic discs,” *Nano Lett.* **15**, 1309–1314 (2015).
- <sup>311</sup>C. Gatel, F. J. Bonilla, A. Meffre, E. Snoeck, B. Warot-Fonrose, B. Chaudret, L.-M. Lacroix, and T. Blon, “Size-specific spin configurations in single iron nanomagnet: From flower to exotic vortices,” *Nano Lett.* **15**, 6952–6957 (2015).
- <sup>312</sup>X. Z. Yu, N. Kanazawa, Y. Onose, K. Kimoto, W. Z. Zhang, S. Ishiwata, Y. Matsui, and Y. Tokura, “Near room-temperature formation of a skyrmion crystal in thin-films of the helimagnet fege,” *Nat. Mater.* **10**, 106 (2011).
- <sup>313</sup>K. Shibata, A. Kovács, N. S. Kiselev, N. Kanazawa, R. E. Dunin-Borkowski, and Y. Tokura, “Temperature and magnetic field dependence of the internal and lattice structures of skyrmions by off-axis electron holography,” *Phys. Rev. Lett.* **118**, 087202 (2017).
- <sup>314</sup>D. Song, Z.-A. Li, J. Caron, A. Kovács, H. Tian, C. Jin, H. Du, M. Tian, J. Li, J. Zhu, and R. E. Dunin-Borkowski, “Quantification of magnetic surface and edge states in an fege nanostripe by off-axis electron holography,” *Phys. Rev. Lett.* **120**, 167204 (2018).
- <sup>315</sup>F. Zheng, F. N. Rybakov, A. B. Borisov, D. Song, S. Wang, Z.-A. Li, H. Du, N. S. Kiselev, J. Caron, A. Kovács, M. Tian, Y. Zhang, S. Blügel, and R. E. Dunin-Borkowski, “Experimental observation of chiral magnetic bobbers in b20-type fege,” *Nat. Nanotech.* **13**, 451–455 (2018).
- <sup>316</sup>M. R. Teague, “Deterministic phase retrieval: a green’s function solution,” *J. Opt. Soc. Am.* **73**, 1434 (1983).
- <sup>317</sup>R. W. Gerchberg and W. O. Saxton, “A practical algorithm for the determination of phase from image and diffraction plane pictures,” *Optik* **35**, 227 (1972).
- <sup>318</sup>S. Lopatin, Y. P. Ivanov, J. Kosel, and A. Chuvilin, “Multiscale differential phase contrast analysis with a unitary detector,” *Ultramicroscopy* **162**, 74–81 (2016).

- <sup>319</sup>T. Matsumoto, Y.-G. So, Y. Kohno, H. Sawada, Y. Ikuhara, and N. Shibata, “Direct observation of  $\Sigma 7$  domain boundary core structure in magnetic skyrmion lattice,” *Sci. Adv.* **2** (2016), 10.1126/sciadv.1501280.
- <sup>320</sup>F. S. Yasin, L. Peng, R. Takagi, N. Kanazawa, S. Seki, Y. Tokura, and X. Yu, “Bloch lines constituting antiskyrmions captured via differential phase contrast,” *Adv. Mater.* **32**, 2004206 (2020).
- <sup>321</sup>C. Ophus and T. Ewalds, “Guidelines for quantitative reconstruction of complex exit waves in hrtem,” *Ultramicroscopy* **113**, 88 – 95 (2012).
- <sup>322</sup>B. T. Thole, P. Carra, F. Sette, and G. van der Laan, “X-ray circular dichroism as a probe of orbital magnetization,” *Phys. Rev. Lett.* **68**, 1943–1946 (1992).
- <sup>323</sup>P. Carra, B. T. Thole, M. Altarelli, and X. Wang, “X-ray circular dichroism and local magnetic fields,” *Phys. Rev. Lett.* **70**, 694–697 (1993).
- <sup>324</sup>C. Donnelly, M. Guizar-Sicairos, V. Scagnoli, S. Gliga, M. Holler, J. Raabe, and L. J. Heyderman, “Three-dimensional magnetization structures revealed with x-ray vector nanotomography,” *Nature* **547**, 328 (2017).
- <sup>325</sup>C. Donnelly, S. Gliga, V. Scagnoli, M. Holler, J. Raabe, L. J. Heyderman, and M. Guizar-Sicairos, “Tomographic reconstruction of a three-dimensional magnetization vector field,” *New J. Phys.* **20**, 083009 (2018).
- <sup>326</sup>A. Hierro-Rodríguez, C. Quirós, A. Sorrentino, L. M. Alvarez-Prado, J. I. Martín, J. M. Alameda, S. McVitie, E. Pereiro, M. Vélez, and S. Ferrer, “Revealing 3d magnetization of thin films with soft x-ray tomography: magnetic singularities and topological charges,” *Nat. Commun.* **11**, 6382 (2020).
- <sup>327</sup>C. Donnelly, S. Finizio, S. Gliga, M. Holler, A. Hrabec, M. Odstrčil, S. Mayr, V. Scagnoli, L. J. Heyderman, M. Guizar-Sicairos, and J. Raabe, “Time-resolved imaging of three-dimensional nanoscale magnetization dynamics,” *Nat. Nanotech.* **15**, 356–360 (2020).
- <sup>328</sup>J. P. Hannon, G. T. Trammell, M. Blume, and D. Gibbs, “X-ray resonance exchange scattering,” *Phys. Rev. Lett.* **61**, 1245–1248 (1988).
- <sup>329</sup>S. Zhang, G. van der Laan, J. Müller, L. Heinen, M. Garst, A. Bauer, H. Berger, C. Pfeiderer, and T. Hesjedal, “Reciprocal space tomography of 3d skyrmion lattice order in a chiral magnet,” *Proc. Natl. Acad. Sci. USA* **115**, 6386 (2018).
- <sup>330</sup>S. L. Zhang, G. van der Laan, W. W. Wang, A. A. Haghighirad, and T. Hesjedal, “Direct observation of twisted surface skyrmions in bulk crystals,” *Phys. Rev. Lett.* **120**, 227202 (2018).
- <sup>331</sup>P. Shafer, P. García-Fernández, P. Aguado-Puente, A. R. Damodaran, A. K. Yadav, C. T. Nelson, S.-L. Hsu, J. C. Woldel, J. Íñiguez, L. W. Martin, E. Arenholz, J. Junquera, and R. Ramesh, “Emergent chirality in the electric polarization texture of titanate superlattices,” *Proc. Natl. Acad. Sci. USA* **115**, 915–920 (2018).
- <sup>332</sup>M. H. Seaberg, B. Holladay, J. C. T. Lee, M. Sikorski, A. H. Reid, S. A. Montoya, G. L. Dakovski, J. D. Koralek, G. Coslovich, S. Moeller, W. F. Schlotter, R. Streubel, S. D. Kevan, P. Fischer, E. E. Fullerton, J. L. Turner, F.-J. Decker, S. K. Sinha, S. Roy, and J. J. Turner, “Nanosecond x-ray photon correlation spectroscopy on magnetic skyrmions,” *Phys. Rev. Lett.* **119**, 067403 (2017).
- <sup>333</sup>M. Mochizuki, X. Z. Yu, S. Seki, N. Kanazawa, W. Koshibae, J. Zang, M. Mostovoy, Y. Tokura, and N. Nagaosa, “Thermally driven ratchet motion of a skyrmion microcrystal and topological magnon hall effect,” *Nat. Mater.* **13**, 241–246 (2014).
- <sup>334</sup>G. Berruto, I. Madan, Y. Murooka, G. M. Vanacore, E. Pomarico, J. Rajeswari, R. Lamb, P. Huang, A. J. Kruchkov, Y. Togawa, T. LaGrange, D. McGrouther, H. M. Rønnow, and F. Carbone, “Laser-induced skyrmion writing and erasing in an ultrafast cryo-lorentz transmission electron microscope,” *Phys. Rev. Lett.* **120**, 117201 (2018).
- <sup>335</sup>X. Zhang, L. Sun, Y. Yu, and Y. Zhao, “Flexible ferrofluids: Design and applications,” *Adv. Mater.* **31**, 1903497 (2019).
- <sup>336</sup>J. McCord, “Progress in magnetic domain observation by advanced magneto-optical microscopy,” *J. Phys. D: Appl. Phys.* **48**, 333001 (2015).
- <sup>337</sup>D. Sanz-Hernández, R. F. Hamans, J.-W. Liao, A. Welbourne, R. Lavrijsen, and A. Fernández-Pacheco, “Fabrication, detection, and operation of a three-dimensional nanomagnetic conduit,” *ACS Nano* **11**, 11066 (2017).
- <sup>338</sup>S. Sahoo, S. Mondal, G. Williams, A. May, S. Ladak, and A. Barman, “Ultrafast magnetization dynamics in a nanoscale three-dimensional cobalt tetrapod structure,” *Nanoscale* **10**, 9981 (2018).
- <sup>339</sup>A. May, M. Hunt, A. Van Den Berg, A. Hejazi, and S. Ladak, “Realisation of a frustrated 3d magnetic nanowire lattice,” *Commun. Phys.* **2**, 13 (2019).
- <sup>340</sup>M. Al Mamoori, L. Keller, J. Pieper, S. Barth, R. Winkler, H. Plank, J. Müller, and M. Huth, “Magnetic characterization of direct-write free-form building blocks for artificial magnetic 3d lattices,” *Materials* **11**, 289 (2018).
- <sup>341</sup>O. Kazakova, R. Puttock, C. Barton, H. Corte-León, M. Jaafar, V. Neu, and A. Asenjo, “Frontiers of magnetic force microscopy,” *J. Appl. Phys.* **125**, 060901 (2019).
- <sup>342</sup>N. Rossi, F. R. Braakman, D. Cadeddu, D. Vasyukov, G. Tütüncüoğlu, A. Fontcuberta i Morral, and M. Poggio, “Vectorial scanning force microscopy using a nanowire sensor,” *Nat. Nanotech.* **12**, 150 (2017).
- <sup>343</sup>H. Corte-León, L. A. Rodríguez, M. Pancaldi, C. Gatel, D. Cox, E. Snoeck, V. Antonov, P. Vavassori, and O. Kazakova, “Magnetic imaging using geometrically constrained nano-domain walls,” *Nanoscale* **11**, 4478 (2019).
- <sup>344</sup>S. Vock, F. Wolny, T. Mühl, R. Kaltofen, L. Schultz, B. Büchner, C. Hassel, J. Lindner, and V. Neu, “Monopolelike probes for quantitative magnetic force microscopy: Calibration and application,” *Appl. Phys. Lett.* **97**, 252505 (2010).
- <sup>345</sup>H. Corte-León, V. Neu, A. Manzin, C. Barton, Y. Tang, M. Gerken, P. Klapetek, H. W. Schumacher, and O. Kazakova, “Comparison and validation of different magnetic force microscopy calibration schemes,” *Small* **16**, 1906144 (2020).
- <sup>346</sup>Y. Anahory, H. R. Naren, E. O. Lachman, S. Buhbut Sinai, A. Uri, L. Embon, E. Yaakobi, Y. Myasoedov, M. E. Huber, R. Klajn, and E. Zeldov, “Squid-on-tip with single-electron spin sensitivity for high-field and ultra-low temperature nanomagnetic imaging,” *Nanoscale* **12**, 3174 (2020).
- <sup>347</sup>L. Rondin, J.-P. Tetienne, T. Hingant, J.-F. Roch, P. Maletinsky, and V. Jacques, “Magnetometry with nitrogen-vacancy defects in diamond,” *Rep. Prog. Phys.* **77**, 056503 (2014).
- <sup>348</sup>L. Thiel, Z. Wang, M. A. Tschudin, D. Rohner, I. Gutiérrez-Lezama, N. Ubrig, M. Gibertini, E. Giannini, A. F. Morpurgo, and P. Maletinsky, “Probing magnetism in 2d materials at the nanoscale with single-spin microscopy,” *Science* **364**, 973–976 (2019).
- <sup>349</sup>I. Gross, W. Akhtar, V. Garcia, L. J. Martínez, S. Chouaieb, K. Garcia, C. Carrétéro, A. Barthélémy, P. Appel, P. Maletinsky, J. V. Kim, J. Y. Chauleau, N. Jaouen, M. Viret, M. Bibes, S. Fusil, and V. Jacques, “Real-space imaging of non-collinear antiferromagnetic order with a single-spin magnetometer,” *Nature* **549**, 252–256 (2017).
- <sup>350</sup>T. Weggler, C. Ganslmayer, F. Frank, T. Eilert, F. Jelezko, and J. Michaelis, “Determination of the three-dimensional magnetic field vector orientation with nitrogen vacancy centers in diamond,” *Nano Lett.* **20**, 2980–2985 (2020).
- <sup>351</sup>T. Schwarze, J. Waizner, M. Garst, A. Bauer, I. Stasinopoulos, H. Berger, C. Pfeiderer, and D. Grundler, “Universal helimagnon and skyrmion excitations in metallic, semiconducting and insulating chiral magnets,” *Nat. Mater.* **14**, 478 (2015).
- <sup>352</sup>A. Aqeel, J. Sahliger, T. Taniguchi, S. Mändl, D. Mettus, H. Berger, A. Bauer, M. Garst, C. Pfeiderer, and C. H. Back, “Microwave spectroscopy of the low-temperature skyrmion state

- in  $\text{Cu}_2\text{OSeO}_3$ ,” *Phys. Rev. Lett.* **126**, 017202 (2021).
- <sup>353</sup>M. A. Boles, M. Engel, and D. V. Talapin, “Self-assembly of colloidal nanocrystals: From intricate structures to functional materials,” *Chem. Rev.* **116**, 11220–11289 (2016).
- <sup>354</sup>F. Liu, Y. Li, Y. Huang, A. Tsyrenova, K. Miller, L. Zhou, H. Qin, and S. Jiang, “Activation and assembly of plasmonic nanosurfactants for encapsulation and triggered release,” *Nano Lett.* **20**, 8773–8780 (2020).
- <sup>355</sup>R. Streubel, X. Liu, X. Wu, and T. P. Russell, “Perspective: Ferromagnetic liquids,” *Materials* **13**, 2712 (2020).
- <sup>356</sup>R. Streubel, N. Kent, S. Dhuey, A. Scholl, S. Kevan, and P. Fischer, “Spatial and temporal correlations of XY macro spins,” *Nano Lett.* **18**, 7428 (2018).
- <sup>357</sup>D. Schildknecht, L. J. Heyderman, and P. M. Derlet, “Phase diagram of dipolar-coupled xy moments on disordered square lattices,” *Phys. Rev. B* **98**, 064420 (2018).
- <sup>358</sup>M. Seul and D. Andelman, “Domain shapes and patterns: The phenomenology of modulated phases,” *Science* **267**, 476 (1995).
- <sup>359</sup>K. Han, G. Kokot, S. Das, R. G. Winkler, G. Gompfer, and A. Snezhko, “Reconfigurable structure and tunable transport in synchronized active spinner materials,” *Sci. Adv.* **6**, eaaz8535 (2020).
- <sup>360</sup>G. Kokot, S. Das, R. G. Winkler, G. Gompfer, I. S. Aranson, and A. Snezhko, “Active turbulence in a gas of self-assembled spinners,” *Proc. Natl. Acad. Sci. USA* **114**, 12870 (2017).
- <sup>361</sup>H. Xie, M. Sun, X. Fan, Z. Lin, W. Chen, L. Wang, L. Dong, and Q. He, “Reconfigurable magnetic microrobot swarm: Multimode transformation, locomotion, and manipulation,” *Science Robotics* **4**, eaav8006 (2019).
- <sup>362</sup>B. A. Grzybowski, H. A. Stone, and G. M. Whitesides, “Dynamic self-assembly of magnetized, millimetre-sized objects rotating at a liquid–air interface,” *Nature* **405**, 1033 (2000).
- <sup>363</sup>U. Agarwal and F. A. Escobedo, “Mesophase behaviour of polyhedral particles,” *Nat. Mater.* **10**, 230–235 (2011).
- <sup>364</sup>P. F. Damasceno, M. Engel, and S. C. Glotzer, “Predictive self-assembly of polyhedra into complex structures,” *Science* **337**, 453–457 (2012).
- <sup>365</sup>L. Cao, D. Yu, Z. Xia, H. Wan, C. Liu, T. Yin, and Z. He, “Ferromagnetic liquid metal putty-like material with transformed shape and reconfigurable polarity,” *Adv. Mater.* **32**, 2000827 (2020).
- <sup>366</sup>J. Lee, S. Dubbu, N. Kumari, A. Kumar, J. Lim, S. Kim, and I. S. Lee, “Magnetothermia-induced catalytic hollow nanoreactor for bioorthogonal organic synthesis in living cells,” *Nano Lett.* **20**, 6981–6988 (2020).
- <sup>367</sup>S. H. Skjærvø, C. H. Marrows, R. L. Stamps, and L. J. Heyderman, “Advances in artificial spin ice,” *Nat. Rev. Phys.* **2**, 13 (2020).
- <sup>368</sup>Z. Luo, A. Hrabec, T. P. Dao, G. Sala, S. Finizio, J. Feng, S. Mayr, J. Raabe, P. Gambardella, and L. J. Heyderman, “Current-driven magnetic domain-wall logic,” *Nature* **579**, 214–218 (2020).
- <sup>369</sup>D. Ambika, V. Kumar, H. Imai, and I. Kanno, “Sol-gel deposition and piezoelectric properties of (110)-oriented  $\text{Pb}(\text{Zr}_{0.52}\text{Ti}_{0.48})\text{O}_3$  thin films,” *Appl. Phys. Lett.* **96**, 031909 (2010).
- <sup>370</sup>M. A. Ruderman and C. Kittel, “Indirect exchange coupling of nuclear magnetic moments by conduction electrons,” *Phys. Rev.* **96**, 99–102 (1954).
- <sup>371</sup>T. Kasuya, “A theory of metallic ferro- and antiferromagnetism on zener’s model,” *Progress of Theoretical Physics* **16**, 45–57 (1956).
- <sup>372</sup>K. Yosida, “Magnetic Properties of Cu-Mn Alloys,” *Phys. Rev.* **106**, 893–898 (1957).
- <sup>373</sup>A. A. Khajetoorians, M. Steinbrecher, M. Ternes, M. Bouhassoune, M. dos Santos Dias, S. Lounis, J. Wiebe, and R. Wiesendanger, “Tailoring the chiral magnetic interaction between two individual atoms,” *Nat. Commun.* **7**, 10620 (2016).
- <sup>374</sup>A. Roy, Y. Wu, R. Berkovits, and A. Frydman, “Universal voltage fluctuations in disordered superconductors,” *Phys. Rev. Lett.* **125**, 147002 (2020).
- <sup>375</sup>Y. Jiang, H. Y. Yuan, Z.-X. Li, Z. Wang, H. W. Zhang, Y. Cao, and P. Yan, “Twisted magnon as a magnetic tweezer,” *Phys. Rev. Lett.* **124**, 217204 (2020).
- <sup>376</sup>G. S. Cañón Bermúdez and D. Makarov, “Magneto-sensitive e-skins for interactive devices,” *Adv. Funct. Mater.* , 2007788 (2021).
- <sup>377</sup>M. Vázquez, “Giant magneto-impedance in soft magnetic wires,” *J. Magn. Magn. Mater.* **226–230**, Part 1, 693–699 (2001).
- <sup>378</sup>D. Karnaushenko, D. Makarov, C. Yan, R. Streubel, and O. G. Schmidt, “Printable giant magnetoresistive devices,” *Adv. Mater.* **24**, 4518–4522 (2012).
- <sup>379</sup>J. J. Beato-López, J. G. Urdániz-Villanueva, J. I. Pérez-Landazábal, and C. Gómez-Polo, “Giant stress impedance magnetoelastic sensors employing soft magnetic amorphous ribbons,” *Materials* **13** (2020), 10.3390/ma13092175.
- <sup>380</sup>D. Makarov, M. Melzer, D. Karnaushenko, and O. G. Schmidt, “Shapeable magnetoelectronics,” *Appl. Phys. Rev.* **3**, 011101 (2016), <https://doi.org/10.1063/1.4938497>.
- <sup>381</sup>G. S. Cañón Bermúdez, D. D. Karnaushenko, D. Karnaushenko, A. Lebanov, L. Bischoff, M. Kaltenbrunner, J. Fassbender, O. G. Schmidt, and D. Makarov, “Magneto-sensitive e-skins with directional perception for augmented reality,” *Sci. Adv.* **4** (2018), 10.1126/sciadv.aao2623.
- <sup>382</sup>G. S. Cañón Bermúdez, H. Fuchs, L. Bischoff, J. Fassbender, and D. Makarov, “Electronic-skin compasses for geomagnetic field-driven artificial magnetoreception and interactive electronics,” *Nat. Electron.* **1**, 589–595 (2018).
- <sup>383</sup>P. Makushko, E. S. Oliveros Mata, G. S. Cañón Bermúdez, M. Hassan, S. Laureti, C. Rinaldi, F. Fagiani, G. Barucca, N. Schmidt, Y. Zabala, T. Kosub, R. Illing, O. Volkov, I. Vladymyrskyi, J. Fassbender, M. Albrecht, G. Varvaro, and D. Makarov, “Flexible magnetoreceptor with tunable intrinsic logic for on-skin touchless human-machine interfaces,” *Adv. Funct. Mater.* , 2101089 (2021).
- <sup>384</sup>I. Mönch, D. Makarov, R. Koseva, L. Baraban, D. Karnaushenko, C. Kaiser, K.-F. Arndt, and O. G. Schmidt, “Rolled-up magnetic sensor: Nanomembrane architecture for in-flow detection of magnetic objects,” *ACS Nano* **5**, 7436–7442 (2011).
- <sup>385</sup>C. Müller, C. C. Bof Bufon, M. E. Navarro-Fuentes, D. Makarov, D. H. Mosca, and O. G. Schmidt, “Towards compact three-dimensional magnetoelectronics–Magnetoresistance in rolled-up Co/Cu nanomembranes,” *Appl. Phys. Lett.* **100**, 022409 (2012).
- <sup>386</sup>C. Müller, C. C. Bof Bufon, D. Makarov, L. E. Fernandez-Outon, W. A. A. Macedo, O. G. Schmidt, and D. H. Mosca, “Tuning giant magnetoresistance in rolled-up Co–Cu nanomembranes by strain engineering,” *Nanoscale* **4**, 7155–7160 (2012).
- <sup>387</sup>A. Richter, G. Paschew, S. Klatt, J. Lienig, K.-F. Arndt, and H.-J. P. Adler, “Review on hydrogel-based ph sensors and micro-sensors,” *Sensors* **8**, 561 (2008).
- <sup>388</sup>N. Farhoudi, H.-Y. Leu, L. B. Laurentius, J. J. Magda, F. Solzbacher, and C. F. Reiche, “Smart hydrogel micromechanical resonators with ultrasound readout for biomedical sensing,” *ACS Sens.* **5**, 1882 (2020).
- <sup>389</sup>S. Van Berkum, J. T. Dee, A. P. Philipse, and B. H. Erné, “Frequency-dependent magnetic susceptibility of magnetite and cobalt ferrite nanoparticles embedded in paa hydrogel,” *Int. J. Mol. Sci.* **14**, 10162 (2013).
- <sup>390</sup>S. Song, J. Park, G. Chitnis, R. Siegel, and B. Ziaie, “A wireless chemical sensor featuring iron oxide nanoparticle-embedded hydrogels,” *Sens. Actuators B Chem.* **193**, 925 (2014).
- <sup>391</sup>R. Niu, C. X. Du, E. Esposito, J. Ng, M. P. Brenner, P. L. McEuen, and I. Cohen, “Magnetic handshake materials as a scale-invariant platform for programmed self-assembly,” *Proc. Natl. Acad. Sci. USA* **116**, 24402–24407 (2019).